Aus dem Institut für Virologie

Direktor: Prof. Dr. Stephan Becker

des Fachbereichs Medizin der Philipps-Universität Marburg

Characterization of Ebola Virus VP30 Phosphorylation with a Phosphospecific Antibody

Inaugural-Dissertation zur Erlangung des Doktorgrades

der gesamten Humanmedizin

dem Fachbereich Medizin der Philipps-Universität Marburg

vorgelegt von

Clemens Lier

aus Bonn

Marburg, 2019

Angenommen vom Fachbereich Medizin der Philipps-Universität Marburg
am: 25.04.2019

Gedruckt mit Genehmigung des Fachbereichs.

Dekan: Herr Prof. Dr. H. Schäfer
Referent: Herr Prof. Dr. S. Becker
1. Korreferent: Herr PD Dr. F. Sommer

Table of Contents

1 Introduction

1.1 Taxonomy and Epidemiology

Ebolavirus, *Marburgvirus,* and *Cuevavirus* form the family *Filoviridae* in the order *Mononegavirales*. The order *Mononegavirales* further includes *Bornaviridae*, *Mymonaviridae*, *Nyamiviridae*, *Paramyxoviridae*, *Pneumoviridae*, *Rhabdoviridae*, and *Sunviridae*, which all have a nonsegmented, negative-sense RNA genome in common.

Family	**Genus**	**Species**	**Distinct Filovirus / Virus name**
Filoviridae	*Cuevavirus*	*Lloviu cuevavirus*	Lloviu virus (LLOV)
	Ebolavirus	*Bundibugyo ebolavirus*	Bundibugyo virus (BDBV)
		Reston ebolavirus	Reston virus (RESTV)
		Sudan ebolavirus	Sudan virus (SUDV)
		Taï Forest ebolavirus	Taï Forest virus (TAFV)
		Zaire ebolavirus	Ebola virus (EBOV)
	Marburgvirus	*Marburg marburgvirus*	Marburg virus (MARV)
			Ravn virus (RAVV)

Table 1: Taxonomy of *Filoviridae* According to ICTV, 2016.
Order, Family, Genus, and Species are written in italics. The virus name is never italicized and may be abbreviated[113].

Five virus species constitute the genus *Ebolavirus*. Ebola virus (EBOV), the only member of the species *Zaire ebolavirus,* and Sudan virus (SUDV), the sole member of the species *Sudan ebolavirus*, sporadically cause epidemics of a severe feverish disease in sub-Saharan Africa. In 1976, both viruses first emerged in two near simultaneous outbreaks in southern Sudan and in the Democratic Republic of Congo (DRC, formerly known as Zaire)[65,66]. In Sudan, 284 people were infected with a lethality of 53 %, whereas 318 humans were infected in Zaire with a lethality of 88 %. The isolated virus was named after the nearby river Ebola, which in the local language means "black river"[192]. Only later it was realized that the two outbreaks were caused by two distinct viruses, SUDV and EBOV, respectively[50]. After their discovery, both viruses caused infrequent outbreaks in equatorial Africa[273]. In 1995, an outbreak of EBOV in Kikwit (DRC) received worldwide attention. Of the 315 infected persons, 250 died[124]. In 2000, a large outbreak of SUDV was reported with 425 cases and 224 deaths[184].
From 2013 to 2016, West Africa experienced the so far largest EBOV outbreak in history. 28 616 suspected, probable, and confirmed cases of Ebola virus disease (EVD) and 11 310 deaths were reported[268]. Cases of EBOV were imported to several European countries and the USA with isolated local transmission[49].

Since 1976, three laboratory infections with EBOV and SUDV have been documented with a mortality rate of 66 % [4,30,69].

Taï Forest virus (TAFV), the only member of the species *Taï Forest ebolavirus,* was discovered in 1994, when an ethnologist became ill after conducting an autopsy of a wild chimpanzee in the Côte-d'Ivoire[135]. Retrospectively, it was demonstrated that the chimpanzee and several other members of the chimpanzee community died of an infection with the same filovirus[77]. So far, no other cases of TAFV infection in humans have been described.

In 1989, Reston virus (RESTV) was first discovered in Cynomolgus monkeys (*Macaca fascicularis*). The animals were imported from the Philippines to a primate facility in Reston, Virginia, and developed a severe hemorrhagic disease[117]. In later years, several outbreaks among monkeys from the Philippines were noted [93,161,201]. In 2008, RESTV was also discovered in pigs on the Philippines[13]. No human infections with RESTV have been reported so far, but several workers who came into contact with infected animals developed antibodies against the virus[161,162].

Bundibugyo virus (BDBV), representing the species *Bundibugyo ebolavirus*, *was* the latest filovirus to be discovered. The virus was isolated after a large hemorrhagic fever outbreak in December 2007 in Bundibugyo District, Western Uganda, among the local population[242]. In June 2012, the only other known outbreak of BDBV occurred in the Democratic Republic of Congo[273].

The species *Marburg marburgvirus*, belonging to the genus *Marburgvirus*, comprises the two distinct filoviruses Marburg virus (MARV) and Ravn virus (RAVV). MARV was discovered in 1967, when 31 people developed a severe hemorrhagic disease simultaneously in Marburg, Frankfurt (both Germany), and in Belgrade (Serbia, former Yugoslavia). A so far unknown virus was isolated from the patients. All the primary 25 cases were laboratory members, who acquired the infection from African green monkeys (*Cercopithecus aethiops*). The monkeys were imported from Uganda for the production of poliovirus vaccine in monkey kidney cell cultures[154,225].
In the following years, sporadic epidemics of MARV disease were reported in central Africa[188]. The so far largest outbreak happened in Angola in October 2004, with 252 human cases and a mortality of 90 %[187,241].

The first known infection with Ravn virus (RAVV) occurred in 1987 in a 15 year old boy after he visited Kitum cave in Mount Elgon National Park [121]. RAVV also co-circulated during an outbreak from 1998-2000 in the Democratic Republic of Congo[15].

Sequences specific for a new filovirus, the Lloviu virus (LLOV), genus *Cuevavirus*, were discovered in bat carcasses (*Miniopterus schreibersii*) in Cueva del Lloviu (Spain) in 2002[176]. No human infections with LLOV have been described until today.

1.2 Pathogenesis and Clinical Features

Ebola virus disease (EVD) is a typical zoonosis. The virus is transmitted into the human population by direct contact with infected animals, both alive and dead. The reservoir for human pathogenic filoviruses remained a mystery for many years. Today bats are considered the natural host for filoviruses[34,66,97,138,168,196,232,243]. Immunoglobulin G specific for EBOV was detected in the serum of *Hypsignathus monstrosus*, *Epomops franqueti*, and *Myonycteris torquata* fruit bats. In the liver and spleen of these animals, viral RNA sequences specific for EBOV were identified[141,193]. The geographic distribution of the three fruit bat species overlaps with the outbreak regions[141]. In 2007, a massive annual fruit bat migration was linked to an EBOV outbreak in the DRC. The index person of the epidemic ate freshly killed fruit bats, making direct transmission from the reservoir into the human population likely[140].

Besides humans, gorillas (*Gorilla gorilla gorilla)*, chimpanzees (*Pan troglodytes troglodytes)*, and duikers (*Cephalophus* spp) can develop symptomatic EBOV infection, leading to dramatic declines in their populations. These periods of decline were accompanied by outbreaks in the human population, suggesting transmission between humans and great apes / duikers[21,37,106,202,258]. During outbreaks between 2001 and 2003, the human infections resulted from direct handling of infected wild animal carcasses[202]. In the recovered animal carcasses, different Ebola virus strains were detected[142]. The multi-emergence hypothesis favors independent virus spillovers by the reservoir into human populations and susceptible animals during certain ecological conditions[142,266]. Similar to EBOV, MARV-specific RNA and antibodies were detected in Egyptian fruit bats (*Rousettus aegyptiacus*), and MARV was even successfully isolated from these bats[125,240].

Introduction of filoviruses into the human population follows a recognizable pattern: the virus is transmitted to a single person from direct contact with the reservoir or infected wild animals. After manifestation of the infection, the disease spreads from human-to-human through the local communities by direct contact with infected patients or corpses at funerals [61,65,66,124,150]. The epidemic may be self-limiting because of the high mortality associated with EVD, but diagnosis and measures to control disease spread are often delayed[44]. Most outbreaks are eventually stopped by the combination of infection-control practices and quarantine measures[190]. During the 1976 outbreak, virus

spread was accelerated by the medical use of unsterilized needles[66]. The route of exposure also partly determines the lethality of the virus. Parenteral exposure is associated with a higher mortality than viral invasion through broken skin or mucous membranes[189]. The oral route of ingestion is linked with a high infectious dose, as organ virus titers of dead animals can be as high as 10^8 pfu/g[81,114]. Airborne transmission has not been described for EBOV, and direct physical contact with an ill person or bodily fluids is required[61]. Aerosol transmission has been documented under laboratory conditions only[120,262].

EBOV replicates in a wide range of cells, including monocytes, macrophages, dendritic cells, endothelial cells, epithelial cells, fibroblasts, interstitial cells of the testis, hepatocytes, and adrenal cortical cells[14,32,81,114,205,276]. Lymphocytes are resistant to EBOV infection, but profound lymphopenia is often observed[80,111]. Lymphopenia has been attributed to direct cytotoxic effects of the viral glycoprotein[111]. Infection of mobile cells like monocytes and macrophages plays an important role in the rapid dissemination of the virus, first to local lymph nodes, liver, and spleen, and later throughout the infected host[33,81]. In the acute phase of infection, filoviruses are present in the blood as free virions. The viral RNA can be detected by RT-PCR in various body fluids, such as saliva, feces, urine, semen, breast milk, tears, and sweat[16,45].

Histopathologically, very little inflammation is seen around the infected cells, which is a hallmark of EBOV infection. Infected cells develop signs of necrosis, in early stages predominantly affecting lymph nodes, liver, spleen, thymus, and later also lung and kidney[14,205,275]. Necrosis of adrenal cortex cells impairs steroid biosynthesis, leading to sodium loss, hypovolemia, and hypotension[73]. Destruction of endothelial cells, either by EBOV-induced necrosis or by dysregulated immune mechanisms, might be responsible for coagulation abnormalities observed during EBOV infection[6,83]. A rise in the levels of tissue factor, released by infected macrophages, is associated with disseminated intravascular coagulation often seen in EVD[83]. During early stages of infection, macrophages release massive amounts of pro-inflammatory cytokines, such as interleukin-1beta (IL-1beta), tumor necrosis factor alpha, and IL-6 as well as the chemokines IL-8 and gro-alpha. Infection of dendritic cells is associated with a poor immune response, impaired type I Interferon production, and downregulation of costimulatory molecules[31,149,227]. EBOV-specific B- and T-cell activation during the acute EBOV infection has recently been described in four survivors of EVD[156].

After an incubation period of 2-21 days (mean 4-10 days), Ebola virus disease (EVD), previously known as Ebola hemorrhagic fever, manifests itself with clinical symptoms, such as fever, headache, asthenia, arthralgia, myalgia, or back pain. Patients often

develop gastrointestinal symptoms, like abdominal pain, diarrhea, and vomiting, leading to hypovolemia and electrolyte imbalances. The initial presentation is very unspecific and similar to other infections, such as malaria, typhoid fever, cholera, Lassa fever, or other tropical diseases. In later stages, infected persons may develop a maculopapular rash or even extensive hemorrhages, respiratory exhaustion, neurological symptoms (headaches, confusion, seizures, and coma), shock, and multiple organ failures, eventually leading to death. Patients usually die 7 to 11 days after onset of symptoms, the mortality rate ranges from 30 to 90 % [28,264]. Because of the high mortality rate associated with EVD, the virus is classified as a biosafety-level 4 (BSL-4) pathogen and must be handled in specialized research laboratories.

Laboratory abnormalities include anemia, lymphopenia, granulocytosis, thrombocytopenia, prolongation of PTT and INR, and elevated D-dimers as signs of disseminated intravascular coagulation, severe electrolyte imbalances (especially hypokalemia, hypocalcemia, and hyponatremia) as well as elevation of blood urea nitrogen, creatinine, and hepatic enzymes, reflecting renal and hepatic organ dysfunction[78,212,213,248].

Survivors often suffer from prolonged convalescence and long-term sequelae, such as ocular deficits, hearing loss, arthralgia, headache, depression, and insomnia. This range of symptoms is summarized as the "post-Ebola syndrome"[46,174]. Occurence of post-traumatic stress disorder, potentiated by stigmatization and isolation of survivors from the communities, is common[147].

EBOV can persist for long times in immunologically privileged organs. Viral RNA was detected by RT-PCR in the semen of male patients up to one year after acute infection[1,56]. Sexual transmission of EBOV was documented in one case 5 months after the patient had recovered[155]. Another probable case of sexually transmitted EBOV was reported 531 days after onset of symptoms[58]. Viral RNA was also detected in other bodily fluids following infection[45,223]. In one case, persistence of viable EBOV in ocular fluids led to acute uveitis, 14 weeks after the onset of symptoms[250]. Even more astonishingly, viable virus was detected in the cerebrospinal fluid of a nurse from Scotland, 9 months after the initial infection. She presented with neurological symptoms and received a diagnosis of acute meningitis due to a late EBOV relapse[116].
Survivors of EVD develop neutralizing antibodies, which have been detected up to 40 years after infection[133,198,226]. Serosurveys in central Africa detected EBOV-specific antibodies in up to 18 % of the human population, suggesting asymptomatic infections or a high burden of infection[36,171].

1.3 Diagnosis, Therapeutic Options, and Prevention

Rapid and accurate diagnosis of EVD is essential to initiate adequate infection control measures. Since there is no specific symptom for EBOV infection, laboratory diagnosis plays a crucial role. Today, RT-PCR tests to detect viral RNA or ELISA tests to detect viral antigens are can confirm an acute infection with EBOV, but tests are only reliable after the onset of symptoms. Depending on the specific assay, blood, urine, or saliva may be used. These molecular tests have replaced traditional viral culture techniques and electron microscopy[35,104].

So far, no proven therapy is available for treatment of EVD. Treatment is symptomatic with oral and intravenous fluid replacement, targeted electrolyte replacement, treatment of hypoglycemia, parenteral nutrition, and antibiotics against secondary bacterial infections. In selected cases, respiratory supportive care or renal replacement therapy might be needed[108,131,246].

Experimental immune therapies and drugs have been investigated in response to the large and unanticipated outbreak from 2013 to 2016. One trial investigated the effect of passive immunization with a mixture of three monoclonal antibodies (designated ZMapp) directed against the surface protein GP for treatment of acute EVD[54]. Other approaches evaluated the use of siRNA (TKM-Ebola), nucleotide analoga (Favipiravir, Brincidofovir, GS-5734) and convalescent whole blood or plasma[62,63,224,249]. So far, no statistical significant survival benefit could be demonstrated for any of these therapies[92].

Efforts also concentrated on the development of an active immunization[3,72]. First phase III study results suggest that the rVSV-ZEBOV vaccine is very effective and safe. No cases were reported in the vaccine groups 10 days or more after randomization, and antibody titers persisted for up to one year[94,95].

Prevention plays an invaluable role in controlling an EBOV outbreak. According to the WHO and the CDC, prevention measures include reducing the risk of wildlife-to-human transmission (e.g. proper cooking of meat), reducing the risk of human-to-human transmission (e.g. by wearing appropriate personal equipment and practicing careful hygiene), reducing the risk of possible sexual transmission (e.g. male survivors should practice safe sex for 12 months after onset of symptoms), and outbreak containment measures (e.g. contact tracing and safe burial of the dead) [67,194].

1.4 Morphology and Genome Organization

Filoviruses were named for their characteristic threadlike shape (filo = thread in Latin). The diameter of the virions is about 80 nm, the length varies from several hundred nm up to 14 µm[73]. The filamentous viral particles may be straight, rod-shaped, branched, or curved, and are enveloped by a lipid bilayer, which is derived from the host cell plasma membrane. Glycoprotein (GP) trimers are inserted into the lipid membrane and form spikes, which can be seen by electron microscopy[211].

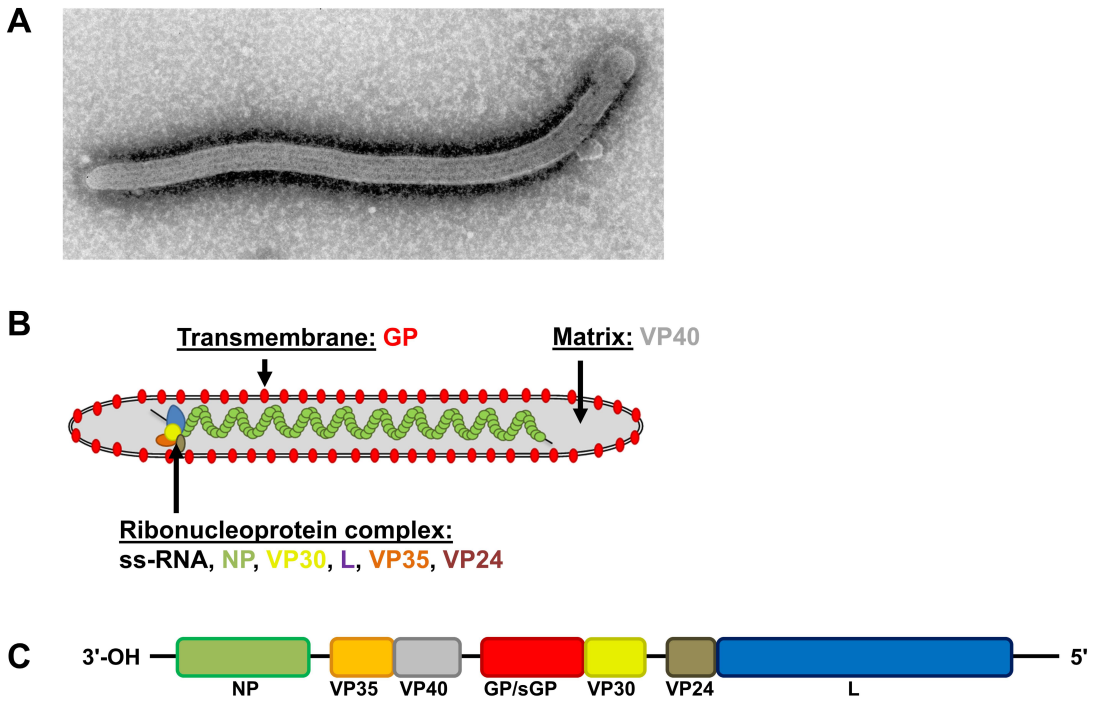

Figure 1: Morphology and Genome Organization of Ebola virus.
A. Electron microscopy of a single EBOV particle. Copyright by Dr. Larissa Kolesnikova. **B.** Schematic representation of an EBOV particle. **C.** Genome structure of EBOV.

The filamentous EBOV particles contain a negative-sense single-stranded RNA genome, surrounded by a complex of viral proteins, the so-called nucleocapsid[68,195]. The open reading frames of the 19 kB-genome encode for 7 structural proteins [NP, VP35, VP40, GP, VP30, VP24, and L] and several nonstructural secreted glycoproteins (sGP, ssGP, and Δ-peptide) [158,170,170,209,255,256]. The viral genome is flanked by noncoding regions, the 3' leader and the 5' trailer region. These regions contain important signals for encapsidation and replication of the viral RNA[170]. In addition, the viral genes are surrounded by conserved extragenic regions, which contain promotors and stop signals for transcription. Gene overlaps, which are limited to transcription signals, were found between VP35 and VP40, GP and VP30, and the VP24 and L genes[209].

The nucleocapsid complex is composed of the nucleoprotein NP, which encapsidates the viral RNA and forms helical coiled structures, the viral proteins VP35, VP30, VP24, and the RNA-dependent RNA polymerase L[10,22,180]. Four of these proteins, namely NP, L, VP30, and the polymerase cofactor VP35, also mediate transcription and replication of the viral genome. VP24 is not needed for viral replication and transcription. It was also referred to as the minor matrix proteins for many years, but more recently it was discovered that VP24 instead plays an essential role in the formation of nucleocapsids[10,105,179,181,260]. VP40, the viral matrix protein, locates to the inner side of the viral membrane. It is required for the filamentous appearance of the virions and the release of new virions at the cellular plasma membrane[118,182,238].
Synthesis of the glycoprotein GP is dependent on mRNA editing. It exists in two major forms, the full length GP, which is inserted into the viral envelope, and smaller secreted glycoproteins[254,255]. The surface GP is synthesized as a precursor protein (GP0) and proteolytically cleaved by furin into the two subunits GP1 and GP2 in the Golgi apparatus, which are linked by a disulfide bond and noncovalent interactions[74,137,255].

1.5 VP30 and NP

VP30 (288 aa) is an essential activation factor of viral transcription, but is not needed for replication of the viral genome[153,163]. Together with the nucleoprotein NP, the polymerase L, and the polymerase cofactor VP35, it forms the transcription complex[170]. VP30 is required for initiation of transcription at the first gene start site probably to overcome an RNA secondary structure and also plays a role in transcription reinitiation at the following genes[153,261].

Homologues of VP30 exist in all filoviruses. In MARV, VP30 is not absolutely required for transcription initiation, but enhances reporter activity when tested in model systems[160]. The rescue of a recombinant MARV was not possible without VP30, suggesting an essential role of the protein in MARV as well[71]. Moreover, EBOV VP30 also shares structural and functional characteristics with the M2-1 transcription factor of the human respiratory syncytial virus[236].

EBOV VP30 consists of an N-terminal region, which contains several phosphorylation sites, a Cys_3-His type zinc-finger motif, as well as an RNA-binding site[90,119,163]. The C-terminal domain adopts a helical structure and folds into dimers, which assemble into hexamers that are present in the virions[89,90]. Three intrinsically disordered protein regions have been described, spanning from residues 1 to 44, 120 to 140, and 268 to 288 of VP30[90,119]. VP30 interacts with NP, the polymerase L, and VP35[27,87,90,214]. The VP30-NP interaction is dependent on the binding of a short peptide in the C-terminal part of NP to

the C-terminal domain of VP30[90,125,270]. The interaction between VP30 and VP35 is mediated by RNA[27].

The function of VP30 as a transcription activation factor can be regulated via phosphorylation[24,152,165]. VP30 can be phosphorylated at two N-terminal clusters of conserved serine residues, each containing 3 serine residues (S29-S31 and S42, S44, S46), and at threonine 52[170]. Further VP30 phosphorylation sites (Thr 143 and Thr 146) have been identified more recently by mass spectrometry[112].

While protein phosphatase 1 and 2A (PP1 and PP2A) - and to a lesser extent PP2C - were identified to dephosphorylate VP30 *in vitro*, the responsible catalyzing kinases are unknown[165]. Using okadaic acid (OA), a PP1 / PP2A inhibitor, it was demonstrated that phosphorylation of VP30 impairs its function as a viral transcription factor, thereby favoring replication. This effect of OA could be revoked if the two clusters of VP30 serine residues were replaced by phosphoablative alanine residues (mutant VP30_AA) [165]. In an animal model, inhibition of PP1 blocked viral proliferation by leading to a hyper-phosphorylated form of VP30 that did not support viral transcription[112].

A model was developed in which dynamic phosphorylation of VP30 is regulating the balance between viral transcription and replication: phosphorylated VP30 favors replication of the full genome by NP / VP35 / L alone, but does not allow viral transcription, whereas nonphosphorylated VP30 (together with NP / VP35 / L) supports the transcription of individual viral genes[26,152,153]. It was postulated that VP30 phosphorylation can change the composition of transcription / replication complexes: phosphorylation of VP30 enhances the interaction with NP. Contrary, phosphorylation of VP30 weakens the interaction with VP35, possibly excluding VP30 from the transcription-complex to form a replicase-complex[24,165].

By introducing VP30 serine mutations into recombinant EBOV, it was shown that the generation of a recEBOV without serine residues in the N-terminal region is impossible[152]. More recently, a recombinant EBOV with VP30 serine 29 as the only phosphorylation acceptor site in the N-terminal region was described, with similar growth characteristics as EBOV_wt. Phosphorylation of VP30 was needed during early time points of infection for primary transcription, and phosphorylation of VP30 serine 29 was sufficient to fulfill this function[26].

The amino acids surrounding the N-terminal phosphorylation cluster of VP30 contribute to RNA-binding activity. RNA-binding was mapped to residues 26 to 40, a region rich in arginines[119]. The RNA-binding function of VP30 can be weakened by hyper-phosphorylation of VP30[27].

The nucleoprotein **NP** (739 aa) is the major component of the nucleocapsid complex. It encapsidates the viral RNA, protecting it from digestion by cellular nucleases. As such, NP is indispensable for replication and transcription of the viral genome[68,170]. The protein consists of a hydrophobic N-terminal half and a hydrophilic C-terminal half[210]. The N-terminal part is required for the formation of NP homo-oligomers and important for RNA-binding, whereas the C-terminal part is crucial for interaction with VP40 and subsequent incorporation of nucleocapsids into virions[143,173,179,183,260].

NP has a predicted molecular weight of 85 kDA. In SDS-PAGE it migrates at 115 kDA, which was attributed to two acidic domains in the C-terminal part of the protein. This region also mediated incorporation of nucleocapsids into viral particles[219]. Other reports suggested that glycosylation and sialyation of NP are responsible for the aberrant SDS migration[105].

In mammalian cells, recombinant expression of NP leads to the formation of perinuclear cytoplasmic inclusion bodies. In these, nucleocapsid-like helical structures with a diameter of 20 nm can be observed by electron microscopy[180,260]. But only after expression of NP, VP35, and VP24, nucleocapsid structures similar to those observed during infection are formed[105].

Inclusion bodies also represent a characteristic feature of EBOV infection[14]. Here, inclusion bodies represent the site of viral genome replication[98]. During infection, VP35, VP30, and L colocalize with NP in the NP-induced inclusion bodies[29,87]. Interactions between VP35 - L and VP35 - NP have been described, leading to the formation of heterotrimeric complexes, in which VP35 serves as a bridge between NP and L[19]. Interactions between NP and VP24 facilitate genome packaging and formation of nucleocapsids in inclusion bodies[10].

1.6 Viral Life Cycle

The viral replication cycle can be divided into three major stages: I) Attachment of virions to susceptible host cells, endocytosis, and membrane fusion. II) Transcription and replication of the viral genome. III) Assembly and budding of new virions.

I) EBOV can infect many cell types and exploits different endocytotic pathways. This includes caveolae-dependent entry, receptor-mediated endocytosis, and macropinocytosis[17,70,107,172,206–208]. The GP1 subunit plays a central role in binding attachment factors on the surface of susceptible host cells. Many binding partners have been identified, which probably reflects the broad cellular tropism of EBOV. The folate receptor, different C-type lectins (DC-SIGN, DC-SIGNR, L-SIGN, hMGL, ASGP-R, LSECtin), integrins, TIM-1, and Axl all have been described to mediate attachment of EBOV particles to host cells[8,20,42,86,130,216,221,222,235]. After binding to the plasma membrane, virions are internalized into acidified endosomes, where fusion of viral and cellular membranes take place[234]. In the endosome / lysosome, GP is cleaved by Cathepsin proteases and subsequently able to bind the endosomal / lysosomal cholesterol transporter NPC-1[39,43,215]. Fusion of viral and cellular lipid membranes is supported by the fusion peptide of the GP2 subunit[43,100]. After fusion, the nucleocapsids are released into the cytoplasm, where transcription and replication of the viral genome take place.

II) Immediately after infection, the viral negative-sense RNA genome needs to be transcribed into individual mRNAs by the incorporated viral proteins only (primary transcription). Transcription of viral mRNAs is accomplished by the viral proteins NP, the RNA-dependent RNA polymerase L, the polymerase cofactor VP35, and VP30. The monocistronic mRNAs contain a 3' poly (A)-tail and a 5' cap. It is thought that the individual genes are transcribed sequentially from the 3' to the 5' end of the viral genome. Polyadenylation of the viral mRNAs by the viral polymerase slows down transcription at the gene ends and re-initiation at the following gene start site does not occur in all cases. Consequently a gradient of viral mRNAs is produced, with NP mRNA being transcribed the most and L mRNA the least[98,169]. Following transcription, the mRNAs are translated by the cellular translation machinery into new viral proteins. The new viral proteins amplify synthesis of individual viral mRNAs (secondary transcription) and replicate the full-length positive-sense antigenomes and genomes, which are simultaneously encapsidated by NP (replication). For replication of the full length genome, VP30 is dispensable. Both the viral transcription and replication machinery use RNA encapsidated by NP as their template, rather than naked RNA. Encapsidation of the viral genome by NP is also thought to protect the RNA from degradation by cellular nucleases [reviewed by Mühlberger et al. 2007[169]].

EBOV transcription and replication is accompanied by the formation of small viral inclusion bodies around the nucleus[200]. The viral inclusion bodies contain mainly viral proteins and represent the sites of viral replication[98,173]. As such, they contain the viral proteins NP, VP35, and L, which are necessary for replication, but VP30, VP24, and VP40 also localize to the inclusion bodies[10,173]. During the course of the infection the inclusion bodies increase in size, as more and more viral proteins are synthesized[173]. Within the inclusion bodies, the assembly of rod-like nucleocapsids can be observed[105,178].

III) Nucleocapsids are electron-dense helical structures composed of NP, which encapsidates the viral RNA, as well as VP35, VP30, VP24, and L[10,22]. They are formed in viral inclusion bodies and are transported along actin filaments to the plasma membrane, where they are packaged into new virions[217]. For recruitment of the nucleocapsids into new virions, an interaction between the C-terminus of NP and VP40 is regarded as important[82,183]. VP40, the matrix protein, plays a major role in the budding of new virions. EBOV can exploit parts of the Endosomal Sorting Complex Required for Transport (ESCRT) pathway, which involves the formation of multivesicular bodies (MVB) as well as parts of the COPII vesicular transport system, for release of new virions from the host cell[91,144,272]. The ESCRT pathway is usurped by many viruses for cellular egress because this pathway supports "reverse topology" membrane fission[257]. Components of the ESCRT pathway, such as Tsg101 or Nedd4, specifically interact with N-terminal "late domains" of VP40[91,144,197]. The surface protein GP colocalizes with VP40 in MVBs and is incorporated into the membrane of newly formed viral particles[127]. In cell culture, budding of new virions mainly occurs at cellular protrusions, so-called filopodiae[128,217].

1.7 Viral Life Cycle Modeling Systems

EBOV is a highly dangerous pathogen and requires handling under biosafety level 4 conditions (BSL-4). Several systems modeling the EBOV life cycle under BSL-2 conditions have been developed. These systems simulate and dissect certain parts of the virus life cycle. Here, an EBOV-specific minigenome and a transcription and replication competent virus-like particle (trVLP) assay are presented. Both assays are based on a viral genome analogue (so-called minigenome), in which the open reading frames of the viral genome are replaced by a single reporter gene (monocistronic minigenome). The reporter gene is flanked by the original 3' leader and 5' trailer regions of the EBOV genome, which contain important *cis*-regulating elements for transcription and replication. The negative-sense RNA minigenome is produced from cDNA by a T7 RNA polymerase. The EBOV proteins need to be supplied *in trans*[170].

These life cycle modeling systems are based on reverse genetics. It is possible to observe the phenotypic effects of specific genetic alterations, which are inserted into the cDNA of the viral proteins [reviewed by Hoenen et al. 2014[99] and Biedenkopf et al. 2017[25]].

1.7.1 EBOV-Specific Minigenome Assay

The minigenome assay models viral genome replication and transcription (Figure 2). Plasmids encoding the EBOV-specific minigenome, a T7 DNA-dependent RNA polymerase as well as the nucleocapsid proteins NP, VP35, L, and VP30 are transfected into HEK-293 cells. These four viral proteins represent the minimal requirement for viral transcription and replication. The plasmids encoding the T7 polymerase and the viral proteins contain eukaryotic promotors, hence the proteins are produced by the cellular transcription and translation machinery. The EBOV-specific minigenome on the other hand, which is under control of a T7 promotor, is transcribed by the T7 polymerase into a negative-sense RNA minigenome in the cytoplasm. The minigenome is encapsidated by transiently expressed NP and used for transcription and replication by VP35, VP30, and L. The activity of the reporter gene (Renilla luciferase) monitors viral transcription and replication and can be measured in a luminometer. Because the viral proteins are supplied *in trans* and are abundantly available, reporter gene activity reflects late stages of EBOV infection, as secondary transcription and genome replication occur in parallel.

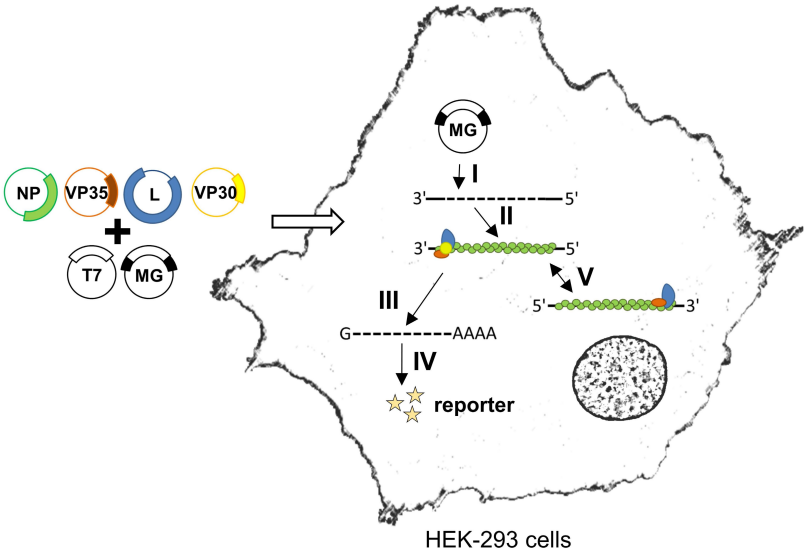

Figure 2: EBOV-Specific Minigenome Assay.

Plasmids encoding the viral transcription complex, a T7 DNA-dependent RNA polymerase and an EBOV-specific minigenome (MG) are transfected into HEK-293 cells. The viral proteins and the T7 polymerase are transcribed and translated by the cellular machinery (not depicted). I) The cDNA of the MG is transcribed into a negative-sense RNA MG by a T7 polymerase. II) The MG is encapsidated by NP and associates with the other viral proteins. III) Secondary transcription of the viral MG into mRNA by NP, VP35, L, and VP30. IV) Translation into the reporter gene (Renilla luciferase). V) Replication of the viral MG by NP, VP35, and L. The activity of the reporter gene Renilla luciferase is measured in relative light units in a luminometer. Reporter gene activity reflects the potential of the viral proteins to support secondary transcription and genome replication. The figure is based on Hoenen et al. 2014[99].

1.7.2 EBOV-Specifc Transcription and Replication Competent Virus-Like Particle Assay

The EBOV-specific transcription and replication competent virus-like particle (trVLP) assay is based on the minigenome assay and simulates a single infectious cycle. Besides modeling viral transcription and replication like in the minigenome assay, it examines the morphogenesis and release of infectious virus-like particles as well as the infection of target cells (Figure 3). In the trVLP assay, all seven EBOV proteins are recombinantly expressed in producer cells (HEK-293 cells) along with a minigenome, which leads to the formation and release of nucleocapsid-containing virus-like particles. The trVLPs are purified from the supernatant to infect naïve indicator cells (HUH-7 cells). In the naïve indicator cells, the minigenome is transcribed by the incorporated viral proteins. The resulting reporter gene activity in the indicator cells not only reflects the primary transcription potential in the indicator cells, but also replication of the minigenome in the producer cells, assembly and budding of trVLPs, and entry into the indicator cells.

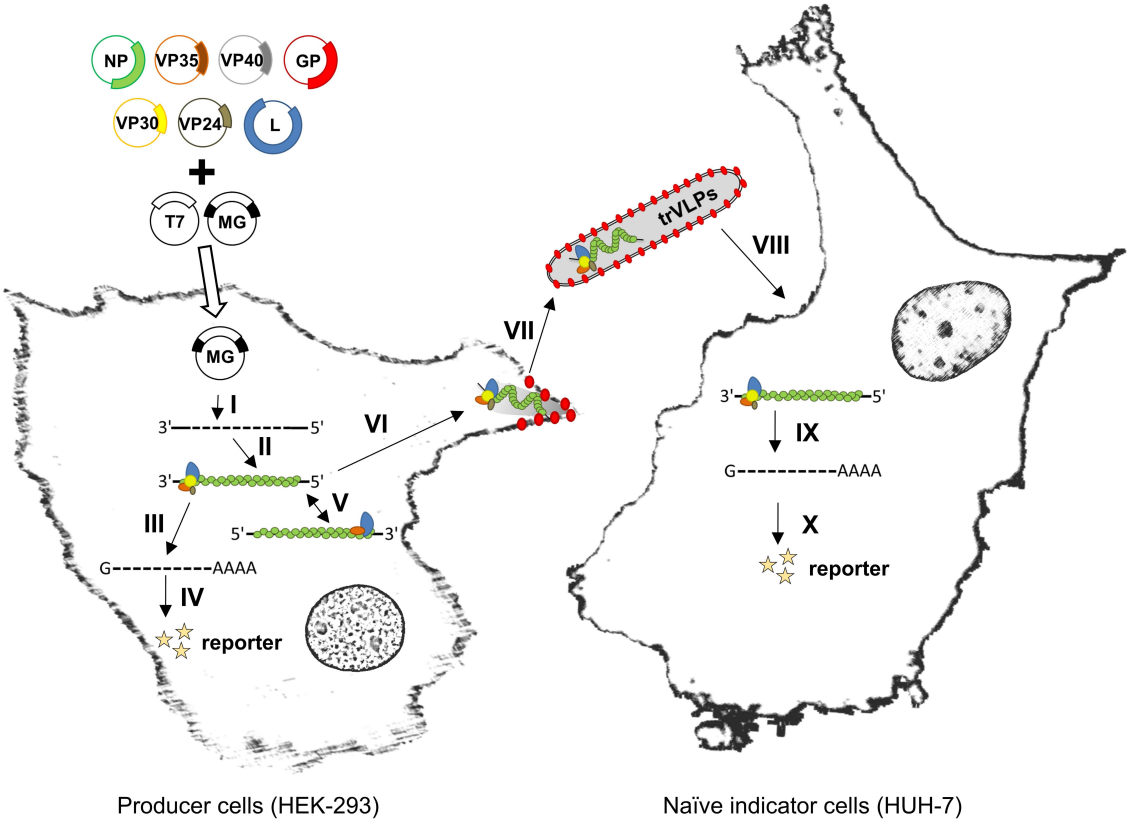

Figure 3: EBOV-Specific Transcription and Replication Competent Virus-Like Particle Assay. Plasmids encoding the seven EBOV proteins, a T7 DNA-dependent RNA polymerase, and an EBOV-specific minigenome (MG) are transfected into HEK-293 cells. The viral proteins and the T7 polymerase are transcribed and translated by the cellular machinery (not depicted). I) The cDNA of the MG is transcribed into a negative-sense RNA minigenome by a T7 polymerase. II) The MG is encapsidated by NP and associating viral proteins. III) Secondary transcription of the viral MG into mRNA by the viral proteins. IV) Translation into the reporter gene (Renilla luciferase). V) Replication of the viral MG by the viral proteins. VI) Assembly of trVLPs containing the MG. VII) Budding of trVLPs. VIII) Infection of naïve indicator cells with trVLPs. IX) Primary viral transcription using only the incorporated viral proteins. X) Translation into the reporter gene (Renilla luciferase). The activity of the Renilla luciferase is measured in relative light units in a luminometer. Reporter gene activity of the producer cells reflects the potential of the viral proteins to support secondary transcription and genome replication. Reporter gene activity of the indicator cells reflects genome replication in the producer cells, viral egress, viral entry, as well as primary transcription in the indicator cells. The figure is based on Hoenen et al. 2014[99].

1.8 Human Protein Kinases and Phosphatases

Reversible protein phosphorylation is a fundamental regulatory mechanism for almost every biological process. Phosphorylation can alter the activity of enzymes, create new recognition sites for binding partners, affect subcellular localization, and influence stability of proteins[122,203]. It is accomplished by the opposing actions of protein kinases and phosphatases. While kinases catalyze the transfer of the γ-phosphate group of ATP to Ser, Thr, or Tyr residues, phosphatases catalyze hydrolysis of the attached phosphate group[237]. In the context of viruses, post-translational dynamic phosphorylation of viral proteins expands the functional repertoire in the background of only a few viral proteins[123,136].

Protein kinases constitute one of the largest gene families in eukaryotes. More than 518 putative kinases have been identified (so-called kinome), making up ~2 % of the human genome[151]. It is estimated that up to 30 % of all eukaryotic proteins can be phosphorylated on at least one site[75]. Kinases can be divided into Ser / Thr kinases (~400) and Tyr kinases (~90), but a few dual-specificity kinases (~40) have been identified as well[7,151]. Proteomic experiments revealed that phosphoserine (pSer) accounts for ~90 % of the phosphorylated amino acids[185]. All protein kinases share a common protein fold with an N- and C-terminal lobe that are connected by a short linker region. The catalytically active center of the kinase is located between the two lobes. Conserved lysine and aspartate residues of the active center are essential for binding of Mg^{2+}-ATP[2]. Different models exist, in which either the protein substrate or the co-substrate ATP bind the catalytic site first[2,259]. Kinases preferentially phosphorylate sites of intrinsically disordered regions because these regions can mold into the active site of the kinase[110]. Very importantly, each kinase specifically phosphorylates only a subset of proteins, in the background of more than 700 000 potential cellular phosphorylation sites[244]. The exquisite substrate specificity is achieved by multiple mechanisms. This includes the structural characteristics of the catalytic kinase site, which interacts with the amino acids surrounding the phosphorylation site of the substrate, distal interactions between kinase and substrate, as well as the formation of multi-protein complexes with scaffolding proteins. Specificity is further accomplished through the subcellular localization of kinase / substrate and system level effects, e.g. the competition between two phosphorylation sites[244].

Protein phosphatases are classified into the three major groups Ser / Thr phosphatases, Tyr phosphatases, and Asp-based protein phosphatases. Ser / Thr phosphatases can be subclassified into the large phosphoprotein phosphatase (PPP) family, which comprises PP1, PP2A, PP2B, PP4, PP5, PP6, and PP7, and the protein

phosphatase family dependent on Mg^{2+} or Mn^{2+} (PPM), which comprises PP2C and pyruvate dehydrogenase phosphatase[220].

Interestingly, only ~40 Ser / Thr phosphatases are encoded by the human genome, in contrast to ~400 Ser / Thr kinases[167]. This discrepancy raises important questions about the regulation and specificity of protein phosphatases. Specificity of many phosphatases seems to be achieved by the combinatorial association of the catalytic phosphatase subunit with various interacting proteins, which target the phosphatase to specific substrates and locations[220]. Contrary to kinases, phosphatase activity and specificity is only modestly dependent on the amino acids adjacent to the phosphorylation site[60].

Protein phosphatase 1 (PP1) is expressed in all eukaryotic cells and is encoded by three different genes (PP1α, PP1β / δ, PP1γ). PP1 can be detected in the cytosol, but is enriched in the nucleus[167]. The holoenzyme consists of a catalytic subunit and one of over 100 regulatory subunits. Regulatory subunits or substrates contain the degenerate consensus sequence [H/K/R]-[A/C/H/K/M/N/Q/R/S/T/V]-[V]-[C/H/K/N/Q/R/S/T]-[F/W], which allows binding to the catalytic subunit[159].

Protein phosphatase 2A (PP2A) is one of the most abundantly available protein in eukaryotic cells. PP2A is a heterotrimeric enzyme: the PP2A core enzyme, consisting of a catalytic subunit (C-subunit) and a scaffolding subunit (A-subunit), interacts with various regulatory subunits (B-subunit). The C subunit and the A subunit exist in two isoforms (α and β). The B-subunit comprises four gene families known as B (also known as B55), B' (also known as B56), B'', and B'''. Each regulatory B-subunit exists in several isoforms that are encoded by different genes. Some isoforms primarily localize to the cytoplasm (such as B56α, B56β, and B56ε), while others are enriched in the nucleus (such as B56γ and B56δ). It is proposed that the regulatory subunits play an essential role for substrate recognition, substrate specificity, subcellular localization, and targeting of the catalytic subunit to its substrates. In 2016, a conserved degenerate [LxxIxE] short linear motif (SLIM) was identified as the binding site of regulatory B56 subunits[96].

Besides being inhibited by endogenous proteins, the catalytic subunits of both PP1 and PP2A are reversibly inhibited by okadaic acid (OA). OA is a tumor-inducing toxin produced by marine dinoflagellates[233].

PP2C is encoded by at least 18 distinct genes and was described in at least 22 isoforms[134,167]. Contrary to PP1 and PP2A, PP2C does not associate with regulatory subunits, and it is not clear how substrate specificity of PP2C is achieved. Many PP2C isoforms can be detected almost exclusively in the nucleus, such as PP2Cα, PP2Cγ, and PP2Cε[51,129,263]. PP2C is not inhibited by OA [reviewed by Shi et al. 2009[220] and Moorhead et al. 2007[167]].

1.9 Aim of the Thesis

Transcription and replication of EBOV is regulated by proteins of the nucleocapsid complex, made up by the RNA genome and the viral proteins NP, VP30, VP35, VP24, and L. VP30 is an EBOV-specific transcription factor, which is not needed for replication of the viral genome. The activity of VP30 as a transcription factor is regulated by phosphorylation of six N-terminal serine residues of the protein (S29-S31 and S42 / S44 / S46). Dephosphorylated VP30 supports the synthesis of viral messenger RNA in a minigenome system, whereas phosphorylated VP30 cannot activate viral transcription. Replication of the viral genome is not dependent on the availability or absence of VP30, although replication is positively enhanced by VP30 phosphorylation or in absence of VP30.

In model systems, phosphorylation of serine residue 29 plays an important role for the initial steps of primary transcription during the early stages of the viral life cycle. A recombinant EBOV with serine 29 as the only phosphoacceptor site could be rescued, showing similar growth characteristics as the wild type virus. In contrast, the generation of a recombinant virus without phosphoacceptor sites within the N-terminal region of VP30 was not possible.

The exact regulation between viral transcription and replication is still unclear. Phosphorylation of VP30 seems to play a role, but it is still uncertain whether replication and transcription happen at different subcellular locations. Experiments conducted so far suggest that replication of the full length genome takes place in NP-induced inclusion bodies, whereas the location for viral transcription is unknown. With the help of additional VP30 phosphorylation mutants we aim to analyze transcriptional regulation in more detail.

Besides the influence of phosphorylation on transcription and replication, VP30 phosphorylation also regulates the interaction with other viral proteins such as the nucleoprotein NP. Evidence suggests that phosphorylated VP30 interacts stronger with NP and is thereby recruited into NP-induced inclusion bodies. The following studies examine VP30 phosphorylation with the help of a phosphospecific peptide antibody directed against phosphorylated serine 29. In immunofluorescence studies, the exact localization of phosphorylated VP30 will be determined. For this, experiments with recombinantly expressed VP30 phosphorylation mutants in combination with the nucleoprotein NP will be conducted. Likewise, phosphorylation of VP30 will be investigated during infection with the recombinant EBOV with serine 29 as the only phosphoacceptor site. Finally, several *in vitro* VP30 phosphorylation assays will be established.

2 Materials

2.1 Equipment

Eppendorf centrifuge 5415R	Eppendorf, Hamburg (GER)
Eppendorf Research Plus® Pipetten	Eppendorf, Hamburg (GER)
Heraeus Multifuge 3S-R	Thermo Fisher, Hudson (USA)
Horizontal Shaker	GFL, Burgwedel (GER)
Ice machine	Ziegra, Isernhagen (GER)
Incubator HERAcell 150 / 240	Thermo Fisher, Hudson (USA)
Light microscope Axiovert200M	Zeiss, Jena (GER)
Luminometer Centro LB 960	Berthold, Bad Wildbad (GER)
Magnetic stirrer	Heidolph, Kelheim (GER)
Mini-centrifuge GMC-060	neoLab, Heidelberg (GER)
Odyssey Infrared Imaging System	Li-Cor Biosciences, Lincoln (USA)
PCR Cycler Primus 25	Beckmann Coulter, Palo Alto (USA)
Pipetting aid Pipetboy	Integra Bioscience, Chur (CH)
Power Supply PowerPacTM HC	Biorad, Hercules (USA)
Power Supply Standard Power Pack P25	Biometra, Göttingen (GER)
Rotor Ultracentrifuge SW32, SW41, SW60	Beckmann Coulter, Palo Alto (USA)
Safety Cabinet BDK SK 1200	BDK, Sonnenbühl-Genkingen (GER)
SDS-polyacrylamide gel chamber Mini-Protean	Biorad, Hercules (USA)
SemiDry Blot chamber Trans-Blot SD	Biorad, Hercules (USA)
Sonifier Branson Ultrasonics S-450	Emerson, St. Louis (USA)
Spectrophotometer NanoDrop Lite	Thermo Fisher, Waltham (USA)
Thermomixer compact	Eppendorf, Hamburg (GER)
Tube Rotator	Heidolph, Schwabach (GER)
Ultracentrifuge Optima™ L-100K / -80XP	Beckmann Coulter, Palo Alto (USA)
UV-Light table 302 nm	Bachofer, Reutlingen (GER)
Vacuumpump Mini-Vac E1	Axonlab, Reichenbach (GER)
Vortex	neoLab, Heidelberg (GER)
Water bath MT	Lauda, Lauda-Königshofen (GER)
Weight scale excellence	Sartorius, Göttingen (GER)

2.2 Consumables

2 ml cryotubes	Corning ®, Acton (USA)
25 cm², 75 cm², 175 cm² cell culture flasks	Greiner bio-one, Frickenhausen (GER)
6-, 24-, 96-well cell culture dishes	Greiner bio-one, Frickenhausen (GER)
96-well plates LumiNunc™	Nunc, Roskilde (DK)
Blotting paper GB 002 (3 mm)	Whatman, Maidstone (UK)
Cell scraper	Sarstedt, Nürnbrecht (GER)
Centrifuge tubes, Ultra-Clear™ for SW41, SW60, SW32, TLA55	Beckmann, Palo Alto (USA)
Coverslips, Ø 12 mm	Menzel, Braunschweig (GER)
Nitrocellulose membranes Protran	Whatman, Maidstone (UK)
Object slide 76 x 22 mm	Menzel, Braunschweig (GER)
Parafilm	Pechiney Plastic, Menasha (USA)
PCR-tubes, 0.2 ml	Biozym, Hess. Oldendorf (GER)
Petri dishes	Sarstedt, Nürnbrecht (GER)
Pipette tips 0.1-1 µl, 10-100 µl, 100-1000 µl TipOne (with and without filter)	Starlab, Ahrensburg (GER)
Pipettes 1, 2, 5, 10, 25 ml Cellstar	Greiner bio-one, Frickenhausen (GER)
Polypropylene reaction tubes 15 / 50 ml	Greiner bio-one, Frickenhausen (GER)
Reaction tube 1.5 ml	Sarstedt, Nürnbrecht (GER)
Reaction tube 2 ml	Eppendorf, Hamburg (GER)
Reaction tubes (screw top)	Sarstedt, Nürnbrecht (GER)

2.3 Kits

Beetle-Juice Kit	PJK GMBH, Kleinblittersdorf (GER)
E.Z.N.A.® FastFilter Plasmid DNA Maxi Kit	OMEGA bio-tek, Norcross (USA)
E.Z.N.A. ® Plasmid DNA Mini I Kit	OMEGA bio-tek, Norcross (USA)
Mix & Go E. coli Transformation Kit and Buffer Set	Zymo Research, Orange (USA)
Pierce™ Silver Stain Kit	Thermo Fisher, Waltham (USA)
QuikChange Multi Site-Directed Mutagenesis Kit	Agilent Technologies, Waldbronn (GER)

QuikChange Site-Directed Mutagenesis Kit	Agilent Technologies, Waldbronn (GER)
Renilla-Juice Kit	PJK GMBH, Kleinblittersdorf (GER)

2.4 Chemicals

1,4 Diazabicyclo-[2.2.2]-octan (DABCO)	Sigma-Aldrich, München (GER)
4',6-Diamidino-2-phenylindol (DAPI)	Sigma-Aldrich, München (GER)
Acetic acid	Merck, Darmstadt (GER)
Acetone	Merck, Darmstadt (GER)
Agarose *PeqGold* universal	Peqlab, Erlangen (GER)
Alcian blue	Sigma-Aldrich, München (GER)
Ammonium persulfate (APS)	Biorad, Hercules (USA)
Ampicillin	Serva, Heidelberg (GER)
Bacto Agar	Becto, Dickinson & Company (USA)
β-Mercaptoethanol	Sigma-Aldrich, München (GER)
Bovine serum albumin (BSA)	Sigma-Aldrich, München (GER)
Bromphenol blue (BPB)	Roth, Karlsruhe (GER)
Calcium chloride ($CaCl_2$ x 2 H_2O)	Merck, Darmstadt (GER)
Casein hydrolysate	Merck, Darmstadt (GER)
Cell extraction buffer (CEB)	Invitrogen, Karlsruhe (GER)

Cell extraction buffer is a denaturing buffer that contains phosphatase (NaF) and kinase inhibitors (EDTA). No additional protease inhibitors were added to cells lysed with CEB.

Chloroform	Merck, Darmstadt (GER)
cOmplete™ Protease Inhibitor Cocktail Tablets, EDTA-free	Roche Diagnostics, Indianapolis (USA)

cOmplete™ (EDTA-free), is a non-denaturing protease inhibitor cocktail and was added to every lysis buffer according to the manufacturer. For the *in vitro* phosphorylation assays it is important to use the EDTA-free variant.

Coomassie Brilliant Blue R250	Serva, Heidelberg (GER)
D(+)- Glucose	Merck, Darmstadt (GER)
Dimethyl sulfoxide (DMSO)	Merck, Darmstadt (GER)

Dithiothreitol (DTT)	Sigma-Aldrich, München (GER)

Dithiotreitol, a reducing agent, was dissolved in DMSO to a stock concentration of 100 mmol/l, stored at -20 °C, and used *in vitro* at a final concentration of 1 mmol/l. DTT reduces the generation of disulfide bonds in order to preserve enzymatic activity of kinases and phosphatases.

EDTA	Roth, Karlsruhe (GER)
EGTA	Sigma-Aldrich, München (GER)
Ethanol abs.	Sigma-Aldrich, München (GER)
Ethanol denatured	Fischar, Saarbrücken (GER)
Fluoprep	BioMérieux, Nürtingen (GER)
Formvar	Sigma-Aldrich, München (GER)
Glutamine 200 mmol/l solution	Invitrogen, Karlsruhe (GER)
Glycerol	Roth, Karlsruhe (GER)
Glycine	Roth, Karlsruhe (GER)
Hydrochloric acid (HCl)	Merck, Darmstadt (GER)
Isopropanol	Sigma-Aldrich, München (GER)
Magnesium chloride ($MgCl_2$ x $6H_2O$)	Merck, Darmstadt (GER)
Magnesium sulfate ($MgSO_4$ x $7H_2O$)	Merck, Darmstadt (GER)
Methanol	Sigma-Aldrich, München (GER)
Milk powder	Saliter, Obergünzburg (GER)
Monopotassium phosphate (KH_2PO_4)	Roth, Karlsruhe (GER)
N(onidet)P40	Merck, Darmstadt (GER)
Nitrogen (99.996 %)	Messer-Griesheim, Siegen (GER)
Nycodenz	Axis-Shield, Oslo (NOR)
Paraformaldehyde (PFA)	Roth, Karlsruhe (GER)
Penicillin / Streptomycin 5000 IU/ml	Invitrogen, Karlsruhe (GER)
Peptone	Merck, Darmstadt (GER)
Phenylmethylsulfonyl fluoride (PMSF)	Sigma-Aldrich, München (GER)

Phenylmethanesulfonyl fluoride, a proteinase K inhibitor, was dissolved in DMSO to a stock concentration of 200 mmol/l, stored at -20 °C, and used at a final concentration of 7.7 mmol/l.

Phosphotungstic acid	Serva, Heidelberg (GER)
Polyacrylamide Rotiphorese® Gel 30	Roth, Karlsruhe (GER)

Polyethylenglykol (PEG) 4000	Sigma-Aldrich, München (GER)
Potassium chloride (KCl)	Merck, Darmstadt (GER)
Sodium azide (NaN_3)	Merck, Darmstadt (GER)
Sodium chloride (NaCl)	Roth, Karlsruhe (GER)
Sodium dodecyl sulfate (SDS)	Merck, Darmstadt (GER)
Sodium hydrogen phosphate (Na_2HPO_4)	Merck, Darmstadt (GER)
Sodium hydroxide (NaOH)	Riedel-de-Haën, Seelze (GER)
Sucrose	Serva, Heidelberg (GER)
Tetramethylethylenediamine (TEMED)	Biorad, Hercules (USA)
TransIT®-LT1 Transfection Reagent	Mirus Bio, Madison (USA)
Tris(hydroxymethyl)aminomethane (Tris)	Acros Organics, Geel (B)
Triton™ X-100	Sigma-Aldrich, München (GER)
Tryptone	Merck, Darmstadt (GER)
Tween® 20	neoLab, Heidelberg (GER)
Yeast extract	Merck, Darmstadt (GER)

Phosphatase inhibitors

Okadaic acid (OA)	Sigma-Aldrich, München (GER) (translucent film, 10 µg) *or* Merck, Darmstadt (GER) (# 495604)

OA is a reversible, membrane-permeable protein phosphatase 1 / 2A inhibitor. OA was dissolved in Dimethyl sulfoxide (DMSO) to a stock concentration of 100 µmol/l, stored at -20 °C, and used within 2 weeks. In cell culture experiments, the final concentration ranged from 1-100 nmol/l. In all *in vitro* assays with OA, the final concentration was 1 µmol/l.

PhosSTOP™, EDTA-free	Roche Diagnostics, Mannheim (GER)

PhosSTOP™ is a non-denaturing, EDTA-free cocktail of phosphatase inhibitors and was used according to the manufacturer.

Kinase inhibitors

Heparin sodium salt	Sigma-Aldrich, München (GER) (# H3393-10 KU)

Heparin sodium salt, a polyanionic substance and casein kinase II inhibitor, was dissolved in dH_2O to a stock concentration of either 50 mg/ml or 5 mg/ml and stored at 4 °C.

N-ethylmaleimide (NEM)	Sigma-Aldrich, München (GER) (# E1271 – 1 G)

N-ethylmaleimide, a protein alkylating agent, was dissolved in ethanol to a stock concentration of 2 mol/l, stored at -20 °C, and used at a final concentration of 5 mmol/l in the lysis buffer. NEM inhibits kinases *in vitro*. When NEM was used *in vitro*, no DTT was added to the lysis buffer.

Staurosporine	Sigma-Aldrich, München (GER) (# S4400 - .1 MG)

Staurosporine, a multi-kinase inhibitor, was dissolved in DMSO to a stock concentration of 250 µmol/l and stored at -20 °C.

Tetrabromocinnamic acid (TBCA)	Merck, Darmstadt (GER) (# 218710 – 5 mg)

TBCA, a selective casein kinase II inhibitor (IC50 = 0.11 µmol/l), was dissolved in DMSO to a stock concentration of 10 mmol/l and stored at -80 °C.

2.5 Cells and Viruses

2.5.1 Prokaryotic Cells

E. coli XL1-Blue	Stratagene, Heidelberg (D)

Genotype: recA1 endA1 gyrA96 thi-1 hsdR17 supE44 relA1 lac [F´ proAB lacIq ZΔM15 Tn10 (Tetr)]

E. coli XL10-Gold	Agilent technologies, Ratingen (GER)

Genotype: TetrΔ (*mcrA*)*183* Δ(*mcrCB-hsdSMR-mrr*)*173 endA1 supE44 thi-1 recA1 gyrA96 relA1 lac* The *F' proAB *lacI*qZΔ*M15* Tn*10* (Tetr) Amy Camr]

2.5.2 Eukaryotic Cells

HEK-293 cells	Human embryonic kidney cells
HUH-7 cells	Human hepatoma cells

2.5.3 Viruses

recEBOV_wt	Institute of Virology, Marburg (GER)
recEBOV_S29	Institute of Virology, Marburg (GER)

2.6 Growth Media

2.6.1 Growth Media for Bacteria

LB medium	10 g	NaCl
	5 g	Yeast extract
	10 g	Tryptone
	ad 1 l dH_2O	
LB agar (1.5 %)	3.75 g	Bacto™ Agar
	ad 250 ml LB Medium	
NZY+ medium	10 g	Casein hydrolysate
	5 g	Yeast extract
	5 g	NaCl
	12.5 ml	1 mol/l $MgCl_2$
	12.5 ml	1 mol/l $MgSO_4$
	20 ml	20 % Glucose in dH_2O
	ad 1 l dH_2O	
SOB medium	20 g	Peptone
	5 g	Yeast extract
	0.58 g	NaCl
	0.19 g	KCl
	10 ml	1 mol/l $MgCl_2$
	10 ml	1 mol/l $MgSO_4$
	ad 1 l dH_2O	

2.6.2 Growth Media for Eukaryotic Cells

$DMEM_{10\,\%\,FCS+Q+P/S}$	500 ml DMEM
(= $DMEM_{+++}$)	50 ml FCS (fetal calf serum)
	5 ml L-Glutamine 200 mmol/l
	5 ml Penicillin / Streptomycin 5000 IU/ml
$DMEM_{5\,\%\,FCS+Q+P/S}$	500 ml DMEM
	25 ml FCS (fetal calf serum)
	5 ml L-Glutamine 200 mmol/l
	5 ml Penicillin / Streptomycin 5000 IU/ml

DMEM $_{+Q+P/S}$	500 ml DMEM 5 ml L-Glutamine 200 mmol/l 5 ml Penicillin / Streptomycin 5000 IU/ml
DMEM $_{+Q}$	500 ml DMEM 5 ml L-Glutamine 200 mmol/l
Dulbecco's modified Eagle's medium (DMEM)	Invitrogen, Karlsruhe (GER)
Fetal calf serum (FCS)	Invitrogen, Karlsruhe (GER)
Opti-MEM™	Invitrogen, Karlsruhe (GER)

2.7 Buffers and Solutions

2.7.1 Buffers

PBS_{def}, pH 7.5	2.7 mmol/l 1.5 mmol/l 8 mmol/l 137 mmol/l in dH_2O	KCl KH_2PO_4 Na_2HPO_4 NaCl
TBS, pH 7.5	50 mmol/l 150 mmol/l in dH_2O	Tris-HCl NaCl
TBS + EDTA, pH 7.5	50 mmol/l 150 mmol/l 2 mmol/l in dH_2O	Tris-HCl NaCl EDTA
TM buffer, pH 7.5	50 mmol/l 5 mmol/l in dH_2O	Tris-HCl $MgSO_4$
TM buffer + $CaCl_2$, pH 7.5	50 mmol/l 5 mmol/l 2 mmol/l in dH_2O	Tris-HCl $MgSO_4$ $CaCl_2$
TM buffer + EGTA, pH 7.5	50 mmol/l 5 mmol/l 5 mmol/l in dH_2O	Tris-HCl $MgSO_4$ EGTA

Co-IP buffer, pH 7.6 (supplemented with 1 % Triton™ X-100 and 1x cOmplete™ prior to use)	5 mmol/l 100 mmol/l 1 % 20 mmol/l in dH_2O	EDTA NaCl NP40 Tris-HCl
TE buffer, pH 7.6	20 mmol/l 1 mmol/l in dH_2O	Tris-HCl EDTA
CIP buffer, pH 7.9	50 mmol/l 10 mmol/l in dH_2O	Tris-HCl $MgCl_2$
TNE buffer, pH 7.4	10 mmol/l 150 mmol/l 1 mmol/l in dH_2O	Tris-HCl NaCl EDTA
Protein sample buffer (4x)	10 ml 200 mg 20 ml 10 ml 4 g ad 50 ml	Mercaptoethanol Bromphenolblue Glycerine 1 mol/l Tris-HCl, pH 6.8 SDS dH_2O
Blocking buffer for WB	5 % in TBS	BSA
Blocking buffer for IFA	2 % 5 % 0.05 % 0.2 % in TBS	BSA Glycerin NaN_3 Tween® 20
Dilution buffer for antibodies (IFA and WB)	1 % 0.1 % in TBS	BSA Tween® 20
Washing buffer for WB	0.1 % in TBS	Tween® 20
SDS-PAGE stacking gel buffer, pH 6.8	0.4 % 0.5 mol/l in dH_2O	SDS Tris-HCl

SDS-PAGE separation gel buffer, pH 8.8	0.4 % 1.5 mol/l in dH_2O	SDS Tris-HCl
Protein gel running buffer (10x)	144 g 10 g 30 g ad 1 l dH_2O	Glycine SDS Tris
Transfer buffer for WB	100 ml 144 mg 300 mg ad 1 l dH_2O	Ethanol Glycine Tris

2.7.2 Solutions

Ampicillin stock solution	100 mg ad 1 ml dH_2O	Ampicillin
Nycodenz 60 % (w / v)	600 g ad 1 l TNE buffer	Nycodenz
Coomassie staining solution	400 ml 100 ml 0.2 % ad 1 l dH_2O	Ethanol Acetic acid Coomassie Brilliant Blue R250
Destaining solution for Coomassie Brilliant Blue R250	400 ml 100 ml ad 1 l dH_2O	Ethanol Acetic acid

2.8 Proteins and Peptides

2.8.1 Enzymes

Calf intestinal alkaline phosphatase (CIP), 1 U/µl	Thermo Scientific, Waltham (USA)
T4 DNA ligase	NEB, Ipswich (USA)
T4 Polynucleotide Kinase (PNK)	Thermo Scientific, Waltham (USA)
DPN I (1 Weiss Unit/µl)	NEB, Ipswich (USA)
Proteinase K (0.9 U/µl)	Fermentas, St.Leon-Rot (GER)
Trypsin-EDTA (0.5 %)	Invitrogen, Karlsruhe (GER)

2.8.2 Peptides

Name	Sequence	Molecular Weight	Company
FLAG-Peptide	DYKDDDDK-amide	1013 g/mol	Sigma-Aldrich, München (GER)
p_S29-Peptide	HHVRAR-pS-AAREN-amide	1484 g/mol	Biogenes, Berlin (GER)
nonp_S29-Peptide	HHVRAR-S-AAREN-amide	1404 g/mol	Biogenes, Berlin (GER)

2.8.3 Primary Antibodies

			Dilution	
Name	**Species**	**Company**	**IFA**	**WB**
α VP30	Guinea pig (g.p.)	Institute of Virology, Marburg (GER)	1:150	1:100
α VP30	Rabbit (R1.61)	Institute of Virology, Marburg (GER)	1:50	1:100
α pS29	Rabbit (7994)	Biogenes, Berlin (GER)	1:50	1:100
α NP	Chicken	Institute of Virology, Marburg (GER)	1:750	1:1000
α GP / NP	Goat	Institute of Virology, Marburg (GER)	---	1:10 000
α ZEBOV	Goat 36.6	Institute of Virology, Marburg (GER)	---	1:2000
α FLAG M2	Mouse	Sigma-Aldrich, München (GER)	1:200	1:500
α FLAG	Rabbit	Sigma-Aldrich, München (GER)	1:200	1:500
α FLAG M2, biotinylated	Mouse	Sigma-Aldrich, München (GER)	---	1:500
α c-myc	Rabbit	Santa Cruz Biotech, Santa Cruz (USA)	---	1:500
α HA, biotinylated	Mouse	Sigma-Aldrich, München (GER)	---	1:1000
α tubulin	Mouse	Sigma-Aldrich, München (GER)	---	1:5000

2.8.4 Secondary Antibodies for IFA

Name		Species	Company	Dilution
α g.p.	*Alexa 488*	Goat	Invitrogen, Karlsruhe (GER)	1:600
α g.p.	*Alexa 594*	Goat	Invitrogen, Karlsruhe (GER)	1:600
α rabbit	*Alexa 488*	Goat	Invitrogen, Karlsruhe (GER)	1:600
α rabbit	*Alexa 594*	Goat	Invitrogen, Karlsruhe (GER)	1:600
α rabbit	*Rhodamin*	Goat	Dianova, Hamburg (GER)	1:100
α chicken	*Alexa 488*	Goat	Invitrogen, Karlsruhe (GER)	1:600
α mouse	*Alexa 488*	Goat	Invitrogen, Karlsruhe (GER)	1:600
α mouse	*Alexa 594*	Goat	Invitrogen, Karlsruhe (GER)	1:600
α mouse	*Rhodamin*	Goat	Dianova, Hamburg (GER)	1:100
DAPI (4',6-Diamidin-2-phenylindol)				1:10 000

2.8.5 Secondary Antibodies for WB

Name		Species	Company	Dilution
α g.p	780 nm	Goat	Li-Cor, Bad Homburg (GER)	1:5000
α rabbit	680 nm	Goat	Invitrogen, Karlsruhe (GER)	1:5000
α rabbit	780 nm	Goat	Li-Cor, Bad Homburg (GER)	1:5000
α chicken	680 nm	Donkey	Invitrogen, Karlsruhe (GER)	1:5000
α chicken	780 nm	Donkey	Li-Cor, Bad Homburg (GER)	1:5000
α goat	680 nm	Donkey	Invitrogen, Karlsruhe (GER)	1:5000
α goat	780 nm	Donkey	Li-Cor, Bad Homburg (GER)	1:5000
α mouse	680 nm	Goat	Invitrogen, Karlsruhe (GER)	1:5000
α mouse	780 nm	Goat	Li-Cor, Bad Homburg (GER)	1:5000
Streptavidin	680 nm	---	Invitrogen, Karlsruhe (GER)	1:5000

2.8.6 Affinity Gels

Name	Species	Company
α *FLAG* M2 affinity gel	Mouse	Sigma-Aldrich, München (GER)
Mouse IgG-Agarose	Mouse	Sigma-Aldrich, München (GER)

2.8.7 Protein Size Markers for WB Analysis

PageRuler™ Plus Prestained Protein Ladder, 10-250 kDa	Fermentas, St. Leon-Rot (GER)
PageRuler™ Prestained Protein Ladder, 10-170 kDA	Fermentas, St. Leon-Rot (GER)

2.9 Nucleotides

dNTP mix, each 10 mmol/l: • 2' desoxyadenosine 5' triphosphate • 2' desoxyzytosine 5' triphosphate • 2' desoxyguanosine 5' triphosphate • 2' desoxythymidine 5' triphosphate	Thermo Scientific, Waltham (USA)
Adenosine 5' triphosphate (ATP) disodium salt hydrate	Sigma-Aldrich, München (GER) (# A2382-1 G)

Adenosine triphosphate disodium salt hydrate was dissolved in dH_2O to a stock concentration of 100 mmol/l and stored at -80 °C. The pH of the stock solution was adjusted to pH = 7.0, using 5 mmol/l and 1 mmol/l NaOH. Unless otherwise stated, the final concentration of ATP is 2 mmol/l in the *in vitro* assays.

2.10 DNA-Oligonucleotides

Primer for sequencing of pCAGGS

#	Name	Sequence (5'→3')
1233	pCAGGS *for*	CCTTCTTCTTTTTCCTACAG

Primers for cloning of VP30 mutants

#	**Name:** EBOV-	**Sequence (5'→3')**
3529	VP30_AA_A29D *for*	CATGTTCGAGCACGA**Gat**GC AGCCAGAGAGAATTATC
3613_a	VP30_AA_A29S_R26A *for*	CACGACCACCATGTT**gcA**GC ACGATCAGCAGCC
3614_a	VP30_AA_A29S_R28A *for*	CACCATGTTCGAGCA**gcA**TC AGCAGCCAGAGAG
3615_a	VP30_AA_A29S_R26A_R28A *for*	CACGACCACCATGTT**gcA**GC A**gcA**TCAGCAGCCAGAGAG

3628	VP30_E33A *for*	CGATCATCATCCAGA**GcG**AA TTATCGAGGTGAG
3629	VP30_Q47A *for*	TCAAGGAGCGCCTCA**gcA**GT GCGCGTTCCTACTG
3638	VP30_AA_A29S_A31S *for*	CGAGCACGATCAGCA***tCC***AG AGAGAATTATCGA GG
3639	VP30_AA_A29S_A31S_R26A *for*	GCAGCACGATCAGCA***tCC***AG AGAGAATTATCGAGG
3640	VP30_AA_A29S_A31S_R28A *for*	CGAGCAGCATCAGCA***tCC***AG AGAGAATTATCGAGG
3641	VP30_AA_A29S_A31S_R26A_R28A *for*	GCAGCAGCATCAGCA***tCC***AG AGAGAATTATCGAGG
3632	VP30_S29A *for*	CATGTTCGAGCACGA**gCA**TC ATCCAGAGAGAATTATC
3633	VP30_S30A *for*	GTTCGAGCACGATCA**tCA**TC CAGAGAGAATTATC
3634	VP30_S31A *for*	CGAGCACGATCATCA**tCC**AG AGAGAATTATCGAG
3635	VP30_S42A *for*	GGTGAGTACCGTCAA***gCA***A GGAGCGCCTCACAAG
3636	VP30_S44A *for*	GTACCGTCAATCAAGG***gcC***G CCTCACAAGTGCGC
3637	VP30_S46A *for*	CAATCAAGGAGCGCC**gCA**C AAGTGCGCGTTCC
3531	VP30_R26A_R28A *for*	GACACGACCACCATGTT**gcA** GCA**gcA**TCATCATCCAGAGA GAATT
3657	VP30_AA_A30S_A44S *for*	GTTCGAGCACGAGCA**tCA**G CCAGAGAGAATTATCG
3658	VP30_AA_A44S_A46S *for*	CAAGCAAGGTCCGCC**tCA**CA AGTGCGCGTTCCTAC

Primers for cloning of a FLAG construct

#	Name	Sequence (5'→3')
3720_a	FLAG *for*	GACGATGACAAGTAAGAAG CCCCTTGAGCATCTGACTTC TGG
3721_a	FLAG *rev*	GTCCTTGTAGTCCATGATCT GCTAGCTAATTAAGAGCTC GCGGC

Primers were synthesized by Invitrogen, Karlsruhe (GER).

for: forward primer (complementary to the sense DNA strand)

rev: reverse primer (complementary to the antisense DNA strand)

small: changed base(s)

bold: mutated amino acid

underlinded: insertion

#: internal primer number in the Institute of Virology, Marburg

2.11 Vectors and Plasmids

2.11.1 Vectors

pCAGGS MCS	Institute of Virology, Marburg (GER)

2.11.2 Plasmids Encoding Recombinant Proteins

Vector	Protein	Origin
pCAGGS	T7	Y. Kawaoka, Wisconsin (USA)
pANDY	3E-5E (Renilla luciferase minigenome)	Institute of Virology, Marburg (GER)
pGL4	Firefly luciferase	Institute of Virology, Marburg (GER)
pCAGGS	GP	Institute of Virology, Marburg (GER)
pCAGGS	NP	Institute of Virology, Marburg (GER)
pCAGGS	NP_{myc}	Institute of Virology, Marburg (GER)
pCAGGS	L	B. Moss, NIH, Bethesda (USA)
pCAGGS	VP24	Institute of Virology, Marburg (GER)
pCAGGS	VP35	Institute of Virology, Marburg (GER)
pCAGGS	$VP35_{HA}$	Institute of Virology, Marburg (GER)
pCAGGS	$VP35_f$	Institute of Virology, Marburg (GER)
pCAGGS	VP40	Institute of Virology, Marburg (GER)

pCAGGS	VP30 wt	Institute of Virology, Marburg (GER)
pCAGGS	$VP30_f$ wt	Institute of Virology, Marburg (GER)
pCAGGS	$VP30_f$ AA	Institute of Virology, Marburg (GER)
pCAGGS	$VP30_f$ DD	Institute of Virology, Marburg (GER)
pCAGGS	$VP30_f$ SA	Institute of Virology, Marburg (GER)
pCAGGS	$VP30_f$ AS	Institute of Virology, Marburg (GER)
pCAGGS	$VP30_f$ DA	Institute of Virology, Marburg (GER)
pCAGGS	$VP30_f$ AD	Institute of Virology, Marburg (GER)
pCAGGS	$VP30_f$ AA A29S	Institute of Virology, Marburg (GER)
pCAGGS	$VP30_f$ AA A30S	Institute of Virology, Marburg (GER)
pCAGGS	$VP30_f$ AA A31S	Institute of Virology, Marburg (GER)
pCAGGS	$VP30_f$ AA A42S	Institute of Virology, Marburg (GER)
pCAGGS	$VP30_f$ AA A44S	Institute of Virology, Marburg (GER)
pCAGGS	$VP30_f$ AA A46S	Institute of Virology, Marburg (GER)
pCAGGS	$VP30_f$ R26A	Institute of Virology, Marburg (GER)
pCAGGS	$VP30_f$ R28A	Institute of Virology, Marburg (GER)
pCAGGS	$VP30_f$ R32A	Institute of Virology, Marburg (GER)
pCAGGS	$VP30_f$ R40A	Institute of Virology, Marburg (GER)
pCAGGS	$VP30_f$ R26A R28A R40A	Institute of Virology, Marburg (GER)
pCAGGS	$VP30_f$ R40A R43A	Institute of Virology, Marburg (GER)

Cloned Plasmid (pCAGGS)	**Template (pCAGGS)**	**Primer #**	**Method**
$VP30_f$ AA A29D	$VP30_f$ AA	3529	SDM
$VP30_f$ AA A29S R26A	$VP30_f$ AA A29S	3613_a	SDM
$VP30_f$ AA A29S R28A	$VP30_f$ AA A29S	3614_a	SDM
$VP30_f$ AA A29S R26A R28A	$VP30_f$ AA A29S	3615_a	SDM
$VP30_f$ E33A	$VP30_f$ wt	3628	SDM
$VP30_f$ Q47A	$VP30_f$ wt	3629	SDM
$VP30_f$ S29A	$VP30_f$ wt	3632	SDM
$VP30_f$ S30A	$VP30_f$ wt	3633	SDM
$VP30_f$ S31A	$VP30_f$ wt	3634	SDM
$VP30_f$ S42A	$VP30_f$ wt	3635	SDM
$VP30_f$ S44A	$VP30_f$ wt	3636	SDM
$VP30_f$ S46A	$VP30_f$ wt	3637	SDM

$VP30_f$ AA A29S A31S	$VP30_f$ AA A29S	3638	SDM
$VP30_f$ AA A29S A31S R26A	$VP30_f$ AA A29S R26A	3639	SDM
$VP30_f$ AA A29S A31S R28A	$VP30_f$ AA A29S R28A	3640	SDM
$VP30_f$ AA A29S A31S R26A R28A	$VP30_f$ AA A29S R26A R28A	3641	SDM
$VP30_f$ R26A R28A	$VP30_f$ wt	3531	SDM
$VP30_f$ AA A44S A46S	$VP30_f$ AA A44S	3658	SDM
$VP30_f$ S29A S31A S42A	$VP30_f$ AA A44S	3657 + 3658	SDM
FLAG	pCAGGS MCS	3720_a + 3721_a	Insertion

2.12 Software

BLAST (Basic local alignment search tool, NCBI) www.ncbi.nlm.nih.gov/BLAST/	Sequence alignment
Chromas	Sequence analysis
Citavi 5	Reference management
Clonemanager 9	Cloning strategies
ClustalX2	Protein sequence alignment
Li-Cor Odyssey Image Studio 2.1	Western blot analysis and quantification
Microsoft Excel 2013	Statistical analysis
Microsoft Powerpoint 2016	Graphics and figures
Microsoft Word 2016	Thesis writing
OligoCalc	Calculation of primer melting temperature
Photoshop CS 5 / 6	Image editing

3 Methods

3.1 Molecular Biological Methods

3.1.1 Site-Directed Mutagenesis

Site-directed mutagenesis introduces site-specific mutations into double-stranded plasmid DNA *in vitro*. Mutagenesis was achieved with the QuikChange Multi Site-Directed Mutagenesis Kit (Agilent). The individually designed mutagenic oligonucleotide forward primer included one or several central mismatch base(s) with 12-20 complementary nucleotides on each adjacent site. The melting temperature T_m of the primer was calculated with the following formula, with a target melting temperature of ≥75 °C:

$$T_m = 81.5 + 0.41 \times (\%GC) - \frac{675}{N} - \%\, mismatch$$

% GC: GC-content of primer in a whole number

% mismatch: mismatch between template and primer in percent, as a whole number

N: primer length in bases

In the first step, the mutant strand was synthesized and linearly amplified by the thermostable, high fidelity *Pfu* polymerase during multiple rounds of denaturing, annealing, and elongation.

Reagents

10× QuikChange Multi reaction buffer	2.5 µl
dsDNA template	100 ng
mutagenic forward primer	100 ng each
dNTP mix	1 µl
QuikChange Multi enzyme blend	1 µl
dH_2O	X µl to final volume of 25 µl

Thermal Cycling Conditions

Cycles	Temperature	Time
1	95 °C	1 min
30	95 °C	1 min
	55 °C	1 min
	65 °C	2 min / kb of plasmid length
	8 °C	∞

Following the generation and amplification of the mutant strand, 1 µl DPN I enzyme was added. DPN I (from diplococcus pneumoniae) is a methylation dependent restriction enzyme that degrades the template DNA, which is methylated by E. coli bacteria. The mutant strand on the other hand, which is synthesized *in vitro*, is not methylated and therefore not degraded. The reaction mixture was incubated for 1 h at 37 °C. The DPN I-treated DNA was now ready for transformation into XL10-Gold ultracompetent cells (3.1.3).

3.1.2 DNA Insertion, Phosphorylation, and Ligation

Insertion of new bases into a double-stranded DNA plasmid was achieved by a site-directed mutagenesis procedure (QuikChange site-directed Mutagenesis Kit). The mutagenic primers included around 20 bases on the 3' end, which were complementary to the DNA template, whereas the non-complementary bases designated for insertion were added upstream on the 5' end of the primer. The insertion was split between the forward and reverse primer. Primers were designed in a non-overlapping fashion and in back-to-back orientation. In the first step, the mutant strands were synthesized and exponentially amplified during multiple rounds of denaturing, annealing, and elongation.

Reagents

10× reaction buffer	5 µl
dsDNA template	50 ng
oligonucleotide primer for	0.3 µl (100 µmol/l)
oligonucleotide primer rev	0.3 µl (100 µmol/l)
dNTP mix	1 µl
DMSO	2 µl
*Pfu*Turbo DNA polymerase (2.5 U/µl)	1 µl
dH_2O	X µl to final volume of 50 µl

Thermal Cycling Conditions

Cycles	Temperature	Time
1	95 °C	1 min
18	95 °C	45 sec
	55 °C	1 min
	65 °C	21 min
	8 °C	∞

Following the thermal cycling, 1 µl DPN I was added to the samples to digest the template DNA (1 h, 37 °C).

Phosphorylation and Ligation:

The *in vitro* synthesized DNA strands are linear and not phosphorylated at the 5'-OH ends. The 5'-OH ends were phosphorylated by a polynucleotide kinase (PNK). Alternatively, it would also be possible to order primers with a 5' phosphate group.

A T4 DNA ligase was added to create circular plasmids by joining of the new 5' phosphate group with the 3'-OH group. PEG was added for increased efficiency of the ligation reaction. The reaction was incubated for 1 h at room temperature.

Reagents

polymerase product (linear plasmid)	6 µl
polynucleotide kinase (PNK)	2 µl
T4 DNA ligase buffer	2 µl
T4 DNA ligase	2 µl
PEG 4000 Solution (50 %)	2 µl
dH_2O	6 µl

The circular plasmids were now ready for transformation into XL1-Blue competent cells.

3.1.3 Transformation of Plasmid DNA into Bacteria

Transformation introduces foreign DNA into bacteria, a process during which competent bacterial cells take up and replicate DNA.

For the purpose of amplification, plasmids were transformed into XL1-Blue competent E. coli. The XL1-Blue cells were prepared according to the *Mix & Go E. coli* Transformation Kit and Buffer Set. Aliquots were stored at -80 °C. For transformation, 100 µl XL1-Blue competent E. coli were thawed on ice, mixed with 10 ng of the respective plasmid, and incubated for 20 min on ice.

Plasmids synthesized with the QuikChange Multi Site-Directed Mutagenesis Kit (Agilent) were transformed into XL10-Gold ultracompetent cells. For this, 45 µl XL10-Gold cells were thawed on ice and supplemented with 2 µl β-mercaptoethanol. Following 10 min of incubation, 1.5 µl of the DPN-I digested DNA was added and the mixture was incubated for 30 min on ice. Next, the tubes were heat-pulsed in a 42 °C water bath for 30 sec. Prior to plating, the bacteria were incubated in 500 µl NZY^+ medium for 1 h at 37 °C, 220 rpm.

3.1.4 Growth and Selection of Recombinant Bacteria

For selection of successfully transformed bacteria, plasmids contained an antibiotic resistance gene. Following transformation, 100 µl of the bacteria were plated on LB agar plates, which contained 100 µg/ml Ampicillin. The plates were incubated for 16 h at 37 °C. Since all recombinant plasmids carried the Ampicillin resistance gene, only successfully transformed bacteria could grow colonies.

3.1.5 Isolation of Plasmids from Bacteria

Following transformation of plasmids into competent bacteria and plating of the bacteria on LB-Ampicillin agar plates, single colonies were picked to inoculate either 3 ml (for "miniprep") or 100 ml (for "maxiprep") LB medium. The LB medium contained 100 µl of an Ampicillin stock solution. This only allowed the growth of successfully transformed bacteria. The inoculated medium was incubated for 16 h at 37 °C and 300 rpm.

The plasmid DNA was isolated from the bacteria using the centrifugation protocol of the E.Z.N.A.® Plasmid DNA Mini I Kit (for "miniprep") or the vacuum protocol of the E.Z.N.A.® FastFilter Plasmid DNA Maxi Kit (for "maxiprep").

The DNA was eluted in 50 µl (for "miniprep") or 1.2 ml dH_2O (for "maxiprep").

3.1.6 Nucleid Acid Quantification

DNA concentration of plasmids was assessed by light absorbance at a wavelength of 260 nm in a Nanodrop spectrophotometer. According to the Beer-Lambert law, light absorbance is directly proportional to the concentration of a substance:

$$A = \varepsilon \times \mathrm{B} \times \mathrm{C}$$

or

$$C = \frac{A}{\varepsilon \times \mathrm{B}}$$

where A is light absorbance, ε the wavelength-dependent molar extinction coefficient, B is the path length, and C is the concentration of e.g. DNA. At a wavelength of 260 nm, the molar extinction coefficient of double-stranded DNA is $\frac{1\,ml}{50\,\mu g \times cm}$.

The quotient of absorbance at 260 nm and 280 nm assesses for contamination by proteins, RNA, and phenol. Ratios around 1.8 were considered as "pure" for DNA.

3.1.7 DNA Sequencing

The recombinant DNA plasmids were sequenced by the Sanger method in the SEQLAB Laboratories (Göttingen). Samples were prepared by mixing 1200 ng of the respective plasmid, 30 pmol sequencing primer, and X µl dH_2O to a final volume of 15

3.2 Cell Biological and Virological Methods

3.2.1 Cultivation of HUH-7 and HEK-293 Cells

HEK-293 (human embryonic kidney) and HUH-7 (human hepatoma) cells were grown in 75 cm^2 tissue culture flask at 37 °C and 5 % CO_2. Dulbecco's modified Eagle's medium (DMEM), supplemented with 10 % fetal calf serum (FCS), 5 mmol/l glutamine (Q), and penicillin / streptomycin (P/S) (= $DMEM_{+++}$) was the standard growth medium. Cells were

passaged every 3 to 4 days upon reaching a confluency >80 %. For this, the growth medium was removed and cells were washed twice with pre-warmed PBS_{def}. For detachment of cells from the flask, 2 ml 0.05 % Trypsin / EDTA was added. Cells were incubated for 2-5 min at 37 °C. The reaction was stopped by addition of 8 ml $DMEM_{+++}$. Cells were carefully resuspended and aliquoted into new tissue culture flasks or plates in the desired dilution.

3.2.2 Transient DNA Transfection

Plasmid DNA was transfected into mammalian cells with the TransIT®-LT1 reagent. This reagent contains histones and cationic lipids that mask the negative charge of the DNA. The TransIT®-LT1:DNA-complexes are taken up by cells through endocytosis. The plasmids enter the nucleus, but are not integrated into the cell genome.

Cells were passaged one day prior to transfection to reach a confluency of 60-80 % at the time point of transfection. The TransIT®-LT1:DNA-complexes were prepared as recommended by the manufacturer. For 1 µg DNA, 3 µl transfection reagent was added. Both the DNA and the transfection reagent were preincubated separately with Opti-MEM™ for 5 min at room temperature, followed by combining the DNA / Opti-MEM™ and the TransIT® / Opti-MEM™. The mixture was incubated for 20 min at room temperature. The volume was adjusted according to the growth area of cells that were to be transfected. Around 200 µl of the final mixture was added dropwise onto the cells of one well (6-well plate). In general, the following DNA amounts were transfected:

Assay	**DNA amount per well**
Immunofluorescence analysis	200 ng / plasmid (12-well plate)
Protein expression for western blot analysis, immunoprecipitation, *in vitro* assays	500 ng / plasmid (6-well plate)
trVLP assay	2.5 µg DNA, including 100 ng VP30 (6-well plate)
Minigenome assay	780 ng DNA, including 40 ng VP30 (12-well plate)

The empty vector pCAGGS_MCS was added to adjust the amout of transfected DNA. During the formation of the transfection complexes, cells were washed with $DMEM_{+Q}$. $DMEM_{+Q}$ also was the initial growth medium. If cells were to grow for longer than one day post transfection, the medium was changed to $DMEM_{+++}$ 16-24 h p.t.

3.2.3 Cell Lysis

Depending on the assay, cells were lysed with different buffers and methods (Table 2). The type of lysis buffer is essential for either preservation of enzymatic activity, e.g. the activity of kinases or phosphatases, or likewise, inactivation of the same enzymes.

Buffer	Detergent	Properties and Use
TM	0.5 % Triton™ X-100	Non-denaturing. Contains Mg^{2+}-. *In vitro* phosphorylation assays (test tube, on-blot phosphorylation)
TM	0.1 % Triton™ X-100	Non-denaturing. Contains Mg^{2+}-. *In vitro* trVLP / recEBOV phosphorylation assay
TBS	0.2 % Tween® 20	Non-denaturing. Lysation of HUH-7 cells for *in situ* phosphorylation
TBS	0.5 % Triton™ X-100	Non-denaturing. *In vitro* phosphorylation assays
Co-IP buffer	1 % NP-40 1 % Triton™ X-100	Non-denaturing. Immunoprecipitation assays
CEB (Invitrogen)	1 % Triton™ X-100 0.1 % SDS 0.5 % deoxycholate	Denaturing. Contains phosphatase and kinase inhitibors. Lysis buffer for western blot analysis.
Sample buffer 4x	8 % SDS	Denaturing. Added to every sample prior to SDS-PAGE to a final concentration of 1x (2 % SDS)

Table 2: Lysis Buffers.

Non-ionic detergents, such as Triton™ X-100, Tween® 20, and NP-40, are considered relatively mild detergents with non-denaturing properties, as they preserve the activity of most enzymes and do not disrupt protein-protein interactions. These detergents allow the *in vitro* study of kinases and phosphatases. Since these detergents also preserve the activity of cellular proteases, the protease inhibitor cocktail cOmplete™ (Roche) was always added to non-denaturing lysis buffers according to the manufacturer. In some experiments, cells were additionally disrupted with sonication for 15-30 sec twice to physically disintegrate cellular membranes. DTT, OA, PhosSTOP™, EDTA, EGTA, and NEM were added to the lysis buffers as indicated in the experiments.

In contrast, ionic agents, such as sodium dodecyl sulfate (SDS) and deoxycholate, are considered harsh detergents. They denature proteins and interrupt protein-protein interactions. Therefore, no protease inhibitors were added. When preservation of enzymatic activity was not important, cells were lysed with the commercially available cell extraction buffer. The cells of one well of a 6-well plate were washed with PBS_{def} and gently scraped from the growth area into 1 ml PBS_{def}. 250 µl - 500 µl of the resuspended cells were pelleted by centrifugation at 3000 rpm for 2 min. The supernatant was discarded. Cells were lysed on ice for 20 min by addition of 80 µl CEB. Cellular debris was pelleted for 5 min at 13 000 rpm. 60 µl of the supernatant were mixed with 20 µl 4x sample buffer. Samples were heated for 5 min at 95 °C prior to SDS-PAGE and WB analysis

WB samples from the BSL-4 laboratory, supplemented with sample buffer, were heated for at least 10 min at 95 °C prior to transferring them out of the BSL-4 conditions. Before SDS-PAGE, samples were again heated for at least 10 min at 95 °C.

3.2.4 EBOV-Specific Minigenome Assay and Treatment with Okadaic Acid

A minigenome assay was performed to study the influence of VP30 phosphorylation on viral transcription and replication (chapter 1.7.1 and Figure 2).

HEK-293 cells and HUH-7 cells, seeded at a densitiy of $2x10^5$ cells per well of a 12-well plate, were transfected with plasmids encoding the viral proteins necessary for viral transcription and replication (NP, L, VP35, VP30 wt / mutants), a T7 RNA polymerase, and the EBOV-specific minigenome encoding a Renilla luciferase reporter gene under control of a T7 promotor. A Firefly luciferase was added for normalization of transfection efficiency.

The following DNA amounts were transfected per well of a 12-well plate:

Plasmid		**Promotor**	**Amount in ng**
1	pCAGGS NP	β-actin (chicken)	50
2	pCAGGS VP35	β-actin (chicken)	50
3	pCAGGS L	β-actin (chicken)	400
4	pCAGGS T7 polyermase	β-actin (chicken)	100
5	pGL4 Firefly luciferase	SV40	40
6	pANDY 3E-5E Renilla luciferase (minigenome)	T7	100
7	pCAGGS $VP30_f$_wt / mutant	β-actin (chicken)	40
			780 ng

A mastermix was prepared from plasmids 1-6. $VP30_f$_wt or mutants were added individually. $DMEM_{+Q}$ was used as the growth medium. 24 h p.t. the growth medium was removed. Cells were rinsed with PBS_{def}, scraped into 1 ml PBS_{def}, and pelleted for 2 min at 3000 rpm. The supernatant was discarded. Cells were resuspended in 100 µl 1x pjk Lysis Juice and lysed for 20 min at 1400 rpm and room temperature. Cellular debris was pelleted for 10 min at 13 000 rpm. Renilla and Firefly luciferase activity was measured in the supernatant in a luminometer (in relative light units, RLU). If necessary for a correct measurement, the supernatant was diluted with Lysis Juice up to 1:100. Firefly and Renilla substrates were prepared according to the manufacturer.

T7-driven transcription of the minigenome results in a negative-sense minigenome RNA, which is replicated and transcribed into a positive-sense RNA by the viral nucleocapsid proteins. The effect of VP30 serine or arginine mutations on viral transcriptional / replicational activity was tested either under control conditions (DMSO) or when treated with the phosphatase inhibitor OA. OA and DMSO were added to the medium 0 h p.t.

The activity of the Renilla luciferase represents the replicational and transcriptional potential of the viral proteins. The activity of the Firefly luciferase serves as an internal control reporter for normalization of transfection efficiency and cellular gene expression level. Results are shown as the quotient of the Renilla luciferase activity divided by the Firefly luciferase activity.

Expression of the VP30 constructs and NP was verified by western blotting. For this, 4 µl of 4x sample buffer was added to 12 µl of cell lysate. Samples were heated for 5 min at 95 °C.

3.2.5 EBOV-Specific Transcription and Replication Competent Virus-Like Particle Assay

An EBOV-specific transcription and replication competent virus-like particle (trVLP) assay was performed to study the influence of VP30 phosphorylation on primary viral transcriptional support activity (chapter 1.7.2 and Figure 3). HEK-293 cells, also called producer cells, were seeded at a density of $6x10^5$ cells per well of a 6-well plate. The following day, cells were transfected with plasmids encoding the seven viral proteins, the EBOV-specific minigenome encoding a Renilla luciferase reporter gene under control of a T7 promotor, a T7 RNA polymerase and a Firefly luciferase.

The following DNA amounts were transfected per well of a 6-well plate:

Plasmid		Promotor	Amount in ng
1	pCAGGS NP	β-actin (chicken)	125
2	pCAGGS GP	β-actin (chicken)	250
3	pCAGGS VP40	β-actin (chicken)	250
4	pCAGGS VP24	β-actin (chicken)	30
5	pCAGGS VP35	β-actin (chicken)	125
6	pCAGGS L	β-actin (chicken)	1000
7	pCAGGS T7 RNA polyermase	β-actin (chicken)	250
8	pGL4 Firefly luciferase	SV40	100
9	pANDY 3E-5E Renilla luciferase (minigenome)	T7	250
10	pCAGGS $VP30_f$_wt / mutants	β-actin (chicken)	100
			2480 ng

A mastermix was prepared from plasmids 1-9. $VP30_f$_wt or mutants were added individually. When two VP30 mutants were combined, 50 ng / VP30 mutant was transfected. $DMEM_{+Q}$ was used as the initial transfection medium and was changed to 3 ml $DMEM_{10\,\%\,FCS+Q+P/S}$ per well 16-24 h p.t.

T7-driven transcription of the minigenome results in a negative-sense minigenome RNA, which is replicated and transcribed into a positive-sense RNA by the viral nucleocapsid proteins. Due to the recombinant expression of the viral proteins in the producer cells, viral transcription here represents later stages of infection as in the minigenome system. This is in contrast to the limited amounts of incorporated viral proteins at the very beginning of an infection.

Purification and Analysis of trVLPs

Since all viral proteins are recombinantly expressed in the producer cells, the minigenome assembles together with the viral proteins and forms trVLPs that are released into the supernatant. The growth medium was collected 72 h p.t. and centrifuged for 10 min at 2500 rpm to pellet cellular debris. The supernatant was transferred into Ultra-Clear™ tubes for SW32 ultracentrifuge rotors and underlaid with 5 ml of 20 % sucrose solution in TNE buffer. The tubes were tared with PBS_{def} and centrifuged for 2 h at 28 000 rpm and 4 °C. Following ultracentrifugation, the supernatant was discarded and the trVLP-containing pellet was resuspended in 90 µl PBS_{def}.

30 µl of the resuspended trVLPs were analyzed for the specific incorporation of viral proteins. For this, a proteinase K digestion assay was performed. Proteinase K is a

broad-spectrum serine protease that degrades a broad range of proteins, but cannot digest proteins inside the trVLPs as they are protected by a lipid envelope. When a lysing agent such as Triton™ X-100 is added, proteins inside the trVLPs should be digested by the proteinase as well.

10 µl trVLPs + 2 µl PBS_{def}
10 µl trVLPs + 2 µl proteinase K (diluted 1:20 in PBS_{def})
10 µl trVLPs + 2 µl proteinase K (diluted 1:20 in PBS_{def} + 1 % Triton™ X-100)

The samples were incubated for 40 min at 37 °C. Next, 1 µl of 100 mmol/l PMSF was added. Samples were incubated for 5 min at room temperature for inactivation of proteinase K. Prior to SDS-PAGE and subsequent WB analysis, 4 µl of 4x sample buffer was added. Samples were heated at 95 °C for 5 min.

Measurement of Viral Transcriptional Activity in Producer Cells

After the growth medium was removed for purification of the trVLPs (72 h p.t.), producer cells were rinsed with PBS_{def}, scraped into 1 ml PBS_{def}, and pelleted for 2 min at 3000 rpm. The supernatant was discarded. Cells were resuspended in 200 µl 1x pjk Lysis Juice and lysed for 20 min at 1400 rpm and room temperature. Cellular debris was pelleted for 10 min at 13 000 rpm. Firefly and Renilla luciferase activity was measured in the supernatant at a dilution of 1:100-1:200. The activity of the Renilla luciferase represents the replicational and transcriptional potential of the viral proteins. The activity of the Renilla luciferase is normalized to the internal control reporter (Firefly luciferase). Expression of the VP30 constructs and NP was verified by SDS-PAGE and WB. For this, 4 µl of 4x sample buffer was added to 12 µl of the producer cell lysate. Samples were heated for 5 min at 95 °C.

Infection of Indicator Cells with trVLPs and Measurement of the Primary Viral Transcriptional Activity

The remaining purified trVLPs were mixed with 250 µl $DMEM_{+Q}$ for infection of naïve HUH-7 cells, also called indicator cells. The HUH-7 cells were seeded in 12-well plates at a density of $2x10^5$ cells / well one day prior to infection. First, HUH-7 cells were washed with $DMEM_{+Q}$. The trVLPs were pipetted onto the cells and incubated for 2 h at 37 °C. Next, 2 ml $DMEM_{5\ \%\ FCS+Q+P/S}$ was added. Cells were incubated for 60 h at 37 °C. The growth medium was removed. Cells were rinsed with PBS_{def}, scraped into 1 ml PBS_{def}, and pelleted for 2 min at 3000 rpm. The supernatant was discarded. Cells were resuspended in 100 µl 1x pjk Lysis Juice and lysed for 20 min at 1400 rpm and room temperature. Cellular debris was pelleted for 10 min at 13 000 rpm. Renilla luciferase activity was measured in the supernatant.

The Renilla luciferase activity obtained from the indicator cells reflects the ability of the trVLPs to start primary transcription in newly infected cells, using only the incorporated viral nucleocapsid proteins. In the context of VP30 phosphorylation it was particularly interesting to find out whether the primary transcriptional activity differs among trVLPs containing the various VP30 mutants.

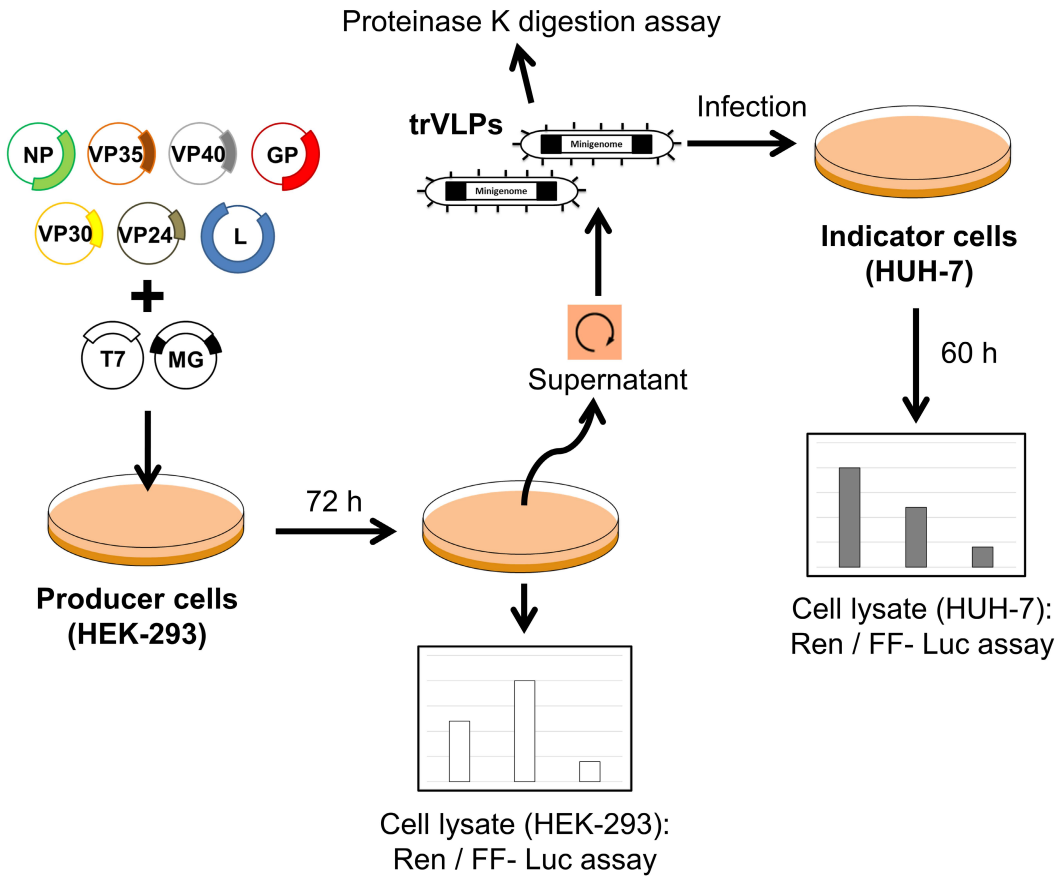

Figure 4: Overview of the EBOV-Specific trVLP Assay.

Producer cells are transfected with plasmids encoding the seven EBOV proteins, an EBOV-specific minigenome, a T7 RNA polymerase, and a Firefly luciferase. 72 h p.t. trVLPs are purified from the supernatant to infect naïve indicator cells. The reporter gene activity is measured in a luciferase assay.

Indirect Immunofluorescence Analysis of Indicator Cells

HUH-7 cells, seeded in 12-well plates on coverslips at a density of $1x10^5$ cells / well, were infected with trVLPs as described above. The trVLPs contained either $VP30_f$_wt or VP30 phosphorylation mutants. At 22 h p.i., cells were fixed with 4 % PFA in DMEM. The permeabilization of cells and blocking of unspecific signals were performed as described in 3.3.5. Cells were stained with anti-VP30 (from guinea pig) and anti-NP (from chicken) antibodies (3.3.5).

3.2.6 Discontinous Nycodenz Gradient Purification of trVLPs

trVLPs pelleted through a sucrose cushion can be further purified into spherical and filamentous particles with a discontinous Nycodenz step gradient purification method. The pelleted trVLPs were resuspended in 730 µl TNE buffer and carefully pipetted on top of the following gradient (Ultra-Clear™ tubes for SW60 ultracentrifuge rotors):

30 % Nycodenz in 1xTNE	730 µl
20 % Nycodenz in 1xTNE	490 µl
15 % Nycodenz in 1xTNE	490 µl
10 % Nycodenz in 1xTNE	490 µl
7.5 % Nycodenz in 1xTNE	490 µl
5 % Nycodenz in 1xTNE	490 µl
2.5 % Nycodenz in 1xTNE	490 µl
trVLPs	730 µl
	4400 µl

Tubes were centrifuged for 15 min at 15 000 rpm and 4 °C. Nine fractions were carefully collected (each 488.88 µl). Fractions 1-3, 4-6, and 7-9 were pooled and pipetted into Ultra-Clear™ tubes for SW41 ultracentrifuge rotors. The tubes were filled up with PBS_{def} and tared. trVLPs were pelleted by centrifugation for 1 h at 36 000 rpm. The supernatant was discarded, and trVLPs were resuspended for *in vitro* phosphorylation (3.4.3) or electron microscopy (3.2.7). Fractions 1-3 were to comprise vesicular trVLPs and contaminating exosomes / microvesicles, whereas fractions 4-6 and 6-9 were to comprise mainly filamentous trVLPs.

3.2.7 Preparation of Purified trVLPs for Negative Staining Electron Microscopy

Nycodenz gradient purified trVLPs were analyzed by Electron microscopy to detect contaminating vesicular particles, such as exosomes and microvesicles.

2 µl of the resuspended trVLPs, purified as described in 3.2.6, were combined with 8 µl of 4 % PFA in DMEM. Sample preparation and electron microscopy were performed by Dr. Larissa Kolesnikova. Briefly, Formvar coated 400-mesh nickel grids - with an additional carbon layer - were pretreated with 1 % alcian blue to improve adherence of virus-like particles. The grid was incubated with the sample, followed by negative staining with 2 % phosphotungstic acid. Images were taken with a JEM1400 transmission electron microscope.

3.2.8 Infection of HUH-7 Cells with recEBOV_wt and recEBOV_S29

The design and rescue of the recombinant viruses recEBOV_wt and recEBOV_S29 was outlined before[23]. One day prior to infection, HUH-7 cells were seeded into 12- or 6-well plates at a density of $5x10^4$ and $4x10^5$ cells / well, respectively. Infection of HUH-7 cells with recEBOV was carried out in $DMEM_{+Q+P/S}$ for 1 h at 37 °C. The supernatant was removed and $DMEM_{5\,\%\,FCS+Q+P/S}$ was added. OA and DMSO were added to the medium 1 h post infection. Cells were infected at a multiplicity of infection (MOI) of 3.
Experiments with recombinant Ebola viruses were performed at the BSL-4 facility of the Philipps-University Marburg by Dr. Nadine Biedenkopf.

3.3 Biochemical and Immunological Methods

3.3.1 Sodium Dodecyl Sulfate-Polyacrylamide Gel Electrophoresis

One-dimensional sodium dodecyl sulfate-polyacrylamide gel electrophoresis (SDS-PAGE) seperates proteins by their molecular weight. The individual net charge of a protein is masked by the negatively charged SDS in the sample buffer. In an applied electric field, the proteins move to the positively charged anode. The speed of migration mainly depends on the molecular size, with smaller proteins moving faster.
The SDS-polyacrylamide gel consists of a stacking gel on top of a seperation gel. The lower acrylamide concentration of the stacking gel allows the proteins to concentrate on the crossing to the separation gel.

	Stacking gel (5 %)	**Separation gel (12 %)**
H_2O	3.38 ml	3.3 ml
SDS-PAGE stacking gel buffer, pH 6.8	1.56 ml	---
SDS-PAGE separation gel buffer, pH 8.8	---	2.6 ml
30 % acrylamide mix (Rotiphorese® 30)	1 ml	4 ml
10 % APS	60 µl	100 µl
TEMED	3 µl	4 µl

Prior to gel electrophoresis, sample buffer was added to every cell lysate, and samples were heated at 95 °C for at least 5 min. Along with a protein size marker, samples were loaded into the wells of the stacking gel. Proteins were separated at 25 mA per gel, at maximum voltage, for approximately 45 min. The outer and inner chambers of the SDS-PAGE system were filled with 1x protein gel running buffer. SDS-PAGE was either

followed by staining of the proteins in the gel with Coomassie (3.3.2) or by the electrophoretic transfer of proteins onto nitrocellulose membranes (3.3.3).

3.3.2 Coomassie Staining of Protein Gels

For detection of proteins that associate with VP30, SDS-polyacrylamide gels from VP30-immunoprecipitates were stained with a Coomassie brilliant blue R250 dye.

Following gel electrophoresis, the SDS-polyacrylamide gel was washed in PBS_{def} twice. The gels were incubated in a Coomassie staining solution for at least 2 h, room temperature, on a horizontal shaker. Eventually, the gels were washed with water several times and incubated in the destainig-solution for 2-4 h until clear protein bands appeared. If necessary, the destaining solution was exchanged several times. Coomassie-stained SDS gels were scanned with the Li-Cor Odyssey imaging scanner at 680 nm wavelength.

3.3.3 Western Blotting and Staining of Nitrocellulose Membranes

Western blotting (WB) was performed for the identification of specific proteins in a heterogeneous mixture of different proteins. Following separation of the proteins by SDS-PAGE, they were transferred via an electric current from the SDS-polyacrylamide gel to a nitrocellulose membrane. The proteins were detected on the membrane by specific primary antibodies.

Using a semi-dry approach, the SDS-polyacrylamide gel, the nitrocellulose membrane (5 x 8 cm), and Whatman blotting papers (6.5 x 8.5 cm) were incubated in transfer buffer for 5 min. From the anode to the cathode, four Whatman blotting papers, the nitrocellulose membrane, the SDS-polyacrylamide gel and, again, four Whatman blotting papers were assembled. Air bubbles and excess transfer buffer were removed by rolling a glas pipette over the sandwich construction. Western blotting was performed at constant voltage (20 V) for 40 min.

Following the electrophoretic transfer of proteins, nitrocellulose membranes were blocked with 5 % BSA in TBS for 2 h on a horizontal shaker at room temperature to diminish unspecific binding of antibodies to the membrane. Subsequently, the blots were washed with WB washing buffer three times for 5 min. The protein of interest was detected by incubating the membrane with a primary antibody for 1 h at room temperature. Alternatively, the membrane was incubated with the primary antibody overnight at 4 °C. Membranes were washed three times for 15 min to remove unspecifically bound antibodies. To visualize primary antibodies, membranes were then incubated with IRDye labeled secondary antibodies for 1 h, followed by three additional washing steps. The IRDye labeled secondary antibodies were detected by the Li-Cor Odyssey infrared imaging system. All antibodies were diluted in an antibody dilution buffer. Note: BSA was used instead of milk powder and TBS buffer instead of PBS_{def}, as

this is a general recommendation when working with phosphospecific antibodies. Since the phosphospecific VP30 antibody is directed against a specific VP30 peptide, unspecific binding of the antibody to phosphoproteins such as casein seems very unlikely. Thus, milk powder and PBS_{def} might be used just as well.

3.3.4 Quantification of VP30 Serine 29 Phosphorylation in WB Analysis

To analyze the influence of other EBOV proteins on the phosphorylation status of VP30 serine 29, HEK-293 cells, seeded in 6-well plates at a density of $6x10^5$ cells / well, were transfected with different combinations of the following plasmids: 100 ng pCAGGS-$VP30_f$_AA_A29S ± 125 ng pCAGGS-NP, 125 ng pCAGGS-$VP35_{HA}$, 1000 ng pCAGGS-L, 30 ng pCAGGS-VP24, 250 ng pCAGGS-VP40, 250 ng pCAGGS-GP, 200 ng pANDY 3E-5E, and 200 ng pCAGGS T7 RNA polymerase. The empty vector pCAGGS_MCS was added to adjust the amout of transfected DNA. 24 h p.t. the medium was changed to $DMEM_{10\,\%\,FCS+Q+P/S}$, supplemented with 0.05 % DMSO (control) or 25 nmol/l OA / 50 nmol/l OA. At 48 h p.t., cells were lysed in CEB buffer. Gel electrophoresis and western blotting were performed. The signal strength obtained with the anti-pS29 antibody was normalized to the signal observed with the anti-FLAG antibody. Signal strength of bands was analyzed with Li-Cor western blot analysis software.

3.3.5 Indirect Immunofluorescence Analysis

Indirect immunofluorescence analysis (IFA) can detect and localize cellular antigens *in situ*. A primary antibody specifically binds the antigen of interest, whereas a secondary antibody is coupled to a fluorophore and directed against the primary antibody. Each fluorophore is excited at a certain wavelength, resulting in light emission at a lower wavelength, which is detected by a fluorescence microscope.

HUH-7 cells, seeded on coverslips in 12-well plates at a density of $5x10^4$ cells / well, were transfected with plasmids encoding EBOV proteins (200 ng each / well) or infected with recEBOV under BSL-4 conditions. When all EBOV proteins were recombinantly expressed, plasmid amounts were adjusted as described in 3.3.4.

20 h p.t. the medium was removed. Transfected cells were washed twice with cold PBS_{def} and fixed with 4 % PFA in DMEM for 15 min at room temperature. HUH-7 cells infected with recEBOV were fixed with 4 % PFA in DMEM 24 h p.i. for at least 16 h. Coverslips were moved to new 12-well plates filled with 4 % PFA / DMEM before export from the BSL-4 laboratory. Prior to continuing, infected cells were incubated for additional 16 h with 4 % PFA / DMEM.

The PFA was washed away, and unspecific surface antigens were blocked by incubating cells for 10 min with 100 mmol/l glycine in TBS. Cells were lysed with 0.1 % Triton™ in

TBS for 7 min at room temperature. Cells were washed again and incubated with blocking buffer for 20 min to remove unspecific intracellular antibody binding sites.
When working with transfected cells, a shorter acetone-methanol fixation / lysis method was used alternatively. First, the growth medium was aspirated. Next, cells were rinsed with TBS twice. Ice-cold 1:1 acetone-methanol was added for 5 min at -20 °C. The acetone-methanol was removed, and cells were washed with TBS twice.
Following fixation and lysis of cells, the coverslips were incubated for 1 h with the respective primary antibodies in a humid chamber at room temperature. Next, coverslips were washed three times with PBS_{def} and incubated with the secondary antibodies for 1 h in the dark, as the fluorescent dyes are very light sensitive. DAPI (4′,6-diamidino-2′-phenylindol) was added to the secondary antibodies at a dilution of 1:10 000. Coverslips were rinsed three additional times with PBS_{def}, followed by shortly immersing them in dH_2O. Excess liquid was carefully blotted onto a Kimtech wipe. Finally, the coverslips were mounted onto microscope slides with Fluoprep (+DABCO), cells facing down. Once the mounting medium had dried, images were taken on the Axiovert 200 M (Zeiss®) fluorescence microscope, at a magnification of 400x or 1000x.

3.3.6 Immunoprecipitation with anti-FLAG M2 Affinity Gel

Immunoprecipitation is considered the gold standard when studying protein-protein interactions. The anti-FLAG M2 affinity gel is a commercially availabe mouse monoclonal anti-FLAG antibody covalently bound to agarose beads. The affinity gel pulls down FLAG-tagged fusion proteins such as a C-terminal FLAG-tagged VP30 construct. Cellular proteins that interact with the FLAG-tagged VP30 are co-immunoprecipitated.
HEK-293 cells, seeded at a density of $6x10^5$ cells / well in 6-well plates, were transfected with 500 ng DNA / well and plasmid (3.2.2). The next day, the growth medium was changed to $DMEM_{+++}$. 48 h p.t. the growth medium was removed. Cells were rinsed with TBS and scraped into 1 ml TBS per well. An aliquot of the resuspended cells was lysed with cell extraction buffer (3.2.3). The remaining cells were pelleted for 2 min at 3000 rpm, the supernatant was discarded, and cells were resuspended in Co-IP buffer supplemented with 1 % Triton™ X-100 and cOmplete™ protease inhibitor cocktail (400 µl buffer / well). No phosphatase inhibitor was added. Cells were lysed for 30 min at room temperature. Cellular debris was pelleted for 10 min at 13 000 rpm. The supernatant was now ready for immunoprecipitation.
The beads of the affinity gel, which are supplied in a 50 % glycerol suspension, were prepared by washing the beads three times with Co-IP buffer for 2 min at 2500 rpm. The gel was then diluted 1:1 with Co-IP buffer. Lysates were added onto the beads (25 µl undiluted affinity gel per lysate of a single well). The lysate / bead mixture was incubated for 2 h at 4 °C in a vertical rotator ("overhead rotator").

In the next step, the beads were pelleted at 4000 rpm. The supernatant was discarded. The beads were washed three times with Co-IP buffer, followed by two additional washing steps with either TM buffer for *in vitro* phosphorylation or TE buffer for subsequent mass spectrometry analysis.
To elute the proteins from the beads, 4x sample buffer was added to a final concentration of 1x. Samples were heated for 10 min at 95 °C. The beads were pelleted by a short centrifugation step. Supernatants were analyzed by SDS-PAGE and WB.

Immunoprecipitation for Mass Spectrometry Analysis

For identification of specific binding partners of FLAG-tagged VP30, the immunoprecipitation protocol was optimized for subsequent mass spectrometry. Apart from large scale immunoprecipitation, two major modifications were made compared to the protocol as described above. 1) Prior to the immunoprecipitation of the FLAG-tagged fusion protein, a preclearing step of the cell lysate was performed with commercially available mouse IgG-agarose, to reduce unspecific binding of cellular proteins to the agarose-coupled mouse anti-FLAG antibody. The mouse IgG-agarose was prepared as described in 3.3.6. Cell lysates were added to the agarose, and the lysate / IgG-agarose mixture was incubated for 1 h at 4 °C in a vertical rotator. The IgG-agarose was pelleted by centrifugation for 2 min at 2500 rpm. The supernatant now was ready for immunoprecipitation of the FLAG-tagged fusion protein. 2) Instead of using the empty vector pCAGGS_MCS as the negative control, a FLAG construct was cloned (3.1.2). For FLAG-tagged fusion proteins, the appropriate negative control is a FLAG-peptide, since the FLAG-part of a FLAG-tagged fusion protein can interact with cellular proteins itself. Additionally, the FLAG-peptide will bind the anti-FLAG antibody of the affinity gel, thereby reducing unspecific binding to the otherwise empty antigen binding region.

3.3.7 VP30 Peptides and a Phosphospecific VP30 Serine 29 Antibody

For detection of phosphorylated serine 29 of EBOV VP30, a polyclonal, phosphospecific IgG peptide antibody was produced in rabbits by Biogenes (Berlin). The antibody was called anti-pS29.
Two 12-mer-peptides were synthesized according to the amino acid sequence position 23 to 34 of VP30, flanking serine 29, with serines 30 and 31 replaced by alanine. Two peptides were synthesized, one with phosphorylated serine at position 29, the other with serine at position 29. The peptides were coupled to a carrier. Following immunization of rabbits, antiserum was isolated. The IgG antibodies were purified by passing the antiserum through affinity columns, with the peptides immobilized in the stationary phase. Following several washing steps, the specifically bound IgG-fraction was eluted with 0.2 mol/l glycine / HCl, pH 2.2, 250 mmol/l NaCl.

The company provided us with the lyophilized phosphorylated 12-mer VP30 peptide. It was assessed to be hydrophil, aliquoted, and dissolved in dH_2O to a concentration of 1 nmol/µl, immediately before the peptide competition assay.

Phosphorylated Peptide (p_S29-peptide)
HHVRAR-**pS**-AAREN-amide
Calculated molecular weight: 1484 g/mol

The p_S29-peptide was dephosphorylated by the calf intestinal phosphatase (CIP) to generate a nonphosphorylated peptide. For this, 20 µl of the 1 mmol/l phosphorylated peptide were mixed with 60 µl CIP buffer and 20 µl of the 1 U/µl CIP. The mixture was incubated for 1 h at 37 °C. The concentration of the dephosphorylated peptide now was 0.2 nmol/µl.

Dephosphorylated Peptide (nonp_S29-peptide)
HHVRAR-**S**-AAREN-amide
Calculated molecular weight: 1404 g/mol

3.3.8 Peptide Competition Assay

A peptide competition assay was carried out to demonstrate the specificity of the anti-pS29 antibody for the phosphorylated form of VP30.
HUH-7 cells, seeded on coverslips at a density of $5x10^4$, were transfected with a plasmid encoding $VP30_f$_AA_A29S. Prior to staining of VP30 in an immunofluorescence assay, the primary antibodies (anti-pS29 and anti-FLAG) were incubated with increasing concentrations of either a FLAG-peptide, the p_S29-peptide, the nonp_S29-peptide, or dH_2O (control). The amount of peptide was calculated in relation to the amount of the anti-pS29 antibody. If there was 100 times more p_S29-peptide in relation to the anti-pS29 antibody during the preincubation, then this means that 50 p_S29-peptides competed for one antigen binding site.
The anti-FLAG antibody served as a control staining of $VP30_f$_AA_A29S on the same coverslip, independent of the phosphorylation status of $VP30_f$_AA_A29S. The concentration of the monoclonal anti-FLAG® M2 antibody (Sigma) was 1 mg/ml. The FLAG-peptide (sequence: DYKDDDDK, molecular weight: 1013 g/mol) was dissolved in TBS to a concentration of 3 mg/ml (= 2.96 nmol/µl).
The concentration of the anti-pS29 antibody was determined as described in 3.3.9. The preincubation was done in TBS buffer for 90 min on a horizontal shaker (300 rpm) at room temperature. Next, reaction tubes were centrifuged for 15 min at 13 200 rpm in order to pellet any immune-complexes formed during incubation. VP30 was stained with

the primary antibody containing supernatant, followed by staining with secondary antibodies (3.3.5).

3.3.9 Protein Quantification

The concentration of the anti-pS29 IgG antibody was estimated in a Nanodrop ND 1000 spectrophotometer (light absorbance at 280 nm). According to the information of the manufacturer Biogenes, the predicted absorbance at 280 nm is 1.35 for a concentration of 1 mg/ml of the phosphospecific antibody. This is equivalent to a molar extinction coefficient$_{280\ nm}$ of the anti-pS29 antibody of $\frac{202.500\ l}{mol \times cm}$.

Using this method, the concentration of the anti-pS29 antibody was 0.8 mg/ml.

3.4 Analysis of VP30 Phosphorylation and Dephosphorylation *in vitro*

Several non-radioactive *in vitro* assays were established to study VP30 phosphorylation. *In vitro*, the reaction equilibrium between the phosphorylated and dephosphorylated state of a protein can be manipulated by addition of phosphatase and kinase activators or inhibitors. The following substances were frequently used in the *in vitro* assays:

Substance	**Characteristics**
Adenosine triphosphate (ATP)	Essential co-substrate of kinases for protein phosphorylation. Is depleted in cell lysates.
Mg^{2+}- ions	Essential for biologically activity of ATP^{4-} . Two ions form a complex with ATP^{4-}. Supplied with the TM buffer.
Dithiothreitol (DTT)	Reducing agent. Prevents formation of disulfide bonds and thereby ensures enzymatic activity. Added to rephoshorylation buffers prior to use.
EDTA	Chelator of Mg^{2+}- and Ca^{2+}- ions.
EGTA	Chelator of Ca^{2+}- ions.
N-ethylmaleimide (NEM)	Irreversible inhibition of enzymes by protein alkylation at cystein residues.
Okadaic acid (OA)	Inhibitor of protein phosphatase 1 and 2A, which were shown to dephosporylate VP30.
Sodium fluoride (NaF)	General protein phosphatase inhibitor.
PhosSTOP™, EDTA-free	Mixture of phosphatase inhibitors, including OA.

Table 3: Reagents for *in vitro* VP30 Phosphorylation and Dephosphorylation.

The *in vitro* approach is based on endogenous cellular kinases and phosphatases, which phosphorylate and dephosphorylate serine 29 of VP30. The enzymes are derived from

HUH-7 or HEK-293 cells, the substrate VP30 is recombinantly expressed in these cells. Phosphorylation of VP30 serine 29 is detected with the phosphospecific peptide antibody anti-pS29.

3.4.1 Dephosphorylation and Phosphorylation of VP30 in Whole Cell Lysates

Hek-293 cells, seeded in 6-well plates at a density of $6x10^5$ cells / well, were transfected with a plasmid encoding $VP30_f$_AA_A29S (500 ng / well). The medium was changed to $DMEM_{+++}$ one day post transfection. 48 h p.t. the growth medium was removed. Cells were rinsed with TBS and scraped into 1 ml TBS.

To analyze the "status quo" or "Input" phosphorylation status of VP30 - at the time of cell harvest – an aliquot of the cells was pelleted for 2 min at 3000 rpm and lysed in the denaturing CEB buffer. Alternatively, the pelleted cells were resuspended in TBS buffer, 4x sample buffer was added immediately, and the sample was heated for 5 min at 95 °C. Denaturation destroys the catalytic activity of phosphatases and kinases, thus the phosphorylation status of VP30 is preserved. It is also possible to preserve the phosphorylation status of a protein in a non-denaturing lysis buffer by addition of a broad-spectrum phosphatase inhibitor, such as PhosSTOP™ or NaF.

The remaining cells were lysed in a non-denaturing TM buffer, supplemented with 0.5 % Triton™ X-100 (350 µl lysis buffer per well). Cell lysates were incubated for at least 30 min at 37 °C.

If no phosphatase inhibitor is added to the lysis buffer, endogenous cellular PP1 and PP2A can dephosphorylate VP30 during the incubation time. Kinases, on the other hand, can no longer phosphorylate VP30 during the incubation time, because the essential co-substrate ATP is no longer produced after cell lysis. OA, added to the TM lysis buffer at a concentration of 1 µmol/l, was tested for its ability to prevent dephosphorylation of VP30 in the cell lysate.

Following the 30 min incubation period, one aliquot was set aside to show the phosphorylation status of VP30 at this point in time. Next, ATP and other substances, including OA and kinase inhibitors, were added to the aliquots. Reactions were incubated with 2 mmol/l ATP for 1 h at 37 °C, unless otherwise noted. DTT was added to every aliquot at a concentration of 1 mmol/l. EGTA was added to the lysis buffer at a concentration of 5 mmol/l. EDTA was combined with a TBS lysis buffer for removal of magnesium. NEM was dissolved in ethanol and added 20 min prior to ATP, at a final concentration of 5 mmol/l.

Reactions were stopped by the addition of sample buffer and heating for 5 min at 95 °C. Cell lysates were sonicated twice for 15 sec. Cellular debris was pelleted for 10 min at 13 200 rpm. The supernatants were run on a SDS-polyacrylamide gel, and western blotting was performed. Membranes were incubated with specific primary antibodies

(anti-pS29 and anti-FLAG) and IRDye labeled secondary antibodies for detection by Li-Cor Odyssey imaging.

3.4.2 *In situ* Studies on VP30 Phosphorylation in NP-Induced Inclusion Bodies

In this *in vitro* assay, HUH-7 cells grown on coverslips in a 12-well plate at a density of $5x10^4$ cells / well, were transfected with plasmids encoding $VP30_f$_AA_A29S, NP, and VP35 (200 ng each / well). 20 h p.t. one coverslip was fixed with ice-cold acetone-methanol (5 min, -20 °C) ("Input"). All other coverslips were not fixed, but instead incubated in a non-denaturing lysis buffer (TBS + 0.2 % Tween® 20) for 10 min at 37 °C. It turned out to be particularly important to use Tween® 20 as the lysing agent, since Triton™ X-100 removed most of the cells from the coverslips. Subsequently, coverslips were gently washed four times with TM buffer and incubated for at least 10 min in TM buffer. Next, the buffer was changed again, this time supplemented with reagents, such as ATP and OA. To irreversibly inactivate kinases, NEM was added 10 min prior to addition of ATP and OA at a concentration of 5 mmol/l.

The rephosphorylation assay was done in small volumes of 50 µl per coverslip on a laboratory film (Parafilm), with the cells facing towards the buffer. All buffers were pre-warmed, the incubation temperature was 37 °C. During the following 30 min incubation period, coverslips were kept in a humid chamber to prevent drying. Reactions were stopped by fixation with ice-cold acetone-methanol 1:1 (5 min, -20 °C). Prior to fixation, one of the coverslips that was treated with OA and ATP was washed twiced with TM buffer and incubated for further 30 min in TM buffer. Staining was performed with specific primary antibodies (anti-pS29 and anti-FLAG) and *Alexa-Fluor* labeled secondary antibodies.

3.4.3 Biochemical Analysis of trVLPs for Kinase Activity

HEK-293 cells, seeded in 6-well plates at a density of $6x10^5$ cells / well, were transfected with plasmids encoding the seven viral proteins (including $VP30_f$_AA_A29S), the EBOV-specific minigenome under control of a T7 promotor, plus a T7 RNA polymerase. 72 h p.t. trVLPs were purified from the supernatant by ultracentrifugation through a 20 % sucrose cushion (3.2.5) or a Nycodenz gradient (3.2.6). Producer cell lysates were subjected to *in vitro* phosphorylation (3.4.1).

An aliquot of the purified and resuspended trVLPs was sampled immediately after centrifugation by addition of sample buffer and heating.

The remaining trVLPs, resuspended in TM buffer, were incubated with 5 mmol/l ATP +/- 1 µmol/l OA, either with or without 0.1 % Triton™ X-100. One hour later, the reactions were stopped by addition of sample buffer. Samples were heated for 5 min at 95 °C and

run on a SDS-polyacrylamide gel. Phosphorylation status of VP30 serine 29 was assessed by western blotting.

In order to digest all proteins that were not incorporated into the trVLPs, aliquots of the purified trVLPs were treated with proteinase K for 30 min at 37 °C. Next, PMSF (in DMSO) was added to inactivate proteinase K. The trVLPs were again centrifuged through a 20 % sucrose cushion in a SW32 rotor. Finally, the pelleted trVLPs were subjected to the *in vitro* phosphorylation assay.

3.4.4 Biochemical Analysis of recEBOV_S29 for Kinase Activity

HUH-7 cells were seeded at a density of $1x10^7$ cells / T175-flask and infected with recEBOV_S29 at a MOI of 3. At 24 h p.i., recEBOV_S29 was purified from the supernatant by ultracentrifugation through a 20 % sucrose cushion in a SW32 rotor at 28 000 rpm and 4 °C. Cell lysates and purified virions were treated as outlined for the trVLPs, except that no proteinase K digestion was performed. Prior to exporting the samples from the BSL-4 laboratory, they were heated for 10 min at 95 °C. All work in the BSL-4 laboratory was performed by Dr. Nadine Biedenkopf.

3.4.5 Immunoprecipitation of VP30 in Combination with a Rephosphorylation Assay

HEK-293 cells, seeded in 6-well plates at a density of $6x10^5$ cells / well, were transfected with plasmids encoding (1) $VP30_f$_AA_A29S or (2) $VP30_f$_AA_A29S + NP + $VP35_{HA}$ (500 ng / plasmid and well). At 48 h p.t., cells were lysed. Expression of the viral proteins was confirmed by cell lysis with CEB, SDS-PAGE (3.3.1), and western blotting (3.2.3). The remaining cells were lysed in a non-denaturing Co-IP buffer for 30 min at room temperature, without addition of phosphatase inhibitors. Lysates were centrifuged for 10 min at 13 200 rpm to remove cellular debris. The supernatant was used for immunoprecipitation with anti-FLAG agarose (3.3.6). Subsequently, the beads were washed thoroughly five times: the first three times with the Co-IP buffer and twice with TM buffer. At this point in time, one aliquot was set aside, proteins were eluted with sample buffer, and the sample was heated to show the phosphorylation status of VP30 serine 29 immediately after immunoprecipitation. The other aliquot was treated with 2 mmol/l ATP and 1 µmol/l OA for 1 h at 37 °C (in TM buffer). Reactions were stopped by addition of sample buffer and heating. Following a short centrifugation step, supernatants were run on a SDS-polyacrylamide gel. Phosphorylation status of VP30 serine 29 was assessed by western blotting.

3.4.6 Kinase Inhibitors *in vitro*

In vitro, kinase inhibitors can be tested at high concentrations without having to monitor cytotoxicity. This makes an *in vitro* approach ideal for screening of substances that can inhibit VP30 phosphorylation.

Following the *in vitro* VP30 dephosphorylation step as outlined in section 3.4.1 and 3.4.2, several kinase inhibitors (Table 4) were tested for their ability to prevent rephosphorylation of VP30. The kinase inhibitors staurosporine, TBCA, and heparin were added 5 min prior to addition of ATP in the test tube rephosphorylation assay (3.4.1) and simultaneously with ATP in the *in situ* assay (3.4.2).

Inhibitior	Characteristics
NEM	Irreversible inhibition of enzymes by protein alkylation at cystein residues. Can only be used *in vitro* for kinase inhibition. Used at a concentration of 5 mmol/l. Added 10-20 min prior to rephosphorylation of VP30.
EDTA	Chelator of Mg^{2+}- and Ca^{2+}- ions. Inhibitis protein phosphorylation by removing the essential Mg^{2+}- ions. Used in TBS lysis buffer at a concentration of 2 mmol/l.
EGTA	Chelator of Ca^{2+}- ions, thereby inhibits calcium-dependent kinases such as CAMK. Used in TM lysis buffer at a concentration of 2 mmol/l.
Staurosporine	Broad-spectrum, ATP-competitive kinase inhibitor. Used at concentrations from 10 nmol/l to 25 µmol/l.
TBCA	Selective casein kinase II inhibitor (IC50 = 0.11 µmol/l), ATP-competitive. Used at concentrations from 100 nmol/l to 1 mmol/l.
Heparin	Polyanionic substance. Resembles DNA / RNA because of the high negative charge. Casein kinase II inhibitor. Used at concentrations from 0.1 µg/ml to 500 µg/ml.

Table 4: Kinase Inhibitors.

3.5 Statistical Analysis

For statistical comparison of two sample means, a two-tailed *t-test* for samples with unequal variance was performed in Microsoft Excel.

A p-value below 0.05 is summarized by one asterisk *, a p-value below 0.01 by two asterisks **, and a p-value below 0.001 by three asterisks ***.

4 Results

4.1 Impact of VP30 Phosphorylation on EBOV Transcription

4.1.1 Influence of VP30 Phosphorylation on Viral Transcriptional Activity

VP30 is an essential EBOV transcription factor, but is dispensable for replication of the full length genome[170]. The function of VP30 as a transcription factor is inhibited by extensive phosphorylation of six N-terminal VP30 serine residues, and it was hypothesized that phosphorylation of VP30 can regulate the balance between viral transcription (VP30 dephosphorylated) and replication (VP30 phosphorylated) [165]. The exact mechanism of how VP30 phosphorylation abolishes transcriptional activity is currently unclear. It was demonstrated that phosphorylation of VP30 impairs its RNA-binding capabilities[27]. Moreover, the interaction between VP30 and NP is enhanced upon phosphorylation, whereas the interaction between VP30 and RNA / VP35 is weakened by phosphorylation[24].

Although theoretically possible, simultaneous phosphorylation of all six N-terminal VP30 serine residues seems unlikely under normal cellular conditions. Energetically speaking, the high negative charge of the adjacent phosphate groups would be very unfavorable. Regarding other proteins it is known that phosphorylation of one serine residue can influence the rate at which neighboring serine residues are phosphorylated. Phosphorylations that are mutually exclusive have been described [47,79].

We therefore asked if the transcriptional support activity of VP30 can also be regulated by phosphorylation of fewer or even single serine residues. We also wanted to know whether phosphorylation of each of the six N-terminal serine residues has the same consequence for VP30's function as a transcription factor or if phosphorylation of specific serine residues is of greater significance for transcriptional suppression. Different VP30 phosphorylation mutants were tested in an EBOV-specific minigenome assay in combination with the phosphatase inhibitor OA. OA inhibits PP1 and PP2A, which are both known to dephosphorylate the N-terminal VP30 serine residues[165]. Inhibition of these phosphatases leads to a hyper-phosphorylated $VP30_f$_wt, which is unable to support viral transcription[165]. The following results show the transcriptional support activity of the VP30 phosphorylation mutants in HEK-293 cells, both under control conditions (DMSO) and under phosphatase inhibition with OA. The findings were confirmed in HUH-7 cells to exclude cell-type specific effects. Expression of all VP30 mutants was confirmed by western blotting (data not shown).

Initially, the effect of serine phosphorylation in the first (residues S29-S31, represented by the mutant VP30$_f$_SA) or the second serine cluster (residues S42 / S44 / S46, represented by the mutant VP30$_f$_ AS) was analyzed (Figure 5 A and B). VP30$_f$_wt, VP30$_f$_AA, VP30$_f$_SA, and VP30$_f$_AS were highly transcriptionally active in the minigenome assay under control conditions (white bars). Notably, the viral transcriptional support activity of VP30$_f$_AA, which mimics permanently dephosphorylated VP30, was even higher than that of VP30$_f$_wt, supporting the idea that VP30 phosphorylation impairs viral transcription. VP30$_f$_DD, mimicking permanently phosphorylated VP30, was transcriptionally inactive. When OA was added to the growth medium, VP30$_f$_wt and VP30$_f$_SA lost most of its transcriptional support activity, whereas VP30$_f$_AA and VP30$_f$_AS still supported viral transcription (black bars).

This means that VP30 is either predominantly phosphorylated in the first cluster upon treatment with OA or that phosphorylation of the first serine cluster (S29-S31) affects the transcriptional support activity of VP30 to a greater extent than phosphorylation of the other serine residues (S42 / S44 / S46).

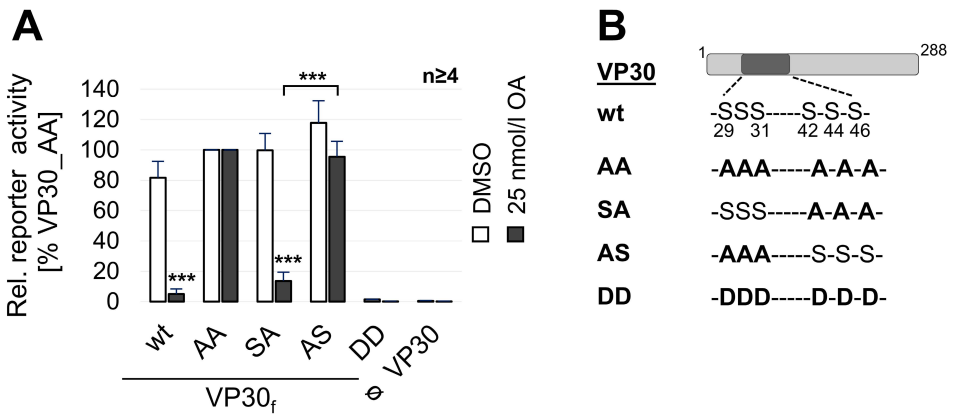

Figure 5: Transcriptional Support Activity of VP30 is Downregulated by Phosphorylation in the First VP30 Serine Cluster.

(A) Reporter gene activity of VP30 phosphorylation mutants in an EBOV-specific minigenome assay under **control conditions (white bars)** or **25 nmol/l OA (black bars)** (3.2.4). HEK-293 cells were transfected with all plasmids needed for the EBOV-specific minigenome assay, including VP30$_f$_wt or mutants. Cells were treated either with 0.025 % DMSO (= control) or 25 nmol/l OA at 0 h post transfection. 24 h p.t. cells were lysed and the reporter gene activity was measured in a luciferase assay. Since the transcriptional activity of VP30$_f$_AA cannot be influenced by phosphorylation in the N-terminal serine cluster, results obtained with VP30$_f$_AA were set to 100 %. Statistical significance is shown in relation to VP30$_f$_AA, unless otherwise noted. **(B)** Schematic presentation of the VP30 phosphorylation mutants. Serine was mutated either to alanine to mimic a permanently dephosphorylated residue or to aspartate to mimic a permanently phosphorylated residue. For a more detailed overview of VP30 phosphorylation mutants refer to the Appendix.

Next we wanted to determine whether phosphorylation of a single serine residue is sufficient to impair VP30's transcriptional potential. For this purpose, mutants with a single serine residue in the N-terminal region were tested in the minigenome assay. The five other serine residues were mutated to alanine ($VP30_f$_AA_A29S to $VP30_f$_AA_A46S, Figure 6 B). We could demonstrate that the transcriptional potential of these VP30 mutants does not differ significantly from $VP30_f$_AA under control conditions (Figure 6, white bars). Also, phosphorylation of a single VP30 serine residue was not sufficient to impair transcriptional activation, since all single serine to alanine mutants kept their transcriptional support activity under phosphatase inhibition to a similar extent as $VP30_f$_AA (black bars).

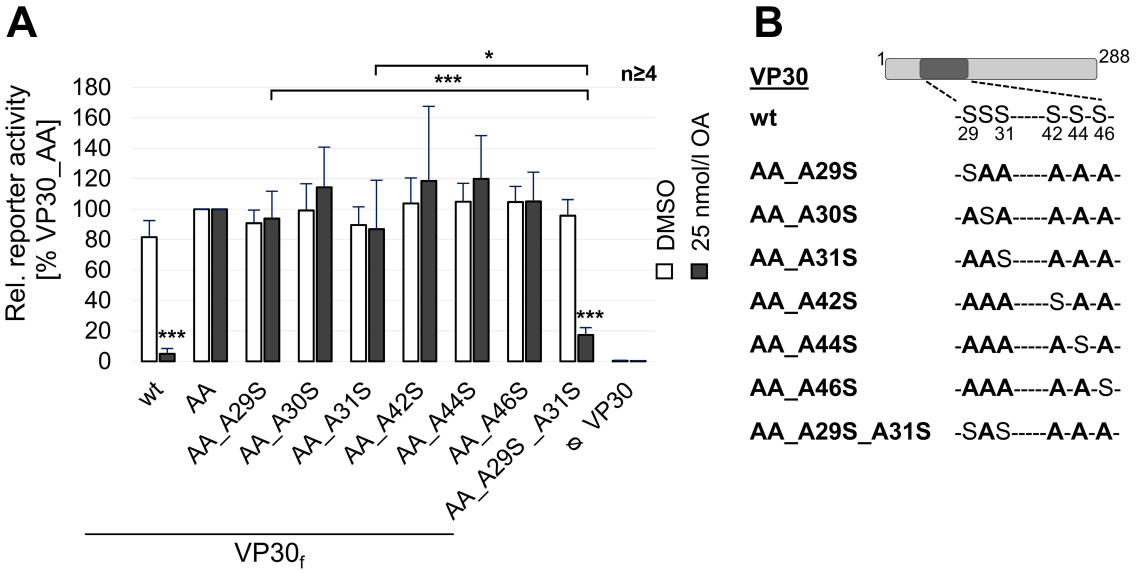

Figure 6: Phosphorylation of VP30 S29 and S31, but not of a Single Serine Residue, is Sufficient for Downregulation of the Transcriptional Support Activity of VP30.

(A) Reporter gene activity of VP30 phosphorylation mutants in an EBOV-specific minigenome assay under **control conditions (white bars)** or **25 nmol/l OA (black bars)** (3.2.4). HEK-293 cells were transfected with all plasmids needed for the EBOV-specific minigenome assay, including $VP30_f$_wt or mutants. Cells were treated either with 0.025 % DMSO (= control) or 25 nmol/l OA at 0 h post transfection. 24 h p.t. cells were lysed and the reporter gene activity was measured in a luciferase assay. Since the transcriptional activity of $VP30_f$_AA cannot be influenced by phosphorylation in the N-terminal serine cluster, results obtained with $VP30_f$_AA were set to 100 %. Statistical significance is shown in relation to $VP30_f$_AA, unless otherwise noted. **(B)** Schematic presentation of the VP30 phosphorylation mutants. Serine was mutated either to alanine to mimic a permanently dephosphorylated residue or to aspartate to mimic a permanently phosphorylated residue. For a more detailed overview of VP30 phosphorylation mutants refer to the Appendix.

Since OA treatment indicated that phosphorylation of the first serine cluster plays an important role regarding the downregulation of viral transcription (Figure 5), we now wanted to know whether simultaneous phosphorylation of only two serine residues, namely S29 and S31, would be sufficient to downregulate the viral transcriptional activity. We generated a VP30 mutant with serine on position 29 and 31 only, while all other serine residues were mutated to alanine ($VP30_f$_AA_A29S_A31S, Figure 6 B). In the DMSO control, this mutant was highly transcriptionally active (Figure 6 A, white bar, far right). When OA was added, however, this VP30 mutant showed a substantial decrease in transcriptional support activity (Figure 6 A, black bar, far right).

To further investigate whether phosphorylation at certain serine residues is particularly important for downregulation of viral transcription, we generated single serine to alanine mutants, in which all other serine residues were maintained (Figure 7 B). With these mutants we tested whether the absence of phosphorylation at a specific serine residue could prevent the transcriptional inactivation of VP30 during phosphatase inhibition with OA. In the absence of OA, the VP30 mutants supported viral transcription equally well (Figure 7 A, white bars). Under phosphatase inhibition, both $VP30_f$_S29A and $VP30_f$_S31A were still able to support transcription, whereas $VP30_f$_S30A, $VP30_f$_S42A, $VP30_f$_S44A, and $VP30_f$_S46A were strongly inhibited (Figure 7 A, black bars). The mutations S29A or S31A prevented the inactivation of VP30 in the presence of OA, although the remaining five other serine residues could potentially be phosphorylated.

These data reveal that, in our system, simultaneous phosphorylation of VP30 serine residues S29 and S31 decisively contributes to the negative effect of phosphorylation on VP30-mediated viral transcriptional activation. We conclude that simultaneous phosphorylation of VP30's serine residues 29 and 31 is both necessary and sufficient for downregulation of viral transcription in the EBOV-specific minigenome assay.

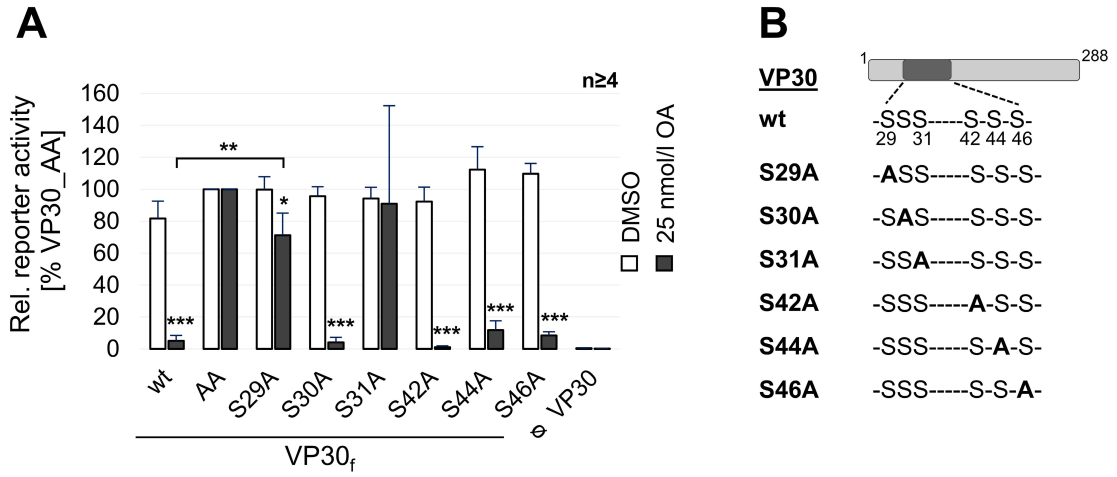

Figure 7: Simultaneous Phosphorylation of VP30 Serine Residues S29 and S31 is Necessary for Downregulation of the Transcriptional Support Activity of VP30.

(A) Reporter gene activity of VP30 phosphorylation mutants in an EBOV-specific minigenome assay under **control conditions (white bars)** or **25 nmol/l OA (black bars)** (3.2.4). HEK-293 cells were transfected with all plasmids needed for the EBOV-specific minigenome assay, including $VP30_f$_wt or mutants. Cells were treated either with 0.025 % DMSO (= control) or 25 nmol/l OA at 0 h post transfection. 24 h p.t. cells were lysed and the reporter gene activity was measured in a luciferase assay. Since the transcriptional activity of $VP30_f$_AA cannot be influenced by phosphorylation in the N-terminal serine cluster, results obtained with $VP30_f$_AA were set to 100 %. Statistical significance is shown in relation to $VP30_f$_AA, unless otherwise noted. **(B)** Schematic presentation of the VP30 phosphorylation mutants. Serine was mutated either to alanine to mimic a permanently dephosphorylated residue or to aspartate to mimic a permanently phosphorylated residue. For a more detailed overview of VP30 phosphorylation mutants refer to the Appendix.

4.1.2 Importance of VP30 Phosphorylation for Primary Viral Transcription

Apart from the role of dephosphorylated VP30 in viral transcription (Figure 5 to Figure 7), VP30 phosphorylation plays an essential role during early steps of the viral life cycle immediately after infection of a new cell. trVLPs containing VP30 with no phosphorylation sites in the serine clusters (VP30_AA) were transcriptionally inactive in the indicator cells, and a corresponding recombinant virus recEBOV_AA could not be rescued[23,26]. Contrary, VP30 with serine 29 as the only phosphoacceptor site was sufficient to activate primary transcription in a trVLP assay and it was possible to rescue a corresponding recEBOV_S29 with similar growth characteristics as recEBOV_wt[23]. The exact role of VP30 phosphorylation during the early time points of infection, however, was unclear. In that respect we wanted to investigate whether the permanent phosphorylation or a dynamic dephosphorylation / phosphorylation of serine 29 is essential for activating primary viral transcription in a trVLP assay. We therefore studied different VP30 phosphorylation mutants, containing either no charge at serine 29 ($VP30_f$_AA), a negatively charged aspartate ($VP30_f$_AA_A29D), or a combination of both (Figure 8).

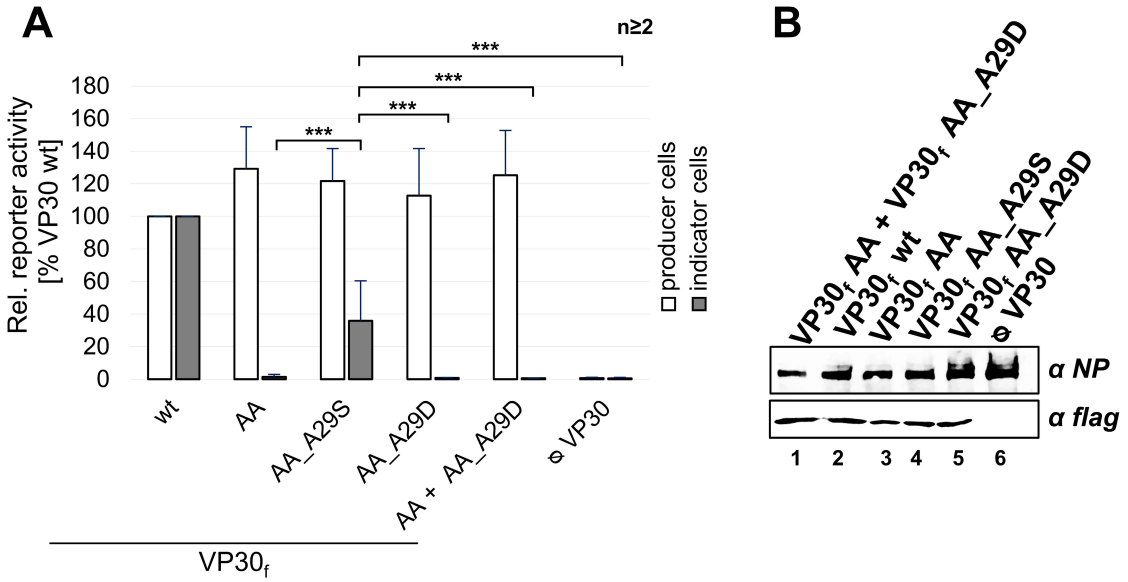

Figure 8: Dynamic Phosphorylation of VP30 is Necessary for Primary Transcriptional Activity.
(A) Reporter gene activity of VP30 phosphorylation mutants in **producer (white bars)** and **indicator cells (grey bars)** in an EBOV-specific trVLP assay (3.2.5). HEK-293 cells (= producer cells) were transfected with all plasmids required for the EBOV-specific trVLP assay, including $VP30_f$_wt or mutants. Producer cells were lysed 72 h p.t. and a luciferase assay was performed (white bars). trVLPs were collected from the supernatants of the producer cells, purified by ultracentrifugation, and used to infect naïve HUH-7 cells (= indicator cells). Reporter gene activity was measured 60 h p.i. (grey bars). Results obtained with $VP30_f$_wt were set to 100 %. For an overview of VP30 phosphorylation mutants refer to the Appendix. **(B)** Western blot analysis (3.3.3) of purified trVLPs. Aliquots of the trVLPs were analyzed for the incorporation of NP and $VP30_f$_wt / phosphorylation mutants (3.2.5). NP was stained with chicken anti-NP and donkey anti-chicken 680 nm antibodies, VP30 was stained with rabbit anti-flag and goat anti-rabbit 680 nm antibodies.

In the producer cells, all VP30 mutants enabled secondary viral transcription (white bars). In the indicator cells, however, only $VP30_f$_wt and – to a lower extent - $VP30_f$_AA_A29S were supporting primary transcription (grey bars). Both $VP30_f$_AA and $VP30_f$_AA_A29D were transcriptionally inactive in the indicator cells. Even the combination of both, phosphoablative $VP30_f$_AA and phosphomimetic $VP30_f$_AA_A29D, could not restore primary transcription. Incorporation of the VP30 mutants into purified trVLPs was confirmed in western blot analysis (Figure 8 B).

These results suggest that dynamic phosphorylation of a specific serine residue is required for primary viral transcription. Since phosphorylation of VP30 actually impairs viral transcription *per se* (Figure 5 to Figure 7), we asked whether the essential dynamic phosphorylation at early stages of infection is required for efficient transport of VP30 to the sites of viral RNA synthesis in the perinuclear region. Therefore, we performed immunofluorescence analyses of naïve indicator cells infected with trVLPs containing different VP30 phosphorylation mutants, and stained for the viral NP and VP30 to detect intruding nucleocapsids (Figure 9). Around the nucleus, small typical NP-positive inclusion bodies were observed upon infection with trVLPs containing no VP30, $VP30_f$_wt, or the VP30 phosphorylation mutants (Figure 9, i-vi). No inclusion bodies could be detected in the negative control (Figure 9, vii). The formation of inclusion bodies was obviously not dependent on newly synthesized NP, since there is no NP open reading frame encoded in the minigenome. Inclusion bodies had to be formed by NP incorporated into the trVLPs. Strikingly, we only observed a signal for $VP30_f$_wt and for $VP30_f$_AA_A29S, but not for the other VP30 phosphorylation mutants, including the combination of $VP30_f$_AA and $VP30_f$_AA_A29D (Figure 9, v). $VP30_f$_wt and $VP30_f$_AA_A29S colocalized with the NP-positive inclusion bodies. The immunofluorescence signal for $VP30_f$_AA_A29S was weaker than for $VP30_f$_wt, in correspondence with the lower activation of primary transcription of this mutant (Figure 8).

These observations suggest that phosphorylation of VP30 ensures adequate transport of VP30 to the site of primary transcription, presumably by enhanced interaction of phosphorylated VP30 with other viral proteins like NP[23].

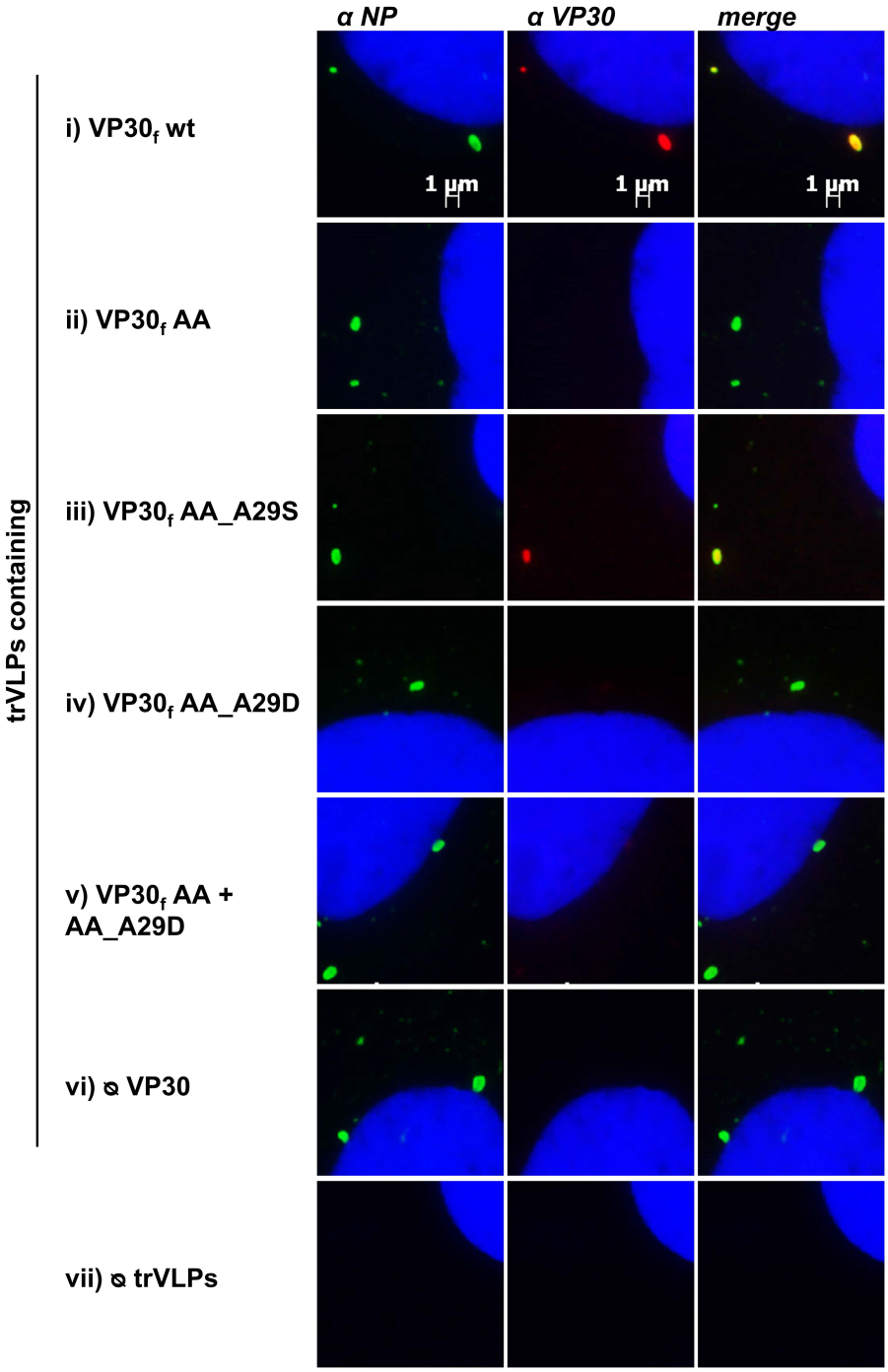

Figure 9: Only VP30$_f$_wt and VP30$_f$_AA_A29S Localize to Small NP-Positive Inclusion Bodies Formed in Naïve Indicator Cells after Infection with trVLPs.

Indirect immunofluorescence analysis (3.3.5) of naïve HUH-7 cells infected with trVLPs. The trVLPs were produced as described in 3.2.5 and contained either VP30$_f$_wt or phosphorylation mutants. Twenty-two h p.i. cells were fixed with PFA. NP was stained with chicken anti-NP and goat anti-chicken *Alexa 488* antibodies, VP30 was stained with guinea pig anti-VP30 and goat anti-guinea pig *Alexa 594* antibodies. Nuclei were visualized with DAPI. Images were taken at a magnification of x1000 in close proximity to the nucleus (blue).

4.2 Characterization of the Phosphospecific VP30 Antibody anti-pS29

With respect to the importance of VP30's serine 29 for phosphorylation-dependent regulation of EBOV transcription, we aimed to further decipher the role of VP30 phosphorylation during the EBOV life cycle with an antibody specifically recognizing phosphorylated serine 29 (anti-pS29). For generation of a polyclonal phosphospecifc antibody, rabbits were immunized with a 12-mer phosphorylated VP30 peptide (3.3.7). This peptide included the original VP30 serine residue 29, centrally arranged (Figure 10 A and E). Importantly, serine residues at the original position 30 and 31 were changed to alanine to mimic nonphosphorylated serine residues. Hence, the new phosphospecific antibody was designed to detect phosphorylation on VP30 AA_A29S without interference of possible phosphorylation events on the neighboring serine residues.

The resulting antibody anti-pS29 was tested for its specificity using FLAG-tagged VP30 phosphorylation mutants (Figure 10 E). HEK-293 cells expressing the FLAG-tagged VP30 mutants were lysed, and expression of the VP30 constructs was verified by an anti-FLAG antibody (Figure 10 B). The phosphospecific antibody anti-pS29 detected both $VP30_f$_wt and $VP30_f$_AA_A29S, suggesting serine 29 to be phosphorylated in cells lysed with phosphatase inhibitors for preservation of the phosphorylation status (lanes 1 and 3). However, when cells were lysed in a non-denaturing buffer without phosphatase inhibitors and incubated for 30 min, $VP30_f$_wt and $VP30_f$_AA_A29S were no longer detected by the phosphospecific antibody, whereas the anti-FLAG antibody was still able to detect the presence of VP30 mutants (lanes 5 and 6). This suggested dephosphorylation of VP30 serine 29 by endogenous phosphatases. $VP30_f$_AA, which mimics permanently dephosphorylated VP30 and differs from $VP30_f$_AA_A29S by the alanine at position 29, was not detected by anti-pS29 (lane 2). $VP30_f$_AA_A29D on the other hand, which mimics phosphorylated VP30 on position 29, was detected by the phosphospecific antibody, albeit weaker (lane 4). The observed lower signal for $VP30_f$_AA_A29D might be explained by a lower affinity of the antibody for the aspartate residue than for phosphorylated serine.

Similar results were obtained upon expression of the VP30 mutants in HUH-7 cells for immunofluorescence analysis (Figure 10 C). Here, expression of constructs was verified by an anti-VP30 antibody from guinea pig, revealing mostly a diffuse staining pattern of VP30. Again, the phosphospecific antibody detected $VP30_f$_wt, $VP30_f$_AA_A29S, and $VP30_f$_AA_A29D, but not $VP30_f$_AA. Furthermore, $VP30_f$_AA_A30S, which has serine on position 30 instead of position 29, was not detected by the phosphospecific antibody.

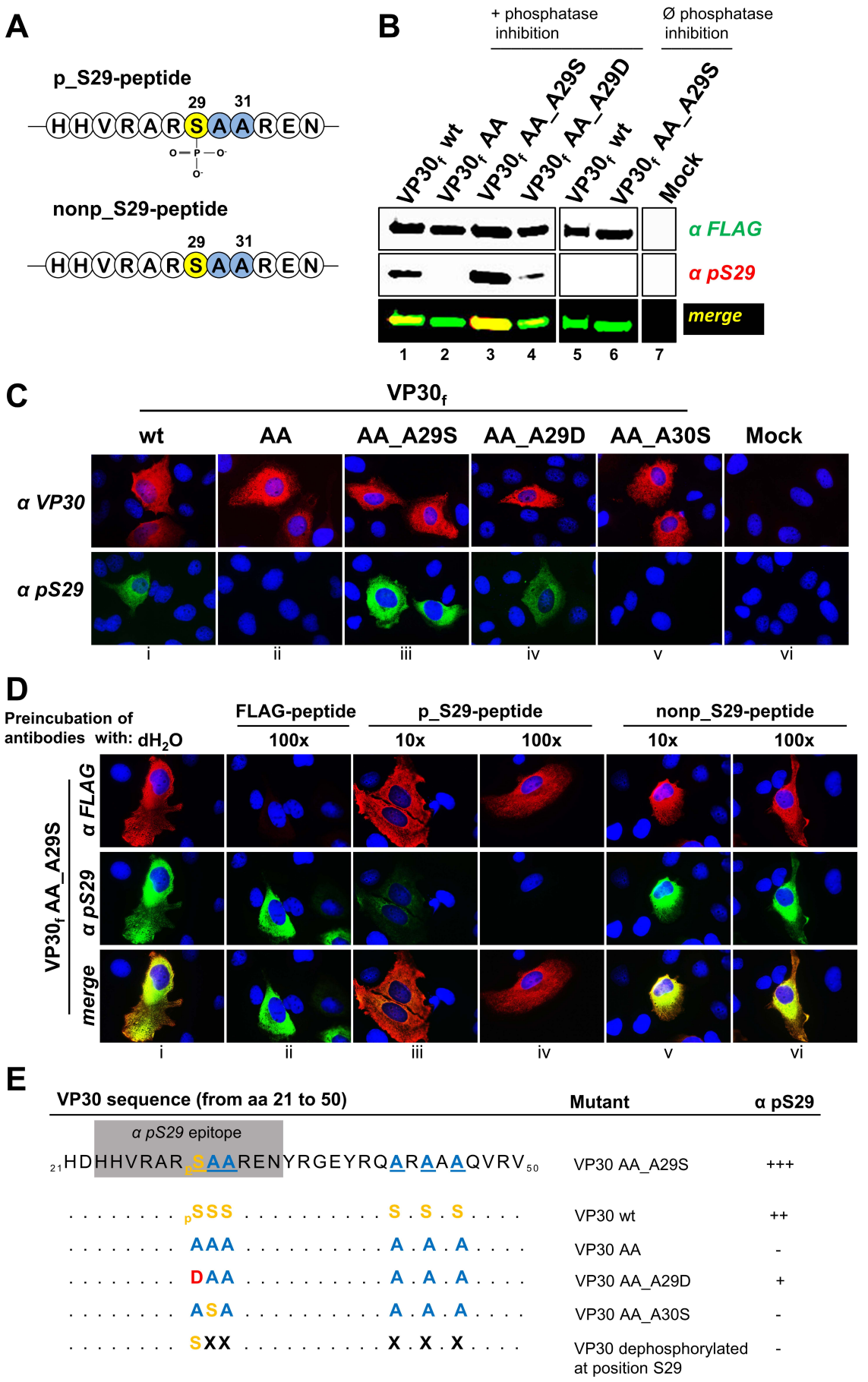

Figure 10: Characteristics of a Phosphospecific VP30 Serine 29 Antibody (anti-pS29).

(A) Illustration of the VP30 peptides used to generate a polyclonal phosphospecific peptide antibody "*anti-pS29"* for detection of VP30 serine 29 phosphorylation. **(B)** Western blot analysis of $VP30_f$_wt / phosphorylation mutants expressed in HEK-293 cells (3.3.3). 24 h p.t. cells were lysed in either a denaturing cell extraction buffer (lanes 1-4 and lane 7) or in a non-denaturing buffer (lanes 5 / 6). Cells lysed with the non-denaturing buffer were incubated for 30 min at room temperature, leading to VP30 dephosphorylation by endogenous phosphatases. SDS-PAGE (3.3.1) and WB (3.3.3) were performed, followed by staining of total VP30 with mouse anti-FLAG and goat anti-mouse 780 nm antibodies and of phosphorylated VP30 with rabbit anti-pS29 and goat anti-rabbit 680 nm antibodies. **(C)** Immunofluorescence analysis of $VP30_f$_wt / mutants expressed in HUH-7 cells (3.3.5). 16 h p.t. cells were fixed with PFA. Total VP30 was stained with guinea pig anti-VP30 and goat anti-guinea pig *Alexa 594* antibodies. Phosphorylated VP30 was stained with rabbit anti-pS29 and goat anti-rabbit *Alexa 488* antibodies. Nuclei were visualized with DAPI. **(D)** Confirmation of the specificity of the VP30 peptide antibody anti-pS29 in a peptide competition assay (3.3.8). The primary antibodies were preincubated with increasing concentrations of either the phosphorylated peptide or dephosphorylated S29-peptide, followed by staining of HUH-7 cells that expressed $VP30_f$_AA_A29S (3.3.5). Preincubation with a FLAG-peptide and dH_2O served as additional controls. Total VP30 was stained with mouse anti-flag and goat anti-mouse *Alexa 594* antibodies, phosphorylated VP30 was stained with rabbit anti-pS29 and goat anti-rabbit *Alexa 488* antibodies. Nuclei were visualized with DAPI. **(E)** Summary of the VP30 phosphorylation mutants and their recognition by the phosphospecific VP30 antibody anti-pS29. Serine was either mutated to alanine (blue, mimicking permanently dephosphorylated VP30) or to aspartate (red, mimicking permanently phosphorylated VP30). X: any amino acid. Grey box: binding site of the anti-pS29 antibody. Right column: recognition of the VP30 mutants by the anti-pS29 antibody. (-): no recognition. (+) to (+++): weak to strong recognition. Figure is based on Lier et al. 2017[145].

As mentioned, all VP30 phosphorylation mutants generally had a diffuse distribution throughout the cytoplasm in IFA, but $VP30_f$_wt had a strong tendency to form cytoplasmic aggregates, especially when highly overexpressed. This feature was not observed for the phosphorylation mutants $VP30_f$_AA or $VP30_f$_AA A29S, suggesting that the formation of $VP30_f$_wt aggregates might be influenced by multisite phosphorylation. This is underlined by the observation that the phosphospecific antibody stained these aggregates strongly and that the mutant $VP30_f$_DD, which mimics permanently phosphorylated VP30 on all six serine residues, aggregated as well (data not shown).

We validated the specificity of the anti-pS29 antibody for phosphorylated $VP30_f$_AA_A29S in a peptide competition assay (Figure 10 D). HUH-7 cells were transfected with the plasmid encoding $VP30_f$_AA_A29S. Prior to staining, increasing concentrations of either the phosphorylated peptide p_S29, the nonphosphorylated S29-peptide, or a FLAG-peptide were added to the primary antibodies (anti-pS29 and anti-FLAG). 24 h p.t., the $VP30_f$_AA_A29S-expressing cells were stained with the preincubated antibodies. With increasing concentrations of the p_S29-peptide, anti-pS29 did no longer detect $VP30_f$_AA_A29S (Figure 10 D, iii and iv), whereas preincubation with the nonphosphorylated S29-peptide did not affect detection by the anti-pS29 antibody

(Figure 10 D, v and vi). Incubation with a FLAG-peptide prevented staining by the anti-FLAG antibody, but not by phosphospecific anti-pS29 antibody (Figure 10 D, ii). Staining of $VP30_f$_AA_A29S with the anti-FLAG antibody was not affected by preincubation with the VP30 S29-specific peptides (Figure 10 D, i and iii-vi).

Overall, these findings confirm that the generated antibody is highly specific for the phosphorylated form of $VP30_f$_AA_A29S and does not bind if serine residue 29 is dephosphorylated by endogenous cellular protein phosphatases or outcompeted by the corresponding phosphospecific peptide.

4.3 Influence of NP and Other Viral Proteins on VP30 Phosphorylation

4.3.1 Co-expression of VP30 with NP

Earlier results obtained with phosphomimetic VP30 mutants carrying permanent charges at the phosphorylation sites indicated that phosphomimetic VP30 located strongly to NP-induced inclusion bodies, whereas a mutant mimicking permanently dephosphorylated VP30 distributed in a more diffuse pattern throughout the cytoplasm[165]. Also, co-immunoprecipitation data revealed a stronger interaction between NP and phosphorylated VP30 as compared with nonphosphorylated VP30[24]. As mentioned, these experiments were performed with VP30 mutants carrying permanent charges at the phosphorylation sites. With the anti-pS29 antibody we now had the opportunity to investigate the localization of dynamically phosphorylatable VP30 in the presence of NP in co-expression studies.

In Figure 11 A, VP30 phosphorylation mutants were stained with an anti-VP30 antibody, independently of their phosphorylation status. The typical NP-induced inclusion bodies were visualized with an anti-NP antibody. $VP30_f$_wt, as well as all VP30 mutants, located to the inclusion bodies, albeit the signal inside the inclusion bodies was weaker for the VP30 phosphorylation mutants. Less prominent, all VP30 phosphorylation mutants had a diffuse cytoplasmic localization upon co-expression with NP.
In Figure 11 B, VP30 was stained with the phosphospecific antibody. For $VP30_f$_wt, a very weak signal was observed, which was mostly located in the NP-induced inclusion bodies, but also diffusely in the cytoplasm. As expected, the anti-pS29 antibody did not stain $VP30_f$_AA. To our surprise, the phosphospecific antibody did not stain $VP30_f$_AA_A29S inside the NP-induced inclusion bodies. Instead, only the diffusely distributed $VP30_f$_AA_A29S was detected in the cytoplasm.

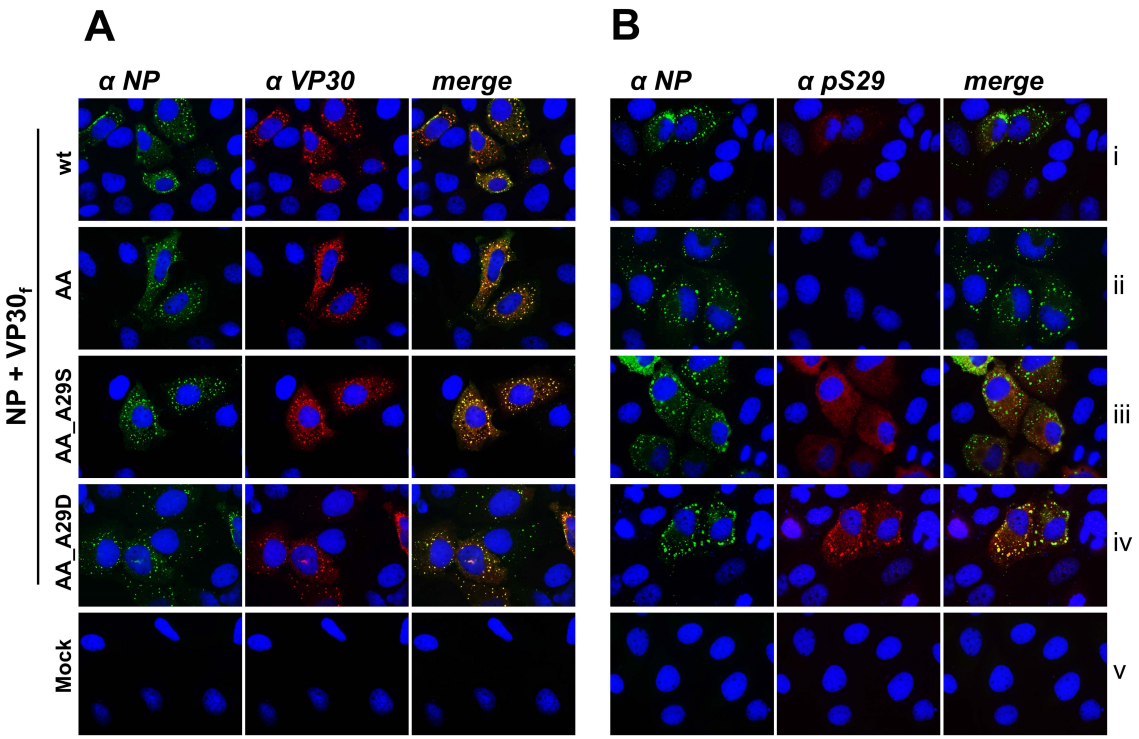

Figure 11: VP30 Serine 29 is Predominantly Dephosphorylated in NP-Induced Inclusion Bodies.
(A) – (B) Indirect immunofluorescence analysis of HUH-7 cells co-expressing $VP30_f$_wt / phosphorylation mutants and NP (3.3.5). 20 h p.t. cells were fixed with PFA. NP was stained with chicken anti-NP and goat anti-chicken *Alexa 488* antibodies. Nuclei were visualized with DAPI. In **(A)**, total VP30 was stained with guinea pig anti-VP30 and goat anti-guinea pig *Alexa 594* antibodies. In **(B)**, phosphorylated VP30 was stained with rabbit anti-pS29 and goat anti-rabbit *Alexa 594* antibodies.

To exclude that the strong interaction of the phosphorylated $VP30_f$_AA_A29S with NP masked the antibody epitope (phosphoepitope masking), we used $VP30_f$_AA_A29D as control. The aspartate on position 29 mimics a permanent phosphorylation and was recognized by the phosphospecific antibody in single expression experiments (Figure 10 B and C). Contrary to $VP30_f$_AA_A29S, $VP30_f$_AA_A29D was recognized perfectly inside the NP-induced inclusion bodies, suggesting that the phosphoepitope *per se* (in this case the negatively charged aspartate) is freely accessible by the anti-pS29 antibody.

This suggests that EBOV VP30 is mainly dephosphorylated in NP-induced inclusion bodies, either due to missing phosphorylation by cellular kinases or, more likely, due to rapid dephosphorylation by cellular phosphatases. We hypothesized that viral NP itself could influence the phosphorylation state of VP30, e.g. by recruiting cellular phosphatases. We therefore used OA to block dephosphorylation of VP30 by cellular PP1 / PP2A during co-expression of NP and $VP30_f$_AA_A29S (Figure 12). In the DMSO-control and at very low concentrations of OA (1 nmol/l), no or only very weak signals of phosphorylated VP30 were observed inside the NP-induced inclusion bodies.

With increasing concentrations of OA, however, the phosphospecific antibody recognized $VP30_f$_AA_A29S strongly inside the inclusion bodies (Figure 12, iii and iv).

We conclude from these results that $VP30_f$_AA_A29S is predominantly dephosphorylated when colocalizing with NP in the inclusion bodies, likely by recruitment of an OA-sensitive phosphatase by NP.

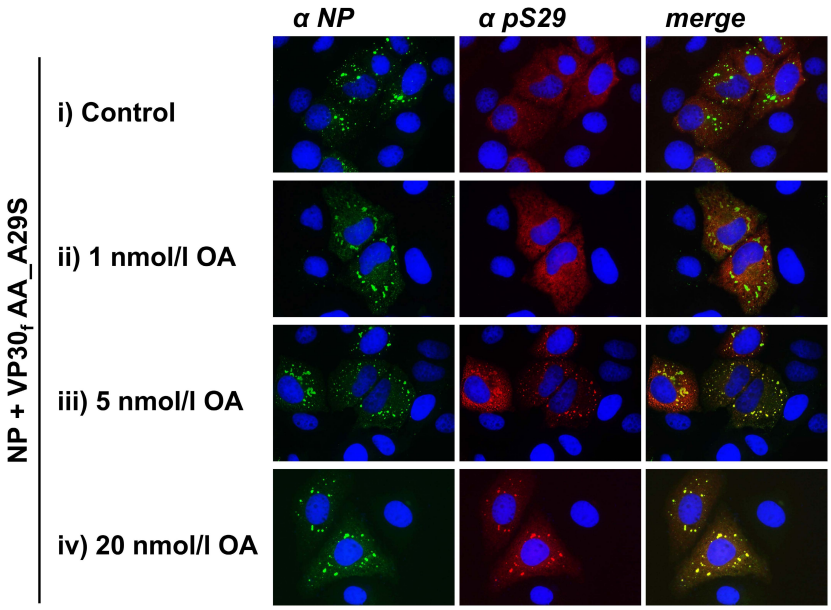

Figure 12: During Phosphatase Inhibition, Phosphorylated VP30 is Detected in NP-Induced Inclusion Bodies.

Indirect immunofluorescence analysis of HUH-7 cells co-expressing $VP30_f$_AA_A29S and NP under the influence of the phosphatase inhibitor OA (3.3.5). OA was added to the growth medium 0 h p.t. Control = DMSO. Cells were fixed 20 h p.t. with PFA. NP was stained with chicken anti-NP and goat anti-chicken *Alexa 488* antibodies, phosphorylated VP30 was stained with rabbit anti-pS29 and goat anti-rabbit *Alexa 594* antibodies. Nuclei were visualized with DAPI.

4.3.2 Co-expression of VP30 with Other Viral Proteins

In the light of the striking influence of NP on VP30 phosphorylation, we wanted to determine whether other viral proteins also influence phosphorylation of VP30 serine 29. We transiently expressed various combinations of EBOV proteins together with $VP30_f$_AA_A29S / $VP30_f$_wt and analyzed their influence on VP30 phosphorylation in IFA (Figure 13). FLAG-tagged VP30 was stained with an anti-FLAG antibody independent of its phosphorylation status. VP35 alone did not influence the phosphorylation status of $VP30_f$_AA_A29S (Figure 13, i). In contrast, when $VP30_f$_AA_A29S was co-expressed with the nucleoprotein NP, the signal for phosphorylated VP30 was strongly diminished and the inclusion bodies could not be visualized with the phosphospecific antibody (Figure 13, ii), supporting the results in

Figure 11. The anti-FLAG staining though revealed the typical concentration of VP30 inside the NP-induced inclusion bodies. When $VP30_f$_AA_A29S was transfected with all other six viral proteins (NP, VP35, VP40, GP, VP24, L), there was no or only a very weak signal for the phosphospecific antibody (Figure 13, iii). The same was true for cells that expressed $VP30_f$_wt together with all other viral proteins (Figure 13, iv).

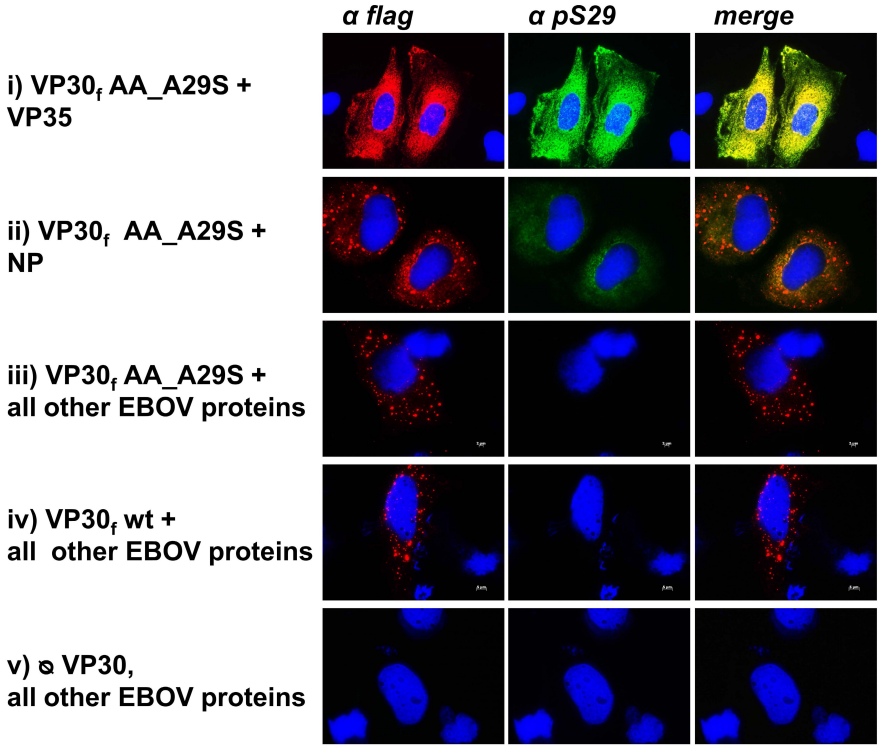

Figure 13: Besides NP, Other EBOV Proteins also Influence Phosphorylation of VP30 Serine 29. Indirect immunofluorescence analysis of HUH-7 cells, which were transfected with plasmids encoding $VP30_f$_AA_A29S / $VP30_f$_wt together with other viral proteins (3.3.5). Cells were fixed 20 h p.t. with PFA. Total VP30 was stained with mouse anti-flag and goat anti-mouse *Alexa 594* antibodies, phosphorylated VP30 was stained with rabbit anti-pS29 and goat anti-rabbit *Alexa 488* antibodies. Nuclei were visualized with DAPI.

These immunofluorescence results were supported by western blot studies in HEK-293 cells (Figure 14 A). Expression of $VP30_f$_AA_A29S was again verified by staining with the anti-FLAG antibody. $VP30_f$_AA_A29S was strongly phosphorylated at position 29 if expressed alone in the HEK-293 cells (lane 1). VP35 or the combination of VP35 / L did not reduce the amount of phosphorylated VP30 (lanes 2 and 5). When $VP30_f$_AA_A29S was expressed together with the viral NP (+/- VP35), a significant weaker signal was observed for the phosphospecific antibody (lane 3 and 4). The same was true when all viral nucleocapsid proteins were expressed. The addition of the minigenome to these expression plasmids had little or no effect (lane 6 versus lane 7). The signal for the phosphospecific antibody was even lower or absent, when all EBOV proteins were expressed (lane 8).

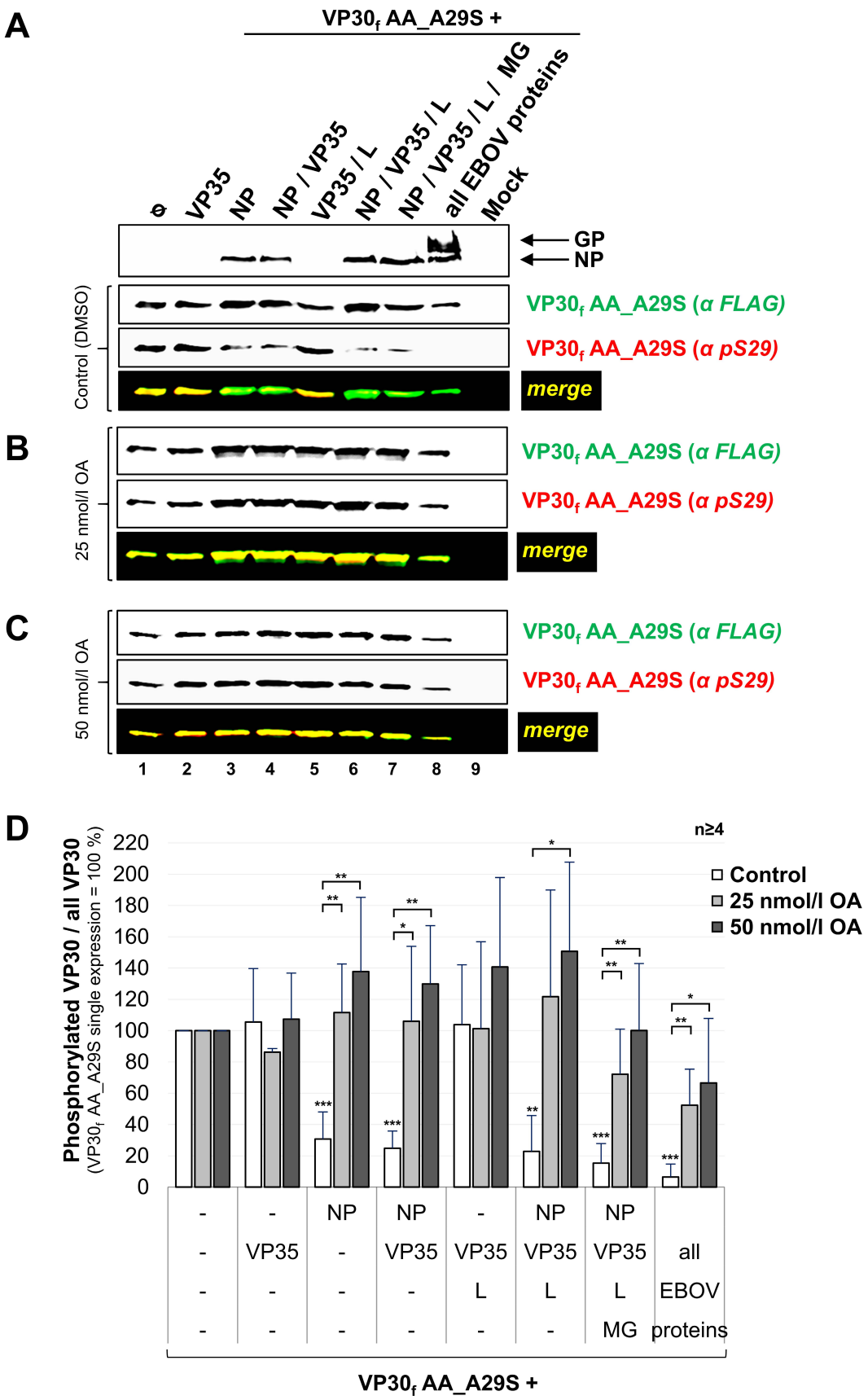

Figure 14: NP and Other EBOV Proteins Decrease Phosphorylation of VP30 by Recruitment of an OA-Sensitive Phosphatase.

(A) - (C) Western blot analysis of HEK-293 cells expressing $VP30_f$_AA_A29S, either alone or in combination with other viral proteins (3.3.4). The empty vector pCAGGS_MCS was added to adjust the amout of transfected DNA. 24 h p.t. the growth medium was changed, with **(A)** 0.05 % DMSO, **(B)** 25 nmol/l OA, or **(C)** 50 nmol/l OA dissolved in the medium. 48 h p.t. cells were lysed using the denaturing CEB. VP30 phosphorylation was assessed by SDS-PAGE (3.3.1) and western blotting (3.3.3). Total VP30 was stained with mouse anti-FLAG and goat anti-mouse 780 nm antibodies, phosphorylated VP30 with rabbit anti-pS29 and goat anti-rabbit 680 nm antibodies. Staining of GP and NP (with goat anti-GP/NP and donkey anti-goat 780 nm antibodies), as well as VP35 (not shown), served as expression controls. **(D)** Quantification of several independent western blot experiments (3.3.4). For normalization of $VP30_f$_AA_A29S amounts, the signal strength obtained with the phosphospecific antibody was divided by the signal-strength obtained with the anti-FLAG antibody. The result obtained for $VP30_f$_AA_A29S single expression was set to 100 %. Unless otherwise noted, asterisks indicate the statistical deviation from $VP30_f$_AA_A29S single expression.

To inhibit VP30 dephosphorylation *in vivo*, we incubated the cells with increasing amounts of OA. Now the signal intensity of the phosphospecific antibody was similar to the anti-FLAG staining for all combinations of viral proteins (Figure 14 B and C).
In Figure 14 D, VP30 protein bands from several independent experiments were quantified. The signal obtained with the phosphospecific antibody was normalized to the signal obtained with the anti-FLAG antibody. The observed differences of the phosphorylation signal were highly significant in the control (white bars). The most obvious decrease in VP30 phosphorylation was seen as soon as NP was co-expressed with $VP30_f$_AA_A29S. The amount of phosphorylated $VP30_f$_AA_A29S was again significantly lower when all viral proteins were expressed. Figure 14 D, grey bars, quantifies the effect of phosphatase inhibition on VP30 phosphorylation. OA was able to reverse the effect of NP on VP30 phosphorylation.

Taken together, we propose that other viral proteins, especially the nucleoprotein NP, can shift the phosphorylation status of serine 29 of VP30 towards dephosphorylation, as serine 29 was preferentially dephosphorylated within NP-induced inclusion bodies. Since the phosphorylation status was changed upon addition of the PP1 / PP2A inhibitor OA, it seems that NP recruits phosphatases, which can dephosphorylate VP30 when interacting with NP. Besides NP, other viral proteins also influence the phosphorylation status of VP30, since the lowest signal for phosphorylated serine 29 was observed when all viral proteins were recombinantly expressed.

4.3.3 VP30 Phosphorylation during Infection with recEBOV_wt and recEBOV_S29

The examination of VP30 phosphorylation during the EBOV life cycle was of great interest. HUH-7 cells were infected with recEBOV_wt and recEBOV_S29, and VP30 phosphorylation was assessed by IFA. Figure 15 A confirms the expression of VP30, Figure 15 B assesses phosphorylation of VP30 serine 29. Staining of the infected cells with an NP-specific antibody served to visualize viral inclusion bodies.

Our first observation was that in EBOV infected cells neither VP30_wt nor VP30_AA_A29S was detected by the phosphospecific antibody (Figure 15 B, i and iv, respectively). However, staining with an anti-VP30 antibody confirmed that VP30 was present and mainly localized inside the NP-induced inclusion bodies (Figure 15 A, i and iv).

In order to block the putative phosphatase activity recruited by viral proteins, we treated the cells with OA to shift VP30 towards a phosphorylated state. In line with our minigenome assay results (Figure 5 to Figure 7), recEBOV_wt was very sensitive to treatment with OA. Most likely, phosphatase inhibition resulted in hyper-phosphorylation of the six N-terminal serine residues of VP30_wt, which then lost its transcriptional support activity. This, in turn, suppressed EBOV propagation, explaining the missing signal for NP or VP30_wt (Figure 15 A and B, ii and iii).

recEBOV_S29 on the other hand, which has serine 29 as the only phosphoacceptor site within the N-terminal VP30 region, was able to propagate under treatment with OA because phosphorylation of a single VP30 serine residue is not sufficient to impair viral transcriptional activity (Figure 6). Upon OA treatment, the phosphospecific antibody detected VP30_AA_A29S in infected cells (Figure 15 B, v and vi), indicating that treatment of cells with the phosphatase inhibitor was able to shift the balance of serine 29 towards the phosphorylated state. The signal was observed mostly in large inclusion bodies. When cell lysates from the same experiment were analyzed in WB analysis, the phosphospecific antibody did not detect phosphorylated VP30_AA_A29S despite treatment with OA, indicating that phosphorylation was still rather weak (data not shown).

Our results reveal that during recEBOV infection only a minor fraction of VP30 serine 29 is phosphorylated, most likely due to the activity of cellular phosphatases. These observations are in agreement with the transfection studies. When all EBOV proteins were recombinantly expressed, we observed a signal for the phosphospecific antibody only after phosphatase inhibition (Figure 14, lane 8).

Even though unexpected, our results do not contradict the earlier observations that phosphorylated VP30 interacts stronger with NP, but rather adds new and complementing information[24,165]. We presume that the high affinity of phosphorylated

VP30 for NP facilitates recruitment of VP30 to viral inclusion bodies where VP30 can initiate viral transcription upon dephosphorylation. The phosphatase activity in the inclusion bodies would assure adequate transcriptional support activity of VP30, since highly phosphorylated VP30 does not support viral transcription.

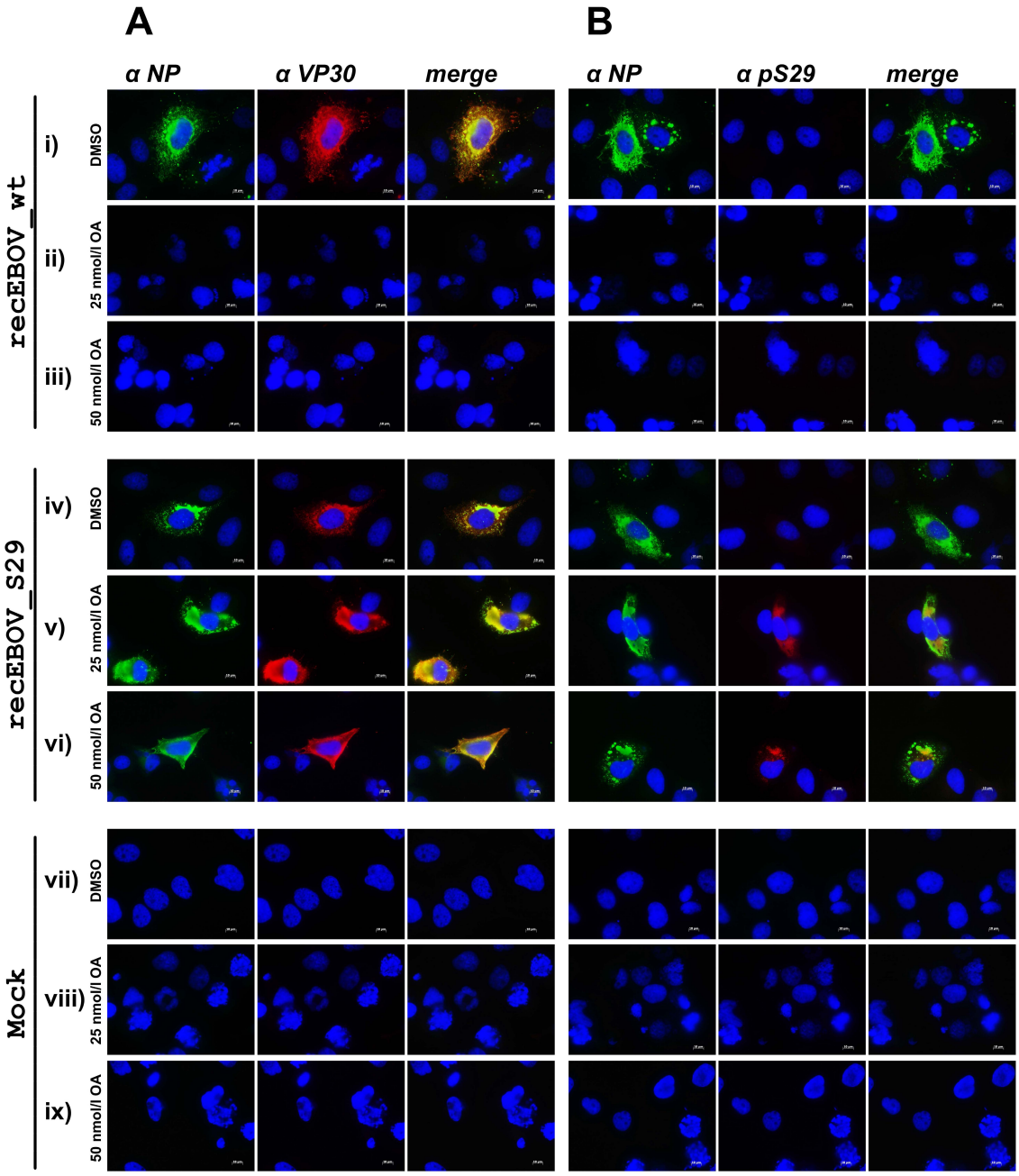

Figure 15: VP30 Serine 29 is Predominantly Dephosphorylated during Infection with recEBOV.
(A) - (B) Indirect immunofluorescence analysis of HUH-7 cells infected with recEBOV_wt or recEBOV_S29 at an MOI of 3 (3.3.5 and 3.2.8). The growth medium contained either DMSO (control), 25 nmol/l OA, or 50 nmol/l OA, 1 h p.i. At twenty-four h p.i. cells were fixed with PFA. NP was stained with chicken anti-NP and goat anti-chicken *Alexa 488* antibodies, nuclei were visualized with DAPI. In **(A)**, total VP30 was stained with rabbit anti-VP30 and goat anti-rabbit *Alexa 594* antibodies. In **(B)**, phosphorylated VP30 was stained with rabbit anti-pS29 and goat anti-rabbit *Alexa 594* antibodies.

4.4 Investigations on Putative VP30 Kinase Recognition Motifs

An efficient interaction between the catalytic center of the kinase and the phosphoacceptor site of the substrate is largely dependent on the neighboring amino acids of the phosphorylation site (P-site), both N- and C-terminal of the P-site[244]. The amino acids of the substrate interact with the active site of the kinase to ensure efficient phosphorylation and positioning of the P-site by adding important binding energy to the interaction[244]. Many conserved phosphoacceptor motifs have been described[9]. Some of these, such as the amino acid motif S-X-X-E/D, are relatively specific for a certain kinase. Other phosphorylation motifs, such as the common R-X-X-S sequence, are used by a large number of kinases (Table 5). In Figure 16, potential kinase recognition motifs for the six N-terminal serine residues of VP30 are depicted[9,278]. Many residues of these phosphorylation motifs, including R26 and R28, are conserved in the different *Ebolavirus* species (data not shown).

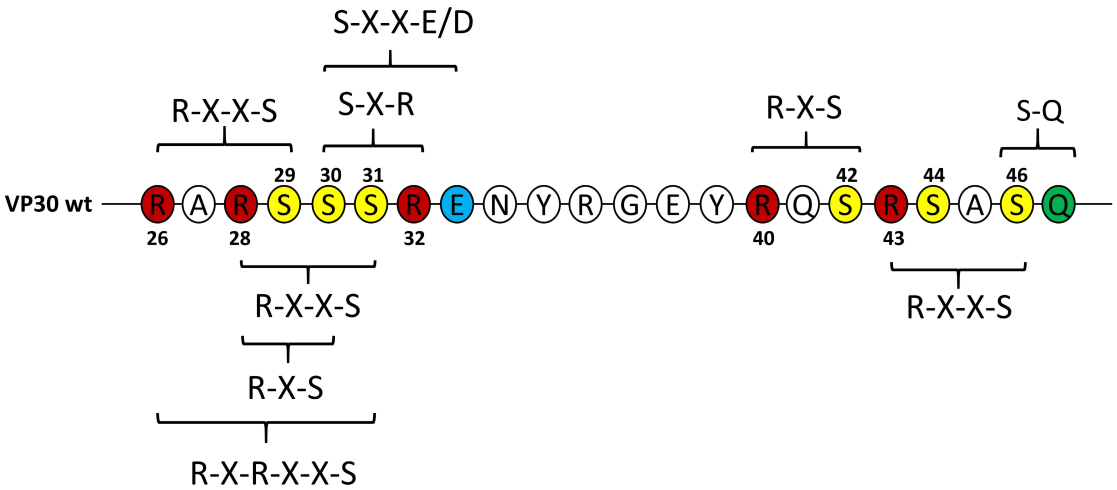

Figure 16: Putative VP30 Phosphorylation Motifs.
Illustration of potential EBOV VP30 phosphorylation motifs in the two N-terminal serine clusters. Many kinases are known to recognize specific amino acids close to the phosphorylation site. The phosphoacceptor serine residue is depicted in yellow, arginine in red, glutamate in blue, and glutamine in green. X = any amino acid.

Minimal phosphorylation motif	Substrate motif for
R-X-X-**S**	PKA, PKC, CAMK, ROCK, RSK, CHK2, PKG
R-X-R-X-X-**S**	PKB (Akt), MAPKAPK1, RSK, p70 S6
R-X-**S**	PKA
S-X-X-E/D	Casein kinase II
S-X-R	PKC, PKG
S-Q	ATM / ATR, DNA-dependent protein kinase
R-X-X-**S**-X-X-R	CLK1

Table 5: Putative VP30 Phosphorylation Motifs and Examples of Relevant Kinases.

In the following experiments, we tried to confirm the biological relevance of the putative kinase recognition motifs for VP30 phosphorylation.

Initially, we expressed VP30 arginine mutants and analyzed the phosphorylation status of serine 29 with the phosphospecific anti-pS29 antibody. The arginine residues of the putative kinase recognition motifs were replaced by the uncharged alanine in the background of $VP30_f$_AA_A29S (Figure 17 C). In immunofluorescence analysis, the expression of the VP30 mutants was verified with an anti-VP30 antibody (Figure 17 A), and in western blot analysis with an anti-FLAG antibody (Figure 17 B). In both assays, the phosphospecific antibody did not recognize $VP30_f$_AA_A29S_R26A, which does not contain the putative R-X-X-S kinase recognition motif for S29 (Figure 17 A, ii and Figure 17 B, lane 5). Likewise, a double arginine mutant was not recognized (Figure 17 A, iv and Figure 17 B, lane 7). The mutant $VP30_f$_AA_A29S_R28A on the other hand, which still contains the R-X-X-S motif for phosphorylation of serine 29, was recognized by the phosphospecific antibody, albeit weaker than $VP30_f$_AA_A29S (Figure 17 A, iii and Figure 17 B, lane 6).

These results are a first hint that phosphorylation of serine residue 29 is dependent on the common kinase recognition motif R-X-X-S involving arginine residue 26. However, this experiment needs to be interpreted carefully, since the phosphospecific antibody is a peptide antibody, and mutation of any amino acids located within the peptide sequence could lead to loss of detection by the antibody without necessarily influencing the phosphorylation status of serine 29 itself.

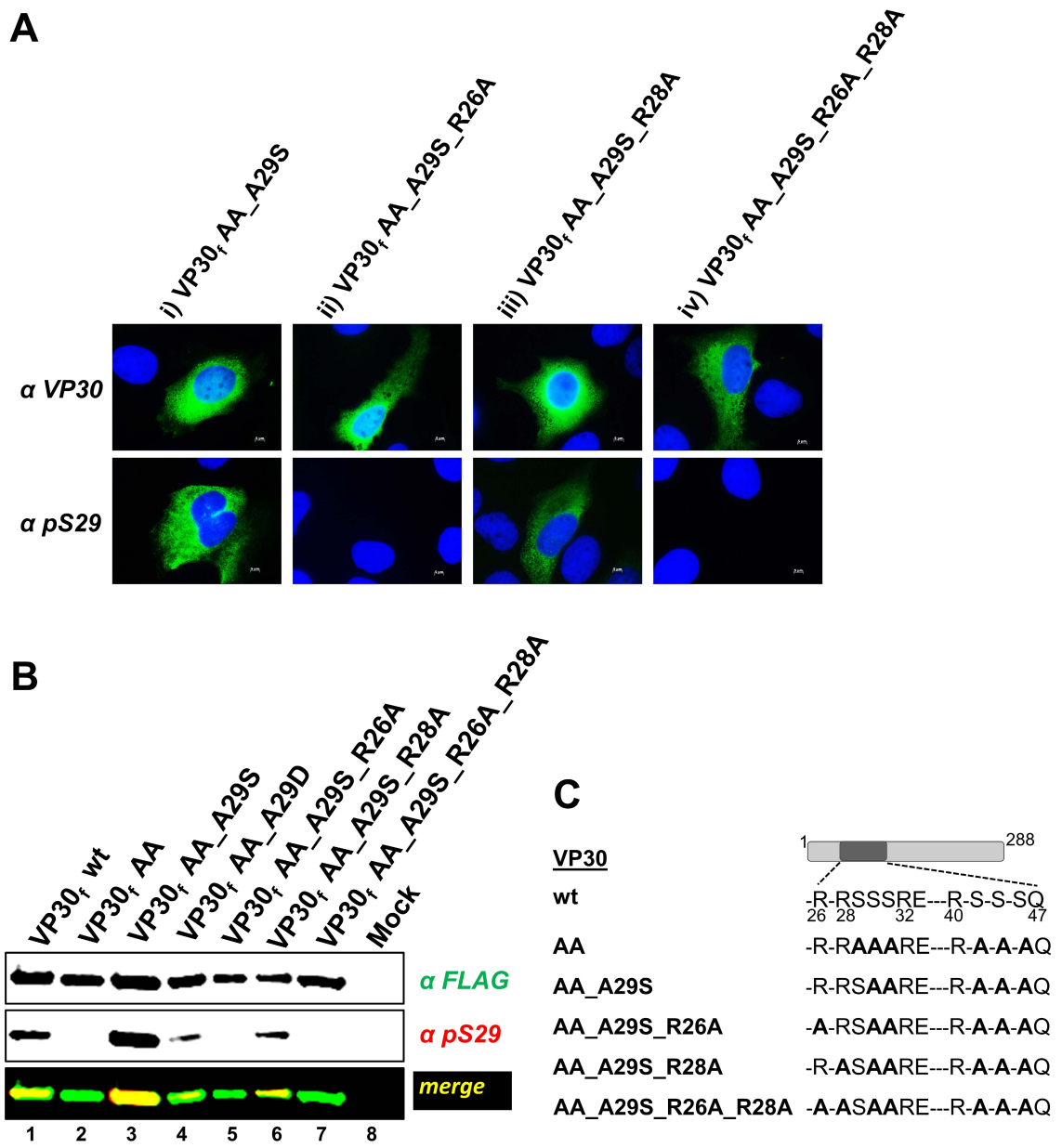

Figure 17: Phosphorylation of VP30 Serine 29 is Dependent on a Common R-X-X-S Kinase Recognition Motif.

(A) Indirect immunofluorescence analysis of HUH-7 cells expressing VP30$_f$_AA_A29S or arginine mutants (3.3.5). Cells were fixed 20 h post transfection. Total VP30 was stained with guinea pig anti-VP30 and goat anti-guinea pig *Alexa 488* antibodies. Phosphorylated VP30 was stained with rabbit anti-pS29 and goat anti-rabbit *Alexa 488* antibodies. Nuclei were visualized with DAPI. **(B)** Western blot analysis of HEK-293 cells expressing VP30$_f$_AA_A29S or arginine mutants (lanes 3 and 5-7) (3.3.3). 24 h p.t. cells were lysed in a denaturing cell extraction buffer. VP30 phosphorylation was assessed by SDS-PAGE (3.3.1) and western blotting (3.3.3). Total VP30 was stained with mouse anti-FLAG and goat anti-mouse 780 nm antibodies, phosphorylated VP30 with rabbit anti-pS29 and goat anti-rabbit 680 nm antibodies. **(C)** Schematic presentation of the VP30 arginine mutants. The putative kinase recognition motifs were mutated to alanine to impair binding of VP30 to the catalytic center of the kinase. For a more detailed overview of VP30 mutants refer to the Appendix.

Hence we wanted to confirm the significance of the putative kinase recognition motifs for VP30 function in an EBOV-specific minigenome assay (Figure 18 A). We mutated the arginine residues of the potential VP30 kinase recognition motifs to alanine, both in the background of $VP30_f$_wt and $VP30_f$_AA_A29_31S (Figure 18 B). The latter mutant showed a high sensitivity to OA, indicating a significant role of phosphorylation events at S29 and S31 for transcriptional regulation (Figure 6 and Figure 7).

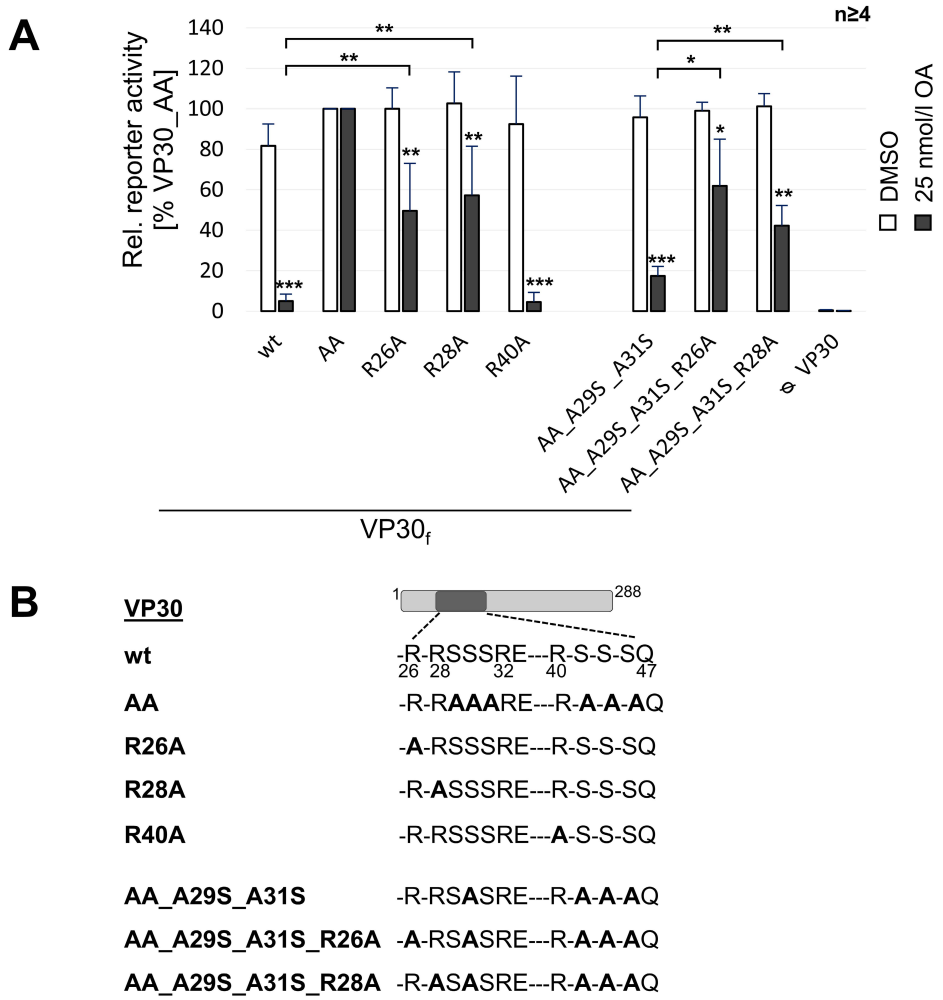

Figure 18: Hyper-phosphorylation of VP30 Serine 29 and Serine 31 Induced by OA Treatment is dependent on Arginine 26 and Arginine 28.

(A) Reporter gene activity of VP30 arginine mutants in an EBOV-specific minigenome assay under **control conditions (white bars)** or **25 nmol/l OA (black bars)** (3.2.4). HEK-293 cells were transfected with all plasmids needed for the EBOV-specific minigenome assay, including $VP30_f$_wt or mutants. Cells were treated either with 0.025 % DMSO (= control) or 25 nmol/l OA at 0 h post transfection. 24 h p.t. cells were lysed and the reporter gene activity was measured in a luciferase assay. Since the transcriptional activity of $VP30_f$_AA cannot be influenced by phosphorylation in the N-terminal serine cluster, results obtained with $VP30_f$_AA were set to 100 %. Statistical significance is shown in relation to $VP30_f$_AA, unless otherwise noted. **(B)** Schematic presentation of the VP30 arginine mutants. The putative kinase recognition motifs were mutated to alanine to impair binding of VP30 to the catalytic center of the kinase. For a more detailed overview of VP30 mutants refer to the Appendix.

In the absence of OA (control experiment, Figure 18 A, white bars), the reporter gene activity of the VP30 arginine mutants was similar to $VP30_f$_wt. When the phosphatase inhibitor OA was added (Figure 18 A, black bars), transcriptional support activity of $VP30_f$_wt was completely abolished as OA results in VP30 hyper-phosphorylation. Contrary, when arginine 26 or 28 were mutated to alanine, OA treatment resulted in only 50 % reduction of the reporter activity (Figure 18 A, black bars, VP30_R26A and VP30_R28A). The same was also true when we introduced the arginine to alanine substitutions in the background of $VP30_f$_AA_A29_31S (Figure 18 A, black bars, $VP30_f$_AA_A29_31S_R26A and $VP30_f$_AA_A29_31S_R28A). As an additional control, the mutant $VP30_f$_R40A was tested. Arginine 40 could serve as a potential R-X-S kinase recognition motif for serine 42 (Figure 16). In Figure 7 we demonstrated that phosphorylation at serine 42 is not essential for transcriptional downregulation, because the serine to alanine mutant VP30_S42A was still transcriptionally inactive during phosphatase inhibition. Accordingly, $VP30_f$_R40A was also transcriptionally inactive in the minigenome assay during treatment with OA (Figure 18 A, black bar).

This results illustrates that the transcriptional support activity of the VP30 arginine mutants is not very sensitive to OA. We think that the respective serine residues cannot become hyper-phosphorylated when arginine 26 or 28 are missing, because the acting kinases are dependent on the two arginine residues. Our results suggest that both arginine 26 and arginine 28 serve as kinase recognition motifs for phosphorylation of serine residues 29 and 31. Mutation of either of the two arginine motifs impairs efficient phosphorylation at these sites.

Finally, the importance of the VP30 kinase recognition motifs was validated in an EBOV-specific trVLP assay. Earlier we demonstrated that phosphorylation of VP30 serine 29 is important to support primary transcription (Figure 8). However, in previous experiments the primary transcriptional support activity of VP30 was not exclusively dependent on serine 29, since phosphorylation of the second serine cluster alone (S42 / S44 / S46) was also sufficient for rendering VP30 active in primary transcription[26]. We therefore hypothesized that mutation of arginine 26 / 28 in the background of $VP30_f$_wt would not impair primary transcriptional activity, because the second serine cluster would not be affected by these mutations and still be available for phosphorylation. Mutation of arginine 26 in the background of $VP30_f$_AA_A29S, however, should abolish primary transcriptional activity if phosphorylation of serine 29 indeed depends on the R-X-X-S motif.

In the producer cells, all VP30 arginine mutants enabled secondary viral transcription (Figure 19, white bars). Mutation of arginine 26 / 28 in the background of all six VP30 serine residues did not affect the primary transcriptional activity in the indicator cells (Figure 19, grey bars, $VP30_f$_R26A and $VP30_f$_R28A). In the background of $VP30_f$_AA_A29S, however, only mutation of arginine 26 abolished primary transcriptional activity completely, whereas mutation of arginine 28 did not (Figure 19, grey bars, $VP30_f$_AA_A29S_R26A and $VP30_f$_AA_A29S_R28A). Incorporation of the VP30 mutants into the purified trVLP's was confirmed by western blotting (Figure 19 B).

Altogether, these findings establish that efficient phosphorylation of VP30 serine 29 and serine 31 is dependent on the R-X-X-S kinase recognition motifs, with arginine 26 playing an essential role for serine 29 phosphorylation.

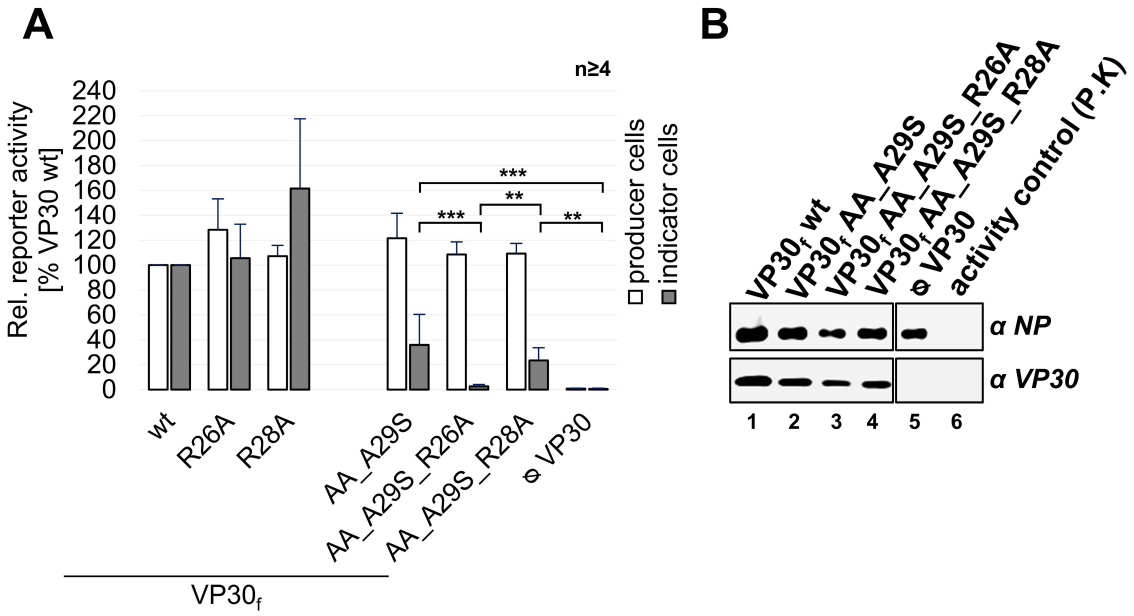

Figure 19: Phosphorylation of VP30 Serine 29 Depends on a R-X-X-S Kinase Recognition Motif.
(A) Reporter gene activity of VP30 arginine mutants in **producer (white bars)** and **indicator cells (grey bars)** in an EBOV-specific trVLP assay (3.2.5). HEK-293 cells (= producer cells) were transfected with all plasmids required for the EBOV-specific trVLP assay, including $VP30_f$_wt or mutants. Producer cells were lysed 72 h p.t. and a luciferase assay was performed (white bars). trVLPs were collected from the supernatants of the producer cells, purified by ultracentrifugation, and used to infect naïve HUH-7 cells (= indicator cells). Reporter gene activity was measured 60 h p.i. (grey bars). Results obtained with $VP30_f$_wt were set to 100 %. Results for $VP30_f$_R26A and $VP30_f$_R28A were kindly provided by Dr. Nadine Biedenkopf. For an overview of VP30 arginine mutants refer to the Appendix. **(B)** Western blot analysis of purified trVLPs (3.3.3). Aliquots of the trVLPs were analyzed for the incorporation of $VP30_f$_wt / mutants in a proteinase K digestion assay (3.2.5). Enzymatic efficiency was controlled by addition of Triton™ X-100 (lane 6). NP was stained with chicken anti-NP and donkey anti-chicken 680 nm antibodies, VP30 was stained with rabbit anti-VP30 and goat anti-rabbit 680 nm antibodies.

4.5 Characterization of VP30 Phosphorylation *in vitro*

For further characterization of VP30 phosphorylation, we established an *in vitro* VP30 phosphorylation and dephosphorylation assay, which is based on the addition of enzyme co-substrates or inhibitors and recognition of phosphorylated VP30 by the anti-pS29 antibody. Cell lysates expressing $VP30_f$_AA_A29S provided the source for kinases and phosphatases. Figure 20 schematically pictures the VP30 serine 29 phosphorylation and dephosphorylation reaction. Cellular kinases need ATP^{4-}, complexed by divalent metal ions, usually two Mg^{2+}-ions, as a co-substrate for phosphorylation of proteins[2]. Ethylenediaminetetraacetic acid (EDTA) complexes and removes Mg^{2+}- and Ca^{2+}-ions from the lysate, whereas Ethylene glycol-bis(β-aminoethyl ether)-N,N,N',N'-tetraacetic acid (EGTA) only chelates Ca^{2+}-ions. N-ethylmaleimide (NEM) irreversibly inactivates kinases *in vitro* by alkylation of thiol-groups[245,274]. Okadaic acid (OA) inhibits PP1 and PP2A and is also part of a commercially available mixture of several phosphatase inhibitors (PhosSTOP™). Sodium fluoride (NaF) is a commonly used general phosphatase inhibitor and is part of the denaturing cell extraction buffer (CEB, Invitrogen).

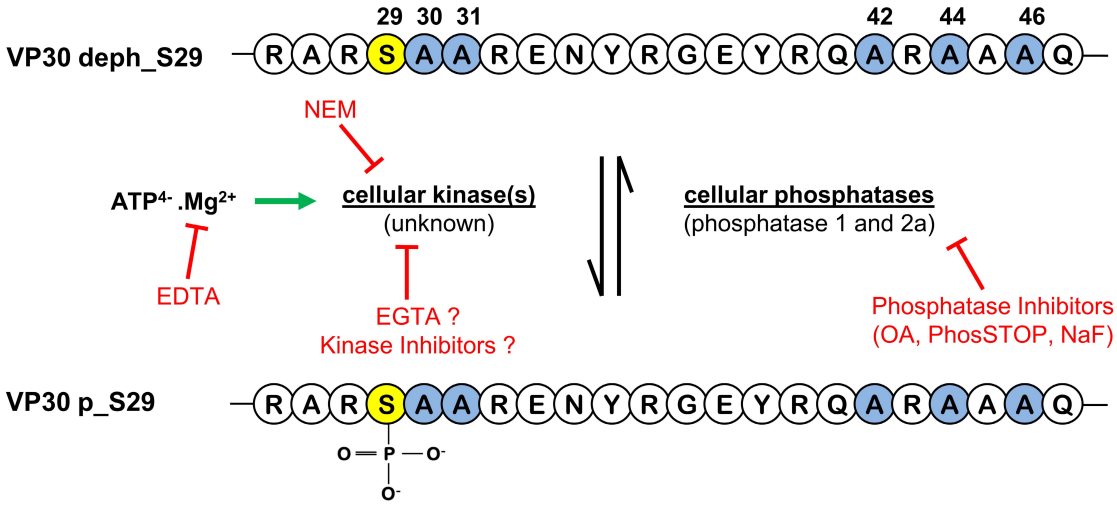

Figure 20: Schematic Model of VP30_AA_A29S Serine 29 Phosphorylation and Dephosphorylation. *In vitro*, the reaction equilibrium between dephosphorylated and phosphorylated VP30 can be shifted by addition of enzyme co-substrates, inhibitors, or activators. Monitoring of VP30 serine 29 phosphorylation status is possible with the phosphospecific peptide antibody anti-pS29. VP30_AA_A29S is depicted from amino acid 26 to amino acid 47.

In Figure 21 A, HEK-293 cells were transfected with a plasmid encoding $VP30_f$_AA_A29S. At 48 h p.t., cells were harvested and the in vitro rephosphorylation assay was started in test tubes. If cells were lysed in a buffer containing phosphatase inhibitors, $VP30_f$_AA_A29S serine 29 phosphorylation could be detected by the phosphospecific antibody in western blot analysis (lanes 1-3, "Input"). Between the tested phosphatase inhibitors, no significant difference in signal strength was observed. In contrast, cell lysis under non-denaturing conditions in a TM lysis buffer without phosphatase inhibition, followed by incubation for at least 20 min at room temperature, resulted in no signal for phosphorylated serine 29 (lane 5). After this dephosphorylation step, it was possible to rephosphorylate VP30 *in vitro* by addition of ATP +/- OA to the cell lysates. Cell lysates were incubated for 1 h at 37 °C to allow rephosphorylation of VP30 by cellular kinases within the cell lysate. With increasing amounts of ATP, the signal for the phosphospecific antibody got stronger (lanes 7-11). The addition of OA to the cell lysate alone did not change the VP30 phosphorylation state (lane 6).
The *in vitro* rephosphorylation reaction was fast and efficient (Figure 21 B). After 10 min of incubation with ATP alone, phosphorylated VP30 was detected by the phosphospecific antibody (lane 4).
We next examined the characteristics of the kinase(s) phosphorylating VP30 *in vitro* in order to narrow down potential kinase candidates, which specifically phosphorylate VP30 serine 29 (Figure 21 C). If no Mg^{2+} was provided with the lysis buffer and endogenous Mg^{2+} was withdrawn from the reaction by EDTA, rephosphorylation did not take place (lane 3). In contrast, Ca^{2+} seemed to be expandable for the phosphorylation reaction (lane 4) and we therefore assume that VP30 can be phosphoylated at serine 29 by kinases that are not dependent on Ca^{2+}. The rephosphorylation reaction was stronger in the presence OA (lane 7 vs lane 6). It was possible to inactivate endogenous kinases with the alkylating agent N-ethylmaleimide (lane 8, VP30 running slightly higher because of protein alkylation). The rephosphoryation reaction was less efficient at lower temperatures (lane 10) and was inhibited by heat-denaturation of cellular kinases prior to addition of ATP (lane 12), which implies that the observed *in vitro* phosphorylation reaction is indeed catalyzed by cellular kinases and not by the spontaneous addition of a phosphate-group to the VP30 serine 29 residue.

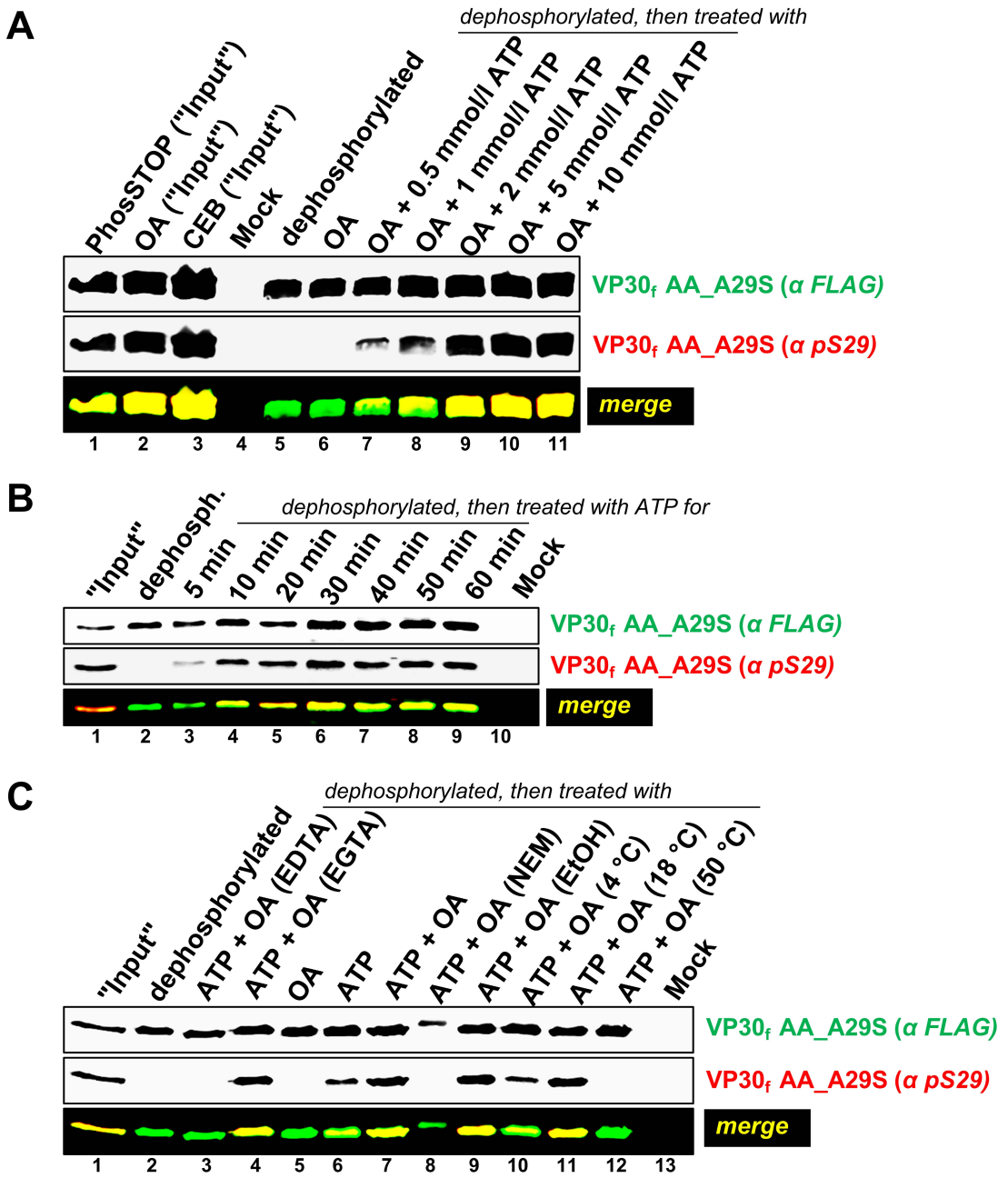

Figure 21: Characteristics of VP30 Serine 29 *in vitro* Phosphorylation.

(A) - (C) Hek-293 cells were transfected with a plasmid encoding VP30$_f$_AA_A29S. At 48 h post transfection cells were lysed for an *in vitro* VP30 dephosphorylation and rephosphorylation assay (3.4.1). VP30 phosphorylation was assessed by SDS-PAGE (3.3.1) and western blotting (3.3.3). Total VP30 was stained with mouse anti-FLAG and goat anti-mouse 780 nm antibodies, phosphorylated VP30 with rabbit anti-pS29 and goat anti-rabbit 680 nm antibodies. (**A**) Several phosphatase inhibitors were tested for their ability to prevent dephosphorylation of VP30 in the cell lysate ("Input", lane 1-3). The remaining cells were lysed in a non-denaturing TM buffer containing no phosphatase inhibitors and incubated for 30 min at 37 °C to allow dephosphorylation of VP30 by cellular phosphatase 1 / 2A (lane 5). After the dephosphorylation step, increasing concentrations of ATP (+1 µmol/l OA) were added to the reaction, and cell lysates were again incubated for 1 h at 37 °C. (**B**) Timeline for the *in vitro* rephosphorylation step with 2 mmol/l ATP (without OA). (**C**) Characteristics of the kinase(s) phosphorylating VP30 serine 29 *in vitro*. EDTA was added to a TBS buffer, EGTA to a TM buffer. ATP concentration was 2 mmol/l. EtOH = Ethanol (NEM-control). *In vitro* reactions were stopped by addition of sample buffer and heating.

In a first attempt to further characterize the kinase(s) that phosphorylate VP30, the broad-spectrum kinase inhibitor staurosporine was tested *in vivo* for its effect on VP30 serine 29 phosphorylation. These experiments suffered from high cytotoxicity and made any observed effects on VP30 phosphorylation difficult to interpret (data not shown).
We therefore tested the potential of several kinase inhibitors to inhibit rephosphorylation of VP30 serine 29 after *in vitro* dephosphorylation (Figure 22). The kinase inhibitors were used at high concentrations since cytotoxicity was no longer an issue. Besides staurosporine, which is a broad-spectrum serine / threonine kinase inhibitor, heparin and TBCA were tested. At low concentrations, TBCA is a selective casein kinase II inhibitor (IC50 = 0.11 µmol/l). According to the known CK2 kinase consensus sequence S-X-X-E/D, this specific kinase is not responsible for phosphorylation of VP30 serine 29 or serine 31. Both TBCA and staurosporine are ATP competitive inhibitors. Heparin, a polyanion, is thought to mimic the viral RNA.
In comparison to the controls without kinase inhibitiors (lane 1), heparin and staurosporine were able to inhibit *in vitro* rephosphorylation of VP30 partially, but only at high concentrations (Figure 22 A and B). TBCA had only a marginal effect on rephosphorylation of VP30 (Figure 22 C).

To sum up, the established VP30 *in vitro* phosphorylation assay shares the common characteristics of known kinase reactions.

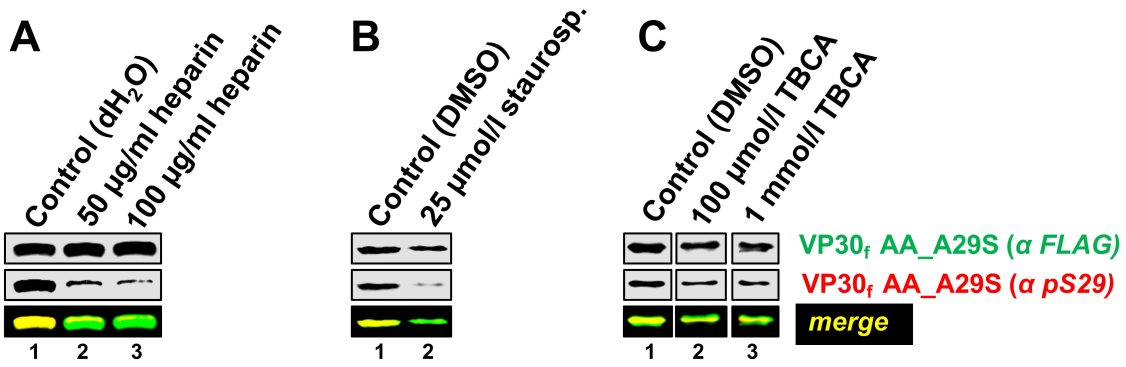

Figure 22: *In vitro* Phosphorylation of VP30 is Inhibited by Kinase Inhibitors.
(A) - (C) Hek-293 cells were transfected with a plasmid encoding $VP30_f$_AA_A29S. At 48 h p.t., cells were lysed in a non-denaturing TM buffer for an *in vitro* phosphorylation assay (3.4.1). Lysates were incubated for at least 30 min at 37 °C to allow dephosphorylation of VP30 by cellular phosphatase 1 / 2A. Next, 2 mmol/l ATP and 1 µmol/l OA were added to the reaction samples and cell lysates were incubated for 1 h at 37 °C, either under control conditions or with a kinase inhibitor (3.4.6). Kinase inhibitors were added 5 min prior to addition of ATP and OA. Reactions were stopped by addition of sample buffer and heating. VP30 phosphorylation was assessed by SDS-PAGE (3.3.1) and western blotting (3.3.3). Total VP30 was stained with mouse anti-FLAG and goat anti-mouse 780 nm antibodies, phosphorylated VP30 with rabbit anti-pS29 and goat anti-rabbit 680 nm antibodies. **(A)** Influence of heparin on VP30 *in vitro* rephosphorylation. (**B)** Influence of staurosporine on VP30 *in vitro* rephosphorylation. (**C)** Influence of TBCA on VP30 *in vitro* rephosphorylation.

4.6 Interaction between VP30 and Kinases

Kinases recognize their substrates on multiple levels, which includes the local consensus sequence of the substrate, e.g. the phosphorylation motif R-X-X-S on VP30 for serine 29, as well as distal kinase docking motifs on the substrate. Although the binding of a specific consensus sequence to the catalytic center of a specific kinase is often required for efficient substrate phosphorylation, this interaction is usually weak and only transient[2]. Contrary, the binding between distal recognition motifs on the substrate and auxiliary domains on the kinase is very important for stable recruitment of the kinase to the substrate and a high affinity enzyme-substrate interaction[2,57,191,244]. For many protein kinases, these distal interactions are based on short linear motifs (SLIMs) either on the substrate itself or scaffolding proteins, which interact with docking surfaces of the kinase domain[85,126,177,247,277]. SLIMs (5-20 amino acids in length), sometimes also termed docking-motifs or D-motifs, are usually located in intrinsically disordered segments of proteins, potentially far away from the phosphorylation site[277]. The disordered regions of the protein adopt a defined structure only when binding interacting proteins[52]. EBOV VP30 contains three regions which are predicted to be intrinsically disordered (aa 1 to 44, 120 to 140, and 268 to 288)[90,119].

To test if VP30 interacts with a cellular kinase, we combined an immunoprecipitation assay with an *in vitro* rephosphorylation assay. $VP30_f$_AA_A29S was immunoprecipitated alone as well as in combination with NP and VP35. For the expression controls, transfected HEK-293 cells were lysed in a buffer containing phosphatase inhibitors (Figure 23, lanes 1-4). Again, VP30 phosphorylation was stronger in single expression (lane 1) in comparison to co-expression with NP and VP35 (lane 3). Other aliquots of the transfected cells were lysed in a non-denaturing buffer without phosphatase inhibitors for immunoprecipitation with anti-FLAG agarose. Immediately after immunoprecipitation and washing of the beads, no signal could be obtained with the phosphospecific antibody (lanes 5 to 8), meaning that VP30 was completely dephosphorylated at serine 29 by cellular PP1 / PP2A during non-denaturing cell lysis. VP30 co-immunoprecipitated NP but not VP35 (lane 7), which might be explained by the low amount of VP35 observed in the expression controls (lanes 3-4).
Next, the washed beads - with the dephosphorylated $VP30_f$_AA_A29S still attached - were subjected to an *in vitro* phosphorylation assay by addition of ATP / OA and incubation at 37 °C (lanes 9-12). Staining of VP30 with the phosphospecific antibody in lanes 9 and 11 demonstrates that it was possible to rephosphorylate $VP30_f$_AA_A29S after the immunoprecipitation. A separate protein gel was stained with Coomassie, and

many distinct bands were seen in the immunoprecipitate of VP30, but not in the respective controls (data not shown).

This result indicates that at least one VP30-specific kinase co-precipitates with VP30 even in the absence of other viral proteins.

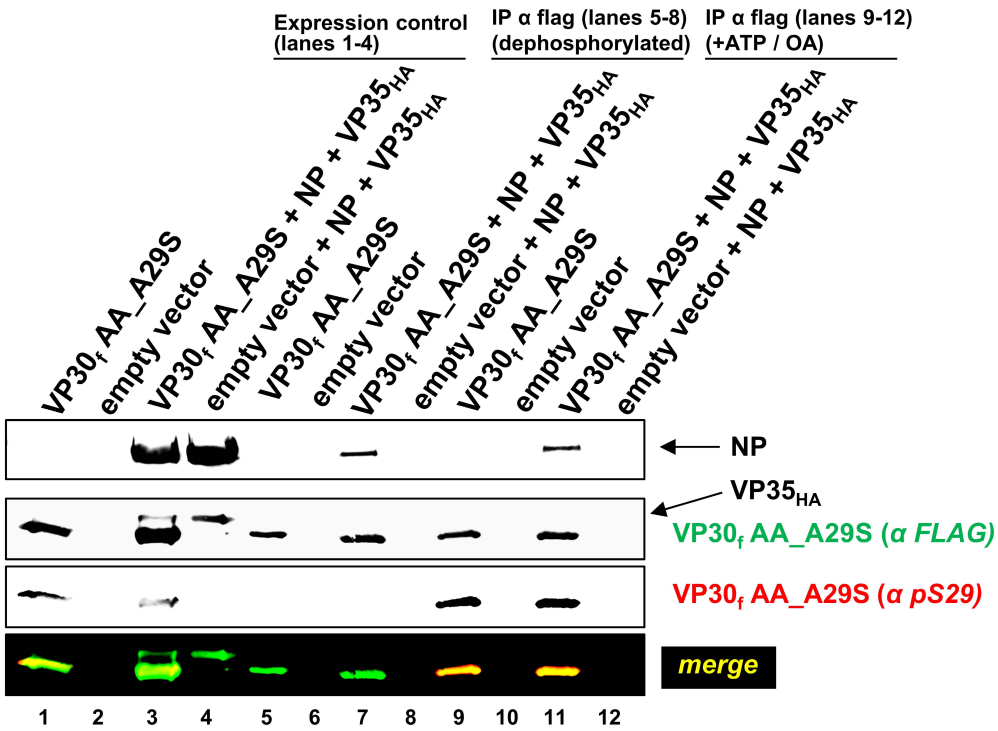

Figure 23: VP30 Co-precipitates an Unknown Cellular Kinase.

Anti-FLAG immunoprecipitation assay of $VP30_f$_AA_A29S (3.3.6) in combination with an *in vitro* phosphorylation assay (3.4.5). HEK-293 cells were transfected with plasmids encoding $VP30_f$_AA_A29S only or the combination of $VP30_f$_AA_A29S, NP, and $VP35_{HA}$. 48 h p.t. cells were lysed and the expression of the viral proteins was confirmed by western blotting using a denaturing cell extraction buffer (lanes 1-4). The remaing cells were lysed in a non-denaturing Co-IP buffer for 40 min at room temperature, without addition of phosphatase inhibitors. The lysate was centrifuged for removal of cellular debris and used for an immunoprecipitation step with anti-FLAG agarose (2 h at 4 °C). Beads were then washed at least four times. Aliquots were set aside immediately after the immunoprecipitation (lanes 5-8), while the other aliquots were treated for 1 h with ATP and OA at 37 °C (lanes 9-12). Reactions were stopped by addition of sample buffer and heating. Samples were analyzed by SDS-PAGE (3.3.1) and western blotting (3.3.3). Total VP30 was stained with mouse anti-FLAG and goat anti-mouse 780 nm antibodies, phosphorylated VP30 with rabbit anti-pS29 and goat anti-rabbit 680 nm antibodies. NP was stained with goat anti-GP / NP and donkey anti-goat 680 nm antibodies. $VP35_{HA}$ was stained with biotinylated mouse anti-HA and Streptavidin 680 nm antibodies.

4.7 Incorporation of a VP30 Serine 29-Specific Kinase into trVLPs

Many viruses incorporate host cell proteins, either actively or as passive bystanders[38]. For HIV, integration of several kinases has been described[41,84]. Since EBOV VP30 phosphorylation is essential during early time points of infection, either before or during primary transcription, we asked if trVLPs and the recEBOV_S29 incorporate a functional cellular kinase into newly formed virus like particles / virions, so that the integrated kinase can phosphorylate VP30 immediately after infection[26].

In Figure 24 A, all viral proteins were recombinantly expressed in HEK-293 cells in order to generate trVLPs. In lane 1, VP30 was for the most part dephosphorylated because of the influence of the other viral proteins on VP30 phosphorylation (see Figure 14), but it was possible to rephosphorylate VP30 in the cell lysate *in vitro* (lanes 3 and 4). Accordingly, no signal was observed for the phosphospecific antibody after the purification of trVLPs, meaning that $VP30_f$_AA_A29S was also mainly dephosphorylated at position 29 in the trVLPs (lanes 6 and 8). When trVLPs were treated with ATP and OA *in vitro* without a lysing agent, the phosphorylation state of $VP30_f$_AA_A29S did not change (lane 7). ATP cannot diffuse through the trVLP membrane due to its negative charge. If Triton™ X-100 was added to the buffer, it was possible to rephosphorylate serine 29 of VP30, indicated by a strong signal for the phosphospecific antibody (lanes 9 and 10).

This suggests VP30-specific kinases to be incorporated or associated with the outer membrane of trVLPs. To exclude an unspecific attachment of a kinase to the trVLPs, we treated the trVLPs with proteinase K to digest all unincorporated proteins. Following a second centrifugation step to purify the trVLPs from the digested proteins, we were still able to detect a signal for the phosphospecific antibody after *in vitro* phosphorylation (lane 13), implying that a VP30-specific kinase is indeed incorporated into the trVLPs. No GP is seen in lanes 12-14 due to digestion of the GP ectodomain by proteinase K.

When we repeated the experiment with recEBOV_S29, the phosphospecific antibody did not detect phosphorylated VP30 after *in vitro* phosphorylation of purified virions (Figure 24 B, lanes 9 and 10). So far, it is unclear whether this is a cell-type specific effect (trVLPs were produced in HEK-293 cells, virus in HUH-7 cells) or whether there is indeed no kinase incorporated into virions. In the cell lysate, a signal for phosphorylated VP30 serine 29 was again only observed after *in vitro* phosphorylation (lanes 3 and 4) because of the influence of the other viral proteins on VP30 phosphorylation status.

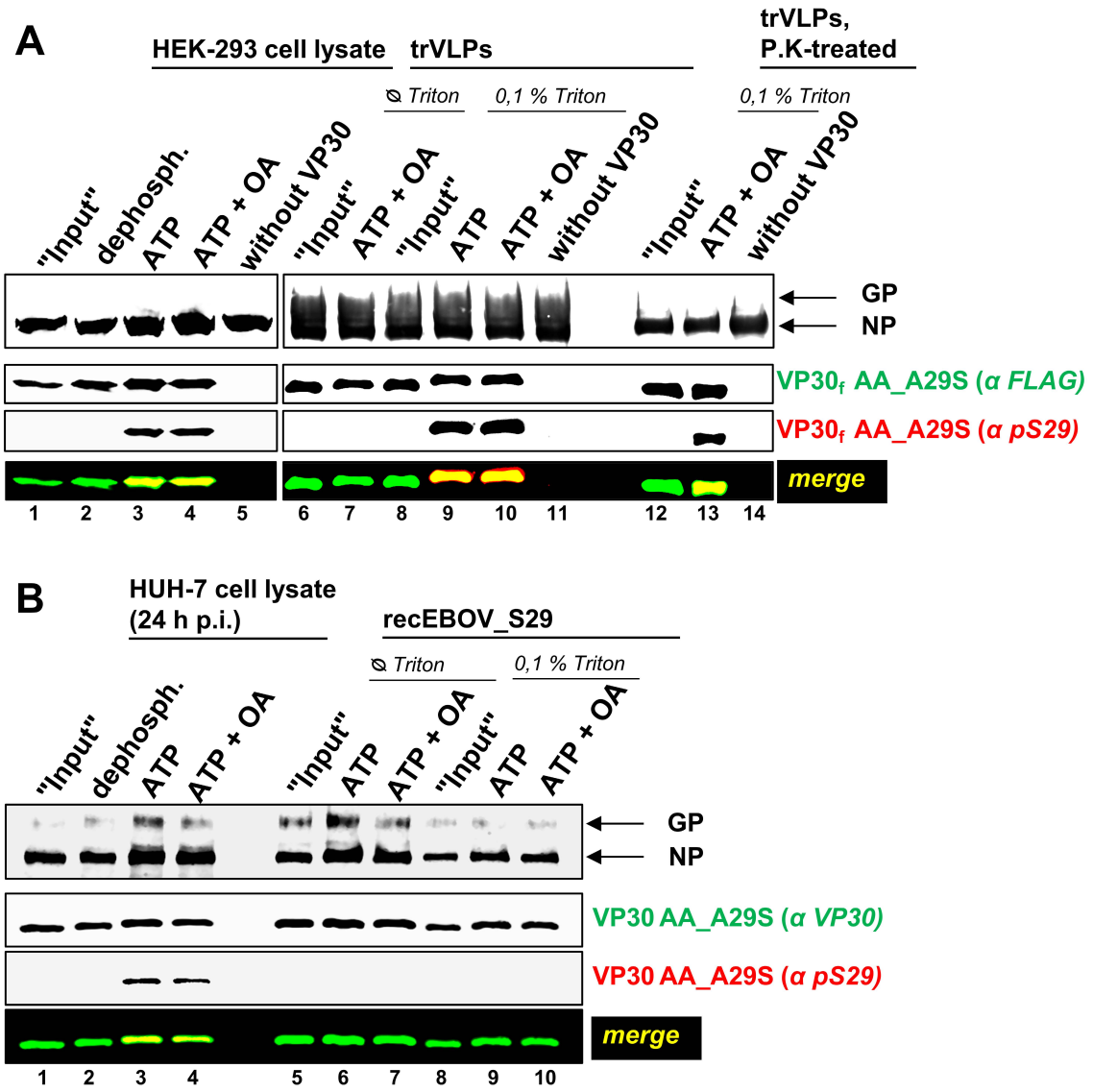

Figure 24: A VP30-Specific Kinase is Incorporated into trVLPs, but not into recEBOV_S29.
(A) Analysis of purified **trVLPs** for VP30-specific kinase activity (3.4.3). HEK-293 cells were transfected with plasmids encoding the seven viral proteins (including VP30$_f$_AA_A29S), the EBOV-specific minigenome under control of a T7 promotor, plus a T7 polymerase. 72 h p.t. cells were lysed and submitted to an *in vitro* phosphorylation assay (lanes 1-4) (3.4.1). trVLPs were purified from the supernatant by ultracentrifugation and incubated with ATP +/- OA, either without (lane 7) or with Triton™ X-100 (lanes 9 and 10). An aliquot of the purified trVLPs was treated with proteinase K for 30 min at 37 °C in order to digest all proteins that are not incorporated into the trVLPs (lanes 12-14). For removal of proteinase K, PMSF was added and trVLPs were again centrifuged through a 20 % sucrose cushion, followed by *in vitro* phosphorylation (lane 13). Phosphorylation of VP30 was assessed by SDS-PAGE (3.3.1) and WB analysis (3.3.3). Total VP30 was stained with mouse anti-FLAG and goat anti-mouse 780 nm antibodies, phosphorylated VP30 with rabbit anti-pS29 and goat anti-rabbit 680 nm antibodies. GP and NP were stained with goat anti-GP / NP and donkey anti-goat 780 nm antibodies. (**B)** Analysis of purified **recEBOV_S29** for VP30-specific kinase activity (3.4.4). HUH-7 cells were infected with recEBOV_S29 at a MOI of 3. Twenty four h p.i. viruses were purified through a 20 % sucrose cushion. The *in vitro* phosphorylation assay was performed as described above. Total VP30 was stained with guinea pig anti-VP30 and goat anti-guinea pig 780 nm antibodies, phosphorylated VP30 with rabbit anti-pS29 and goat anti-rabbit 680 nm antibodies. GP and NP were stained with goat anti-GP / NP and donkey anti-goat 780 nm antibodies.

4.8 VP30 Phosphorylation and Dephosphorylation in NP-Induced Inclusion Bodies

Our results indicated that VP30 dephosphorylation takes place in NP-induced inclusion bodies, most likely by recruitment of phosphatases by NP (Figure 11, Figure 12, and Figure 15). However, it remained an open question whether VP30 also gets phosphorylated by the so far unidentified cellular kinase(s) inside the inclusion bodies. We therefore examined VP30 phosphorylation *in situ* with cells on coverslips. Principally, this assay follows the same rules as outlined for the *in vitro* phosphorylation above, with the exception that it was performed on coverslips and not in test tubes. First, HUH-7 cells were transfected with plasmids encoding NP, VP35, and $VP30_f$_AA_A29S, leading to the formation of large inclusion bodies around the nucleus. After non-denaturing cell lysis, coverslips were washed several times to remove soluble material of the cytoplasm, while the cells were still adhering to the coverslips. The inclusion bodies are embedded in the cytoskeleton and are not washed away [217,218]. Therefore, this assay is assumed to be both *in vitro* and *in situ*.

In Figure 25, i (not *in vitro*, "Input" = "Status quo") the phosphorylated form of $VP30_f$_AA_A29S was detected in the cytoplasm but not in the inclusions bodies. Contrary, the anti-FLAG antibody stained $VP30_f$_AA_A29S also inside the inclusion bodies. After washing and *in vitro* dephosphorylation, no phosphorylated $VP30_f$_AA_A29S could be detected. Moreover, the anti-FLAG antibody no longer detected $VP30_f$_AA_A29S in the cytoplasm, suggesting that the washing of cells after cell lysis was effective (Figure 25, ii). As expected, addition of OA alone did not change the phosphorylation status (Figure 25, iii). We did not obtain a signal for the phosphospecific antibody when ATP alone was added (Figure 25, iv). Opposite to this, a very strong signal for phosphorylated $VP30_f$_AA_A29S was observed in virtually every transfected cell when ATP plus the phosphatase inhibitor OA were added together after the dephosphorylation step (Figure 25, v). After rephosphorylation of $VP30_f$_AA_A29S with ATP and OA, it was even possible to subsequently dephosphorylate VP30 again by washing away the rephosphorylation buffer and incubating the coverslips in a buffer without OA and ATP (Figure 25, vi). The rephosphorylation of VP30 was dependent on Mg^{2+}-, but not on Ca^{2+}-ions (Figure 25, vii and viii), and it was possible to inactivate kinases by the alkylating agent N-ethylmaleimide (NEM) (Figure 25, ix). Similar to Figure 22, it was possible to partially inhibit rephosphorylation of VP30 by addition of heparin or staurosporine (data not shown).

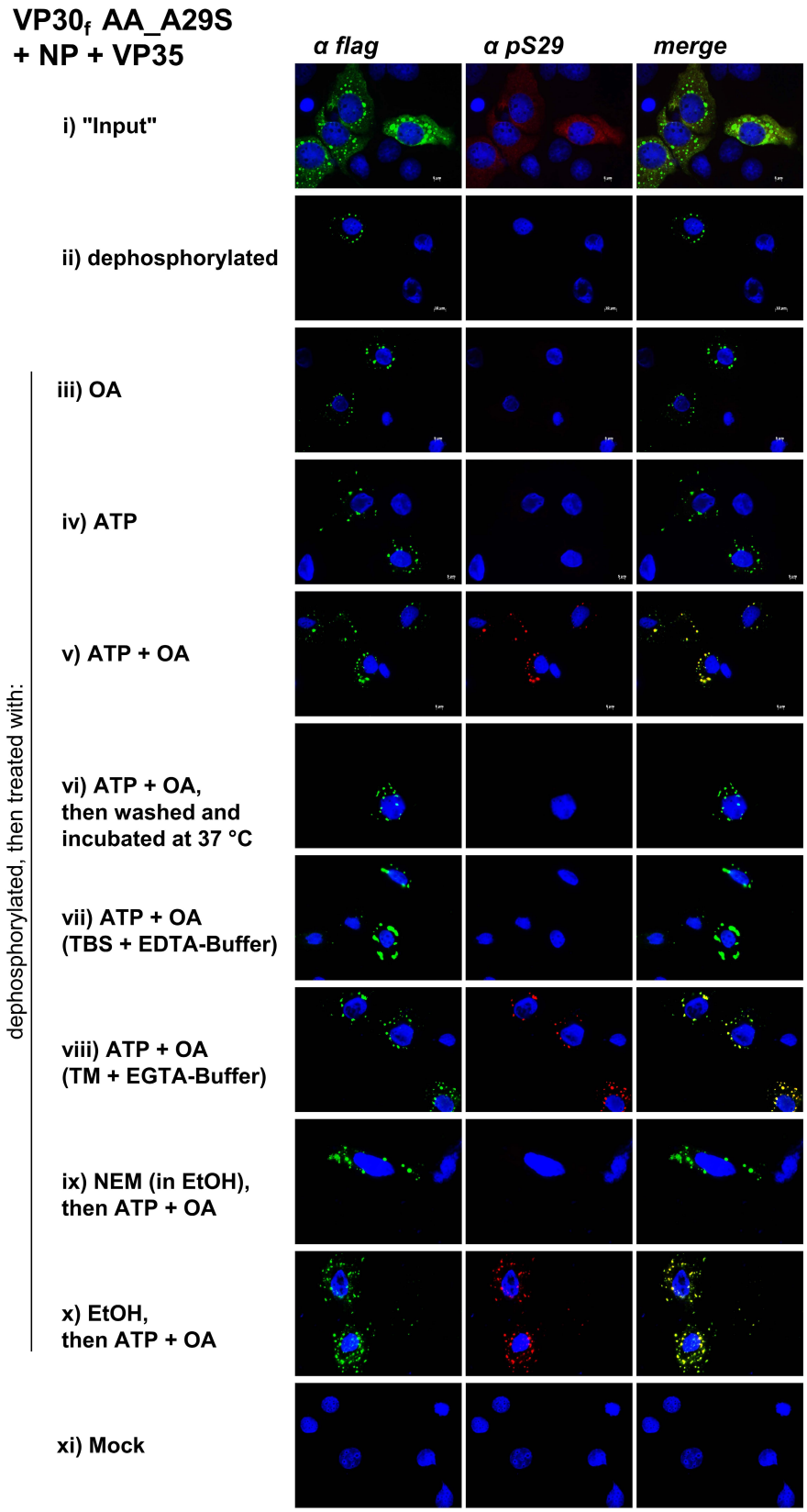

Figure 25: VP30-Specific Kinases and Phosphatases Localize to NP-Induced Inclusion Bodies.

In situ phosphorylation assay of VP30 (3.4.2). For this *in vitro* assay, HUH-7 cells, grown on coverslips, were transfected with plasmids encoding $VP30_f$_AA_A29S, NP, and VP35. 20 h p.t. one coverslip was fixed with acetone-methanol (i, "Input"). The other coverslips were incubated in a non-denaturing lysis buffer containing 0.2 % Tween® 20 for 10 min at 37 °C. After cell lysis, coverslips were carefully washed at least three times with TM buffer and incubated in TM buffer for 10 min at 37 °C to allow complete dephosphorylation of VP30 (ii, dephosphorylated). Rephosphorylation of VP30 serine 29 was achieved by incubation of cells in TM buffer with ATP +/- OA and other substances. EtOH = Ethanol (NEM-control). After rephosphorylation with ATP + OA, one coverslip was washed again and then incubated in TM buffer without phosphatase inhibitors (vi). Reactions were stopped by fixation with acetone-methanol (1:1). Phosphorylation status of VP30 was assessed by IFA (3.3.5). Total VP30 was stained with mouse anti-flag and goat anti-mouse *Alexa 488* antibodies, phosphorylated VP30 was stained with rabbit anti-pS29 and goat anti-rabbit *Alexa 594* antibodies. Nuclei were visualized with DAPI.

Taken together, accumulated evidence indicates that both VP30-specific kinases and phosphatases localize to the NP-induced inclusion bodies. Together with the data from the previous sections, it seems likely that NP recruits the phosphatase(s) for VP30, whereas VP30 interacts directly with the cellular kinase(s).

5 Discussion

Phosphorylation of viral proteins plays an important role in the viral life cycle of many members from the order *Mononegavirales*. Contrary to large DNA viruses, such as Herpesviruses or Poxviruses, which encode for viral protein kinases, RNA viruses from the order *Mononegavirales* hijack components of the cellular phosphorylation machinery[115,139]. Cellular kinases and phosphatases are specifically recruited by negative-sense RNA viruses to modulate, regulate, and extend the function of their viral proteins.

Among the negative-sense RNA viruses, phosphorylation of the P protein is best studied. The P protein is the essential polymerase cofactor of many *Mononegavirales* and represents the VP35 homologue of the *Filoviridae*. In contrast to VP35, the function of the P protein is influenced by phosphorylation at multiple sites (hence the name phosphoprotein). So far, many functions of P protein phosphorylation have been established, but the exact role of phosphorylation remains a mystery and may differ from virus to virus. Phosphorylation of the P proteins of vesicular stomatitis virus (VSV) and respiratory syncytial virus (RSV) was demonstrated to enable or modulate the activity of RNA synthesis[11,252]. Contrary, phosphorylation of measles virus phosphoprotein downregulated viral transcriptional activity[228]. Several host kinases, including CKII, PKC- ζ, AKT, and PLK1, were identified to be responsible for phosphorylation of different P proteins[11,55,229,230,253].

Besides the P Protein, phosphorylation of the nucleoprotein has been reported for many *Mononegavirales*, including Sendai virus, Nipah virus, mumps virus, rabies virus, Marburg virus, and Ebola virus[18,68,102,103,175,269]. For rabies virus, nucleoprotein phosphorylation is a prerequisite for efficient transcription and replication[269]. The MARV nucleoprotein can get phosphorylated in seven regions. Only phosphorylated forms of the MARV NP were detected in virions, suggesting a role of phosphorylation in the formation of nucleocapsid complexes[18,146]. Furthermore, phosphorylation of MARV NP also influences viral RNA synthesis[59]. Ebola NP was found to be phosphorylated in two amino acid stretches. Besides VP30, it is the only other viral protein for which phosphorylation could be detected in purified SUDV[68].

As a special feature among the *Mononegavirales*, *Filoviridae* encode for the structural protein VP30, which is phosphorylated both in MARV and EBOV[68,164]. It was demonstrated that phosphorylation of MARV VP30 at serine residue 40 and 42 is important for the interaction of VP30 with NP-positive inclusion bodies[164]. Similarly, phosphorylation of EBOV VP30 influences the interaction with other viral proteins and

viral RNA, but also impacts viral transcription and replication[24,26,27]. The only known homologue among the *Mononegavirales* with similar functions and structural characteristics to EBOV VP30 is the M2-1 protein of the respiratory syncytial virus (RSV). M2-1 acts as a transcription elongation factor, preventing transcription termination intra- and intergenically[48,236]. Both M2-1 and EBOV VP30 are dynamically phosphorylated, bind RNA, contain a zinc binding region, and are dispensable for replication of the full length genome[236]. Phosphorylation of both proteins reduces their RNA-binding capabilities[27,236]. Although M2-1 and VP30 share similar characteristics, they also display functional differences: phosphomimicry and phosphoablation of M2-1 serine 58 and serine 61, mimicked by either aspartate or alanine mutants, impairs the transcriptional potential[236]. Contrary, mutation of VP30 serines 29-31 and 42 / 44 / 46 to alanine enhanced the transcriptional activity, whereas mutation to aspartate abolished transcriptional activity of VP30[165].

5.1 Regulation of EBOV Transcription and Replication by VP30 Phosphorylation

During the EBOV life cycle, the negative-sense viral genome is sequentially transcribed into individual polyadenylated and capped mRNAs, which are translated by the cellular machinery into viral proteins. mRNA synthesis is regulated by *cis*-acting elements of the viral genome: it is initiated at individual gene start signals and stopped at gene end signals[170]. The viral genome is also replicated to produce full length positive-sense antigenome and negative-sense genome RNA that are neither capped nor polyadenylated. During the process of replication, gene end signals must be ignored by the viral polymerase. EBOV, like the other *Mononegavirales*, encodes only for a single polymerase L[169,170]. This raises the important question, how the balance between transcription and replication is differentially regulated. For other nonsegmented, negative-sense RNA viruses it is believed that encapsidation of the RNA by the nucleoprotein NP allows the viral polymerase to read through gene end signals to replicate the full template[157,251]. Increasing amounts of viral NP would then lead to a switch from viral transcription to replication.

For EBOV, a different model for regulation of transcription and replication was proposed, based on phosphorylation of VP30. Replication of the full-length Ebola genome is achieved by NP, VP35, and L alone, whereas transcription of individual genes additionally requires VP30. It could be demonstrated that the transcriptional support activity of VP30 is abolished when 6 N-terminally serine residues (S29-S31 and S42 / S44 / S46) are replaced by aspartate to mimic permanently phosphorylated VP30

(VP30_DD) [165]. Simultaneously, replication increased by almost twofold[24]. In line with this, the transcriptional activity of VP30_wt was also dramatically reduced when cells were treated with OA in a minigenome assay[165]. OA blocks PP1 and PP2A, which were shown to dephosphorylate VP30 *in vitro*. Conversely, mutation of the six serine residues to alanine (VP30_AA) enhanced transcription and diminished replication[24]. The transcriptional activity of VP30_AA was not inhibited by OA[165]. These results suggested that VP30 phosphorylation serves as an on-off switch to regulate transcription (VP30 dephosphorylated, transcriptionally active) and replication (VP30 phosphorylated, transcriptionally inactive).

However, it was demonstrated that VP30_AA is unable to support primary transcription in a trVLP assay[26]. During primary transcription, transcriptional activity is dependent on viral proteins associated with the incoming trVLPs / virions. In line with this, a recombinant virus encoding VP30_AA could not be rescued[153]. In contrast, recombinant viruses encoding either VP30_SA or VP30_AS were successfully recovered, and these VP30 mutants also enabled primary transcriptional activity in a trVLP assay[26,152]. In further experiments the significance of serine 29 phosphorylation was demonstrated: serine 29 as the only phosphoacceptor site in the N-terminal VP30 region was sufficient to render VP30 transcriptionally active in a trVLP assay. The importance of S29 was further supported by the rescue of a recombinant virus encoding VP30_AA_A29S (recEBOV_S29), which had similar growth kinetics as recEBOV_wt[26]. Altogether, these results indicated that phosphorylation of VP30 is an essential step during the viral life cycle and that phosphorylation of serine 29 is sufficient to fulfill these functions.

5.1.1 Role of VP30 Phosphorylation for Primary Transcriptional Activity

In Figure 8 the importance of serine 29 phosphorylation for primary transcriptional activity was confirmed in a trVLP assay. Here, even the combination of VP30_AA and VP30_AA_A29D was unable to support viral transcription in the indicator cells, which indicates that phosphorylation needs to be dynamic within one and the same VP30 molecule. We observed the formation of small inclusion bodies in the indicator cells (Figure 9), but only VP30_wt and VP30_AA_A29S localized to the inclusion bodies, suggesting that phosphorylation of at least one VP30 site is important for the transport with the incoming nucleocapsids to the inclusion bodies. Remarkably, the greater amount of VP30_wt in the inclusion bodies correlated with a higher transcriptional activity in the indicator cells, which might be attributed to more phosphorylation sites in VP30_wt when compared to VP30_AA_A29S. Because the N-terminal region of VP30 is predicted to be intrinsically disordered, it is conceivable that VP30 phosphorylation allows the dynamic binding to other viral proteins or host cell factors. This theory is supported by the

observation that phosphorylated VP30 has a higher affinity for NP[23,24]. Phosphorylation of VP30 might be necessary during early time points of infection to ensure adequate interaction between VP30 and NP, which allows recruitment of VP30 into the NP-induced inclusion bodies in the indicator cells. In this context it should be mentioned though that enhanced interaction of phosphorylated VP30 with NP can just as well be attributed to greater self interaction of phosphorylated VP30. Although it was demonstrated that VP30_AA can interact with VP30_wt, a comparison between homo-oligomerization of phosphorylated VP30_wt and the homo-oligomerization of VP30_AA was never made[23]. When no VP30 was present in the small inclusion bodies, as was the case for VP30_AA and VP30_AA_A29D, primary viral transcription did also not take place. Because the sensitivity of the IFA is not high enough, it is not clear if VP30_AA and VP30_AA_A29D localized diffusely to the cytoplasm of the indicator cell or if they were degraded by cellular enzymes as they were not associated with the other viral proteins. Formation of inclusion bodies was also observed for trVLPs that did not contain VP30.

Astonishingly, it was possible to rescue the primary transcriptional activity for VP30-deficient trVLPs even if large amounts of VP30_AA were supplied *in trans* in the indicator cells, suggesting that phosphorylation of VP30 is not required for the primary transcription process *per se*, but rather for efficient interaction with the other viral proteins[26]. On the other hand, it was not possible to efficiently rescue trVLPs containing VP30_AA by supplementing VP30_AA *in trans* in the indicator cells[26]. This might partly be attributed to reduced replication of the viral minigenome in the indicator cells expressing VP30_AA, but further unknown functions of VP30 phosphorylation during primary transcription - apart from ensuring transport with the nucleocapsid - cannot be excluded.

The relevance of VP30 phosphorylation was underlined by experiments with arginine mutants of VP30 (Figure 19). Here, mutation of arginine 26 in the background of VP30_AA_A29S destroyed the putative S29 phosphorylation motif and abolished primary transcriptional activity. This implies that the mere presence of the nonphosphorylated serine 29 residue, which we tried to mimic by alanine, is not sufficient to support primary transcription.

Altogether, our results indicate that phosphorylation of VP30 needs to be dynamic in the indicator cells, requiring cycles of phosphorylation and dephosphorylation. However, it should be mentioned that mimicry of phosphorylation by aspartate residues is not optimal because of its different size and unequal negative charge. It is not clear if a constant phosphate group at position 29 (not the aspartate residue!) would also inhibit transport of VP30 with the nucleocapsid to the inclusion bodies.

In the inclusion bodies, VP30 is probably rapidly dephosphorylated because of the high phosphatase activity associated with NP (f.i. Figure 11), which ensures transcriptional activity of VP30_wt. In first experiments it was not possible to detect phosphorylation at position 29 in the inclusion bodies of the indicator cells with the phosphospecific VP30 antibody (data not shown). Phosphorylation of VP30 is probably only transient during early steps of infection and gets rapidly reversed by the high activity of phosphatases. It is conceivable that the phosphospecifc antibody is not sensitive enough to detect low-level, transient phosphorylation of VP30 serine 29. The kinase activity detected in purified trVLPs (Figure 24) might be responsible for the supposed initial phosphorylation step of VP30 in the trVLP assay.

Our data also suggest that the small perinuclear inclusion bodies in the indicator cells represent the sites for primary transcription because the amount of VP30 in the inclusion bodies always correlated with the reporter gene signal in the indicator cells. To confirm this hypothesis, one could use FISH probes to detect positive-sense viral RNA.

5.1.2 Relevance of VP30 Multisite Phosphorylation

Previous experiments discovered that hyper-phoshorylation of VP30 reduces its transcriptional potential, however, no discrimination was made between the six N-terminal VP30 serine residues. Hence the functional significance of phosphorylation at each individual serine residue remained unknown. Here, we were able to demonstrate that simultaneous phosphorylation of VP30 serine 29 and serine 31 is both necessary and sufficient to downregulate the transcriptional support activity of VP30 (Figure 6 and Figure 7). These results are underlined by mutational studies of the putative VP30 phosphorylation motifs, where only the R26A and R28A mutations were able to restore VP30 activity under OA treatment (Figure 18). Phosphorylation of a single serine residue within the N-terminal cluster was not sufficient to impair VP30's function as a transcriptional activator (Figure 6). This finding implies that multisite phosphorylation of at least S29 <u>and</u> S31 is a prerequisite for downregulation of VP30's transcriptional support function. In direct contrast to this, multisite phosphorylation was not a requirement for primary transcriptional activity (Figure 8).

If phosphorylation of a single VP30 serine residue would have a functional impact on the transcriptional activity, VP30 could easily and largely be inactivated by cellular kinases. The requirement for multisite phosphorylation also refines the specificity of VP30 phosphorylation; this is part of the kinetic proofreading concept that was first established in 1974 for DNA replication and protein synthesis, but also applies to protein phosphorylation[101,231]. As demonstrated, VP30 must undergo a series of phosphorylations for inactivation, but at every phosphorylation step, kinases might

dissociate from VP30 and the rapid action of phosphatases would return VP30 to its basal state (also called error correction). The stability of the VP30-kinase complex is tested with each modification, leading to increased specificity of the reaction and less random phosphorylation events. Summarized, multisite phosphorylation reduces false positive signal transduction, ensuring only reliable transcriptional inactivation of VP30[5].

It is also tempting to speculate about the order of VP30 multisite phosphorylation and dephosphorylation. Several Ser / Thr kinases can phosphorylate their substrate sequentially[12,76,148,199]. We demonstrated that VP30 S29 and S31 share the common R-X-X-S phosphorylation motif and thus could potentially be phosphorylated by the same kinase (Figure 16 to Figure 19). Similarly, hierarchical phosphorylations were described for the RSV M2-1 protein, where phosphorylation of S58 creates a new CKI phosphorylation motif for S61[40]. Currently, it is not clear whether VP30 phosphorylation and dephosphorylation follows a fixed order leading to cycles of VP30 activation and inactivation, or whether random VP30 phosphorylation and dephosphorylation takes place.

Our finding that two phosphorylation steps are sufficient to inactivate VP30's function as a transcription factor, a scenario much more likely than simultaneous phosphorylation of all six serine residues, indicates that VP30 phosphorylation could indeed be responsible for a switch from viral transcription to replication. But, at the same time, the demand for several phosphorylation steps also questions whether phosphorylation of VP30 indeed plays a crucial role in regulating the balance between transcription and replication because the recEBOV_S29 showed similar growth kinetics as recEBOV_wt in cell culture experiments[26]. Since recEBOV_S29 contains only the single serine 29 as a phosphoacceptor site within the N-terminal serine cluster of VP30, recEBOV_S29 cannot downregulate transcription by VP30 phosphorylation. Accordingly, recEBOV_wt was inhibited stronger by OA than recEBOV_S29 (Figure 15). If phosphorylation of VP30 would play an essential role in regulating the balance between transcription and replication during the viral life cycle, it would be expected that the recEBOV_wt has a growth advantage over recEBOV_S29. Similarly, a recombinant virus encoding VP30_AS was rescued[152]. In our minigenome assays, VP30_AS was transcriptionally active even under phosphatase inhibition (Figure 5). However, it is possible that both recEBOV_S29 and recEBOV_AS have reduced viral fitness when tested in different cell lines. Likewise, the lack to balance transcription / replication by VP30 phosphorylation might manifest itself only after several serial passages.

One limitation of the current study is that we used OA to study the effect of VP30 phosphorylation on transcriptional regulation. VP30 is dephosphorylated completely by

PP2A / PP1 and partly by PP2C *in vitro*, but it is not clear if all of these phosphatases have a biological relevance for VP30 dephosphorylation[165]. Theoretically, it is even possible that other phosphatases can dephosphorylate VP30 as well. OA is a more potent inhibitor of PP2A (IC50 = 0.1 nmol/l) than of PP1 (IC50 = 15-20 nmol/l). We used OA at 25 nmol/l and repeated the experiments with the same results at 50 nmol/l OA, but higher concentrations would be needed to inhibit all PP1. Similarly, PP2C is not inhibited by OA at all. Although it would be uncommon for phosphatases, PP1 or PP2A could also have a preference for certain phosphorylation sites of VP30. Altogether, the effect of VP30 phosphorylation at certain serine residues might be underestimated in our study design. For this reason, it would be interesting to test other phosphatase inhibitors, like Sanguinarin, Microcystin, Nodularin, or Tautomycin [233].

A potential drawback of the minigenome assay is that not all viral proteins are recombinantly expressed. In Figure 14 A we demonstrated that the additional expression of VP24 / VP40 / GP also influences the phosphorylation status of VP30 serine 29 towards dephosphorylation, which could be due to recruitment of other phosphatases by those viral proteins. Testing the influence of phosphatase inhibition on viral transcriptional activity in the context of all viral proteins would yield a more realistic picture.

Seemingly contradicting our results, VP30_DA, which mimics permanently phosphorylated S29-S31, was transcriptionally active in a minigenome system[153]. Here it should be emphasized again that the attempt to mimic phosphate groups with negatively charged aspartate residues is not optimal. The negative charge induced by phosphorylation is greater than the negative charge of the carboxylic acid group. Most likely, the dynamic phosphate group has unique biological properties that are impossible to imitate by the constant negative charge of aspartate. This is supported by the fact that the phosphospecific antibody detected VP30_AA_A29D only weakly (Figure 10 B and C). Moreover, the phosphomimetic form was not recognized at all by another phosphospecific VP30 antibody (from rabbit 7993, not presented in this thesis), proving that proteins can indeed bind only to phosphorylated but not phosphomimetic VP30. As such, inhibition of phosphatases to produce stable phosphate groups of VP30 is more realistic than imitation of phosphorylation with aspartate residues. Our results suggest that simultaneous phosphorylation of S29 and S31 is sufficient to downregulate transcriptional VP30 activity.

5.2 Regulation of VP30 Phosphorylation

Every phosphorylation reaction must be spatially and temporally regulated to ensure accurate downstream effects. In our study we identified that the interaction between VP30 and other viral proteins, especially the nucleoprotein NP, dramatically modulates the phosphorylation status of VP30. With the help of a phosphospecific VP30 antibody we were able to describe previously unidentified interactions of VP30 with cellular kinases and of NP with cellular phosphatases. We think that these interactions are key regulators of VP30 phosphorylation.

In recent years, much light was shed on the mechanisms by which pathogens hijack host proteins. Many viruses encode and mimic short linear motifs (SLIMs) of the host proteome to specifically recruit cellular factors[53]. Short linear motifs consist of short stretches of typically less than ten amino acids and reside in intrinsically disordered protein regions[239]. The interaction between SLIMs and structured protein domains is typically of low affinity (1-20 µmol/l), which allows the virus to dynamically interact with a range of host proteins. For VP30, three disordered regions are predicted, spanning from residues 1 to 44, 120 to 140, and 268 to 288[119]. Likewise, the C-terminal half of NP (residues 391–739) is mostly disordered[64,125].

5.2.1 Interaction between VP30 and Cellular Kinases

To ensure efficient phosphorylation, a regulated interaction between substrate and kinase is crucial. In immunoprecipitation studies, we were able to identify a specific interaction between VP30 and cellular kinases. Since the responsible kinases for VP30 phosphorylation are unknown so far, it was not possible to detect kinases immunologically. Instead, VP30 kinase activity was detected with an *in vitro* biochemical kinase assay (Figure 23). Auto-phosphorylation by VP30 or by other viral proteins can be excluded (Figure 24 B, lanes 9 and 10). This finding strongly suggests that VP30 interacts with cellular kinases, either by direct interaction or with the help of scaffolding proteins. Future studies might identify the responsible kinases by immunoprecipitation and subsequent tandem mass spectrometry. It should be mentioned though that our biochemical approach is probably very sensitive and as such prone to contamination. Prior to mass spectrometry, an in-gel kinase assay might help to identify relevant bands in the protein gel[267]. Any identified kinase should then be validated by other approaches to confirm its biological relevance, f.i. by experiments with siRNA or specific kinase inhibitors.

Based on the knowledge from other studies, the interaction between VP30 and kinases is likely based on distal interactions between kinase and VP30, outside of the catalytically

active kinase center[2,191,244]. It is possible that VP30 contains a so far unknown SLIM in one of its intrinsically disordered protein regions, which binds one or several cellular kinases. We further demonstrated that phosphorylation of VP30 serine 29 is dependent on a common R-X-X-S motif (Figure 16 to Figure 19). Identification of this phosphorylation narrows down potential kinase candidates, but prediction solely based on the phosphorylation motif has low accuracy. Many kinases do not have a known phosphorylation motif, several kinases share similar motifs, and many motifs are degenerate. Specificity of protein phosphorylation is achieved on many different levels and the presence of a functional phosphorylation motif is probably not necessary for the interaction between VP30 and kinases[57]. Therefore, it is expected that both VP30_wt and VP30_AA_A29S as well as arginine mutants such as VP30_AA_A29S_R26A interact with the same cellular kinase(s). Dephosphorylation of VP30 prior to immunoprecipitation might additionally increase the affinity of VP30 for the kinase, as the dephosphorylated substrate, in contrast to the phosphorylated counterpart, also transiently binds the active site of the respective kinase[2,244].

For a more realistic picture, the interaction between VP30 and kinases could be studied in the context of all viral proteins, either after recombinant expression or after infection with recEBOV. Theoretically, the interaction between VP30 and cellular proteins might be modulated by other viral proteins. In our experiments the kinase was not only co-precipitated during single expression of VP30, but also during co-expression of the viral VP30, NP, and VP35 (Figure 23, lane 11). Similarly, we were able to detect kinase activity for VP30 in inclusion bodies formed by NP, VP35, and VP30, which suggests that the kinase is recruited by VP30 to the sites of viral replication (Figure 25). Although unlikely, our experimental design of the *in situ* assay cannot completely exclude contamination by cytoplasmic kinases / phosphatases, which are not associated with the NP-induced inclusion bodies. The *in situ* phosphorylation assay could also be applied to cells infected with recEBOV.

Moreover, we demonstrated that a cellular kinase is incorporated into trVLPs, likely by interaction with VP30 in the inclusion bodies. However, it was not possible to detect kinase activity in purified recEBOV_S29 (Figure 24). The obvious discrepancy between the trVLPs and the recEBOV_S29 is not resolved. We repeated the experiment with trVLPs purified through a Nycodenz gradient with the same result; kinase activity for VP30 was detected both in fractions 4-6 and 7-9 (data not shown). Nevertheless, it is still possible that kinases are not integrated into filamentous or vesicular trVLPs, but instead are contaminants from small round particles or microvesicles that were present even after gradient centrifugation (data not shown). On the other hand it is also well known

that different cell lines lead to incorporation of different proteins into newly formed virus particles[84]. We used HEK-293 cells to generate the trVLPs because of the good transfection efficiency, and HUH-7 cells for infection with recEBOV_S29. Another explanation would be that recEBOV_S29 is more efficient in eliminating cellular bystander proteins. We also do not know if the observed incorporation of a kinase into trVLPs is of any significance for the early steps of infection prior or during primary transcription, or if the integration of the kinase is merely a passive and random process.

Apart from identification of VP30-specific kinases by mass spectrometry, kinase inhibitors might be tested *in vitro* (and eventually *in vivo*) for further characterization of the responsible kinases. Ideally, kinase inhibitors should be tested in primary cells or primary cell lysates, since immortalised cell lines are likely to have a deregulated and distrupted kinase network. As a general note, it should be mentioned that we cannot know for certain whether the kinases phosphorylating VP30 *in vitro* are the same that phosphorylate VP30 *in vivo*. In Figure 22, phosphorylation of VP30 was at least partially inhibited by staurosporine and heparin *in vitro*, and only marginally by very high concentrations of TBCA. We used very long incubation times (one hour), which makes the observed effects difficult to interpret. If kinase inhibitors are tested in future experiments, incubation times and concentrations of ATP / OA should be adjusted to better evaluate the effects of kinase inhibition. The observed effect of heparin on serine 29 phosphorylation is not an effect of inhibition of CK2, but most likely results from binding of the negatively charged heparin molecule to the arginine residues R26 / R28 / R32 and subsequent sterical inhibition of the responsible kinases. In this way, heparin mimics viral RNA, which also recognizes the arginine residues of VP30[27,214].

From a functional point of view, inhibition of kinases that phosphorylate serine 29 of VP30 would abolish the transcriptional regulation via VP30 phosphorylation because simultaneous phosphorylation of serine 29 and 31 is a necessary condition to downregulate transcriptional activity (Figure 7). Still, the effect of inhibition of responsible kinases on viral proliferation is uncertain. It is likely that VP30 can get phosphorylated redundantly by several cellular kinases, which would complicate targeted inhibition. For example, certain cell types may lack the kinase(s) phosphorylating VP30 serine 29, but may express kinases that phosphorylate the other serine residues of VP30. In this respect, the six serine residues within VP30_wt might enable redundancy of phosphorylation.

5.2.2 Interaction between NP and Cellular Phosphatases

In Figure 11 to Figure 14 we demonstrated that phosphorylation of VP30 is largely influenced by the presence of other viral proteins, especially by the nucleoprotein NP. We further established++ that OA, an inhibitor of PP1 and PP2A, counteracts the effect of NP (Figure 12 and Figure 14). Additionally, our *in situ* assay strongly suggests that the phosphatase activity is very high in the NP-induced inclusion bodies: contrary to the rephosphorylation assay in test tubes (Figure 21), rephosphorylation of $VP30_f$_AA_A29S was only detectable in the presence of ATP and the phosphatase inhibitor OA (Figure 25, iv and v). The idea of high phosphatase activity is supported by the fact that phosphorylation of $VP30_f$_AA_A29S was reversible after washing away of ATP and OA (Figure 25, vi).

We think that NP recruits an OA-sensitive phosphatase and that VP30 is an indirect target. Since the effect was already seen at 5 nmol/l OA, which is below the IC50 value of PP1, it seemed likely that NP recruits PP2A. Moreover, neither NP nor VP30 contain the degenerate consensus sequence [H/K/R]-[A/C/H/K/M/N/Q/R/S/T/V]-[V]-[C/H/K/N/Q/R/S/T]-[F/W], which allows binding to the catalytic PP1 subunit[159]. Nevertheless, binding of PP1 to viral proteins through regulatory subunits would still be a possibility.

Following our studies, a group from Denmark discovered a conserved motif that provides binding specificity to the B56 subunit of PP2A[96]. The degenerated short linear motif [L/F/M]-[X]-[X]-[I/V/L]-[X]-[E] was also detected in the nucleoprotein of all members of the *Filoviridae* (starting at amino acid 562 in EBOV NP). Together, we could recently demonstrate that NP indeed recruits PP2A-B56 via the degenerate LxxIxE motif to NP-induced inclusion bodies in order to dephosphorylate and thereby activate VP30. The influence of PP2A-B56 as a VP30-specific phosphatase was crucial as small peptide inhibitors interfering with the NP-B56 motif resulted in a nearly complete abrogation of viral transcription and virus propagation, although PP1 was also present in the experimental setting[132]. If PP2A can no longer bind to NP and is therefore not recruited into spatial proximity of VP30, the VP30 associating kinases will hyper-phosphorylate VP30 serine 29 and 31, leading to transcriptional inactivation and suppression of virus proliferation (Figure 6).

Generally speaking, recruitment of PP2A by viral proteins seems to be a common strategy [reviewed by Guergnon et al. 2011[88]]. This interaction was described to activate cellular pathways involved in cell transformation, to induce apoptosis and to regulate viral replication and assembly[88,166].

5.2.3 Further Considerations

In addition to the influence of the nucleoprotein NP, other EBOV viral proteins also modulate the phosphorylation status of VP30 serine 29. During co-expression of NP, VP35, L, and VP30 our phosphospecific antibody still recognized a limited amount of phosphorylated VP30 (Figure 14 A, lanes 6 and 7), but when all viral proteins were recombinantly expressed, almost no phosphorylated VP30 could be detected (Figure 14A, lane 8). Similarly, barely any phosphorylated VP30 was detected during infection with recEBOV_S29 and recEBOV_wt (Figure 15). This suggests that the viral VP24 / GP or VP40 further downregulate VP30 phosphorylation, either by recruitment of other phosphatases like PP1 / PP2C or by inhibition of VP30 kinase activity. The idea of PP1 recruitment is supported by the observation that the phosphorylation status of VP30 did not reach 100 % during treatment with 50 nmol/l OA, a concentration too low to inhibit all PP1 (Figure 14 C). Both VP40 and GP do not contain a PP1 docking motif. VP24 contains a HVVNY sequence (aa 168-172), which almost fits the PP1 binding motif, but the presence of tyrosine at position 5 inhibited binding to at least the PP1y1 isoform[159]. Nevertheless, PP1 recruitment via regulatory subunits or recruitment of other phosphatases should be considered, although recently published results argue that PP2A plays the major role in regulating the phosphorylation of VP30, since inhibition of the binding of the B56 subunit to NP resulted in a complete abrogation of transcription[132]. Another possible explanation would be that addition of VP24 / GP or VP40 rearranges the nucleocapsid complex in such a way that phosphatases now have preferred access to VP30 compared to the associating kinases.

In the light of these results it is not surprising that we never obtained a signal for VP30 with the phosphospecific antibody for native trVLPs / recEBOV_S29 / recEBOV_wt, suggesting that VP30 serine 29 is mainly dephosphorylated in viral particles (Figure 15 and Figure 24). Earlier studies revealed that VP30 and NP are the only phosphorylated proteins in preparations of purified SUDV[68]. In contrast to our experiments, radioactive phosphate was added during infection, which was built into phosphorylated VP30. As a consequence, the phosphorylation signal was not specific for a certain amino acid, but represented the phosphorylation status of the whole VP30 protein. In this context it should be noted that the anti-pS29 antibody is polyclonal, and thus represents a mixture of antibodies with probably different binding characteristics and affinities. The peptide sequence of 12 amino acids in length, against which the phosphospecific VP30 antibody was raised, contains several epitope possibilities, usually around 5 to 8 amino acids, against which the antibody can be directed. Because of the purification process of the phosphospecific antibody, all recognized epitopes included the central phosphoserine residue (3.3.7). Our results suggest that when the phosphospecific antibody detects

$VP30_f$_wt, serine residue 29 is indeed phosphorylated. However, in case the antibody does not bind $VP30_f$_wt, it cannot be implicated that serine 29 is dephosphorylated, as phosphorylation at serine residue 30 and 31 could interfere with binding of the peptide antibody. Interestingly, the phosphospecific antibody detected very little amounts of phosphorylated $VP30_f$_wt in co-expression studies with NP inside the inclusion bodies, contrary to no phosphorylated $VP30_f$_AA_A29S (Figure 11). This marginal difference between the phosphorylation status of $VP30_f$_wt and $VP30_f$_AA_A29S might be explained by the assumption that mutation of 5 serines to alanine itself (as in the case of $VP30_f$_AA_A29S) is able to influence the phosphorylation status of serine 29 by allowing access of more phosphatases, as they are no longer needed to dephosphorylate other serine residues (S30 / S31 / S42 / S44/ S46). Since kinases are, in contrast to the phosphatases, almost always specific for a single serine residue, this would then shift the phosphorylation status towards the dephosphorylated state on serine 29 in the mutant $VP30_f$_AA_A29S, at least when compared to $VP30_f$_wt.

Studies with phosphomimetic VP30_DD suggested that phosphorylated VP30 is enriched in viral inclusion bodies[165]. Because VP30_DD is transcriptionally inactive, it was hypothesized that inclusion bodies are the site of viral replication but not viral transcription. Our finding that VP30 is mostly dephosphorylated at position 29 in the inclusion bodies, a form of VP30 that is always transcriptionally active (Figure 7), strongly suggests that inclusion bodies also represent a site of viral transcription. The fact that phosphatase activity is high in inclusion bodies underlines this new finding (Figure 26).

At system level, competition between viral proteins for the catalyzing enzymes should be kept in mind. For example, it is likely that the phosphatase recruited by NP not only indirectly dephosphorylates VP30, but also dephosphorylates NP itself. Thus, the interaction theoretically enhances the extent of NP phosphorylation because VP30 acts as a competitive phosphatase inhibitor. Likewise, it is possible that the kinase(s) recruited by VP30 also phosphorylates other viral proteins, f.i. NP. Hence, the amount of phosphorylated VP30 additionally decreases.

A further mechanism to modulate serine phosphorylation is methylation of arginine residues by protein arginine methyl transferases (PRMTs). Crosstalk between serine phosphorylation and arginine methylation was observed for histones, RNA-binding proteins, and transcription factors[204,271]. Arginine methylation was also described for many viral proteins[109,265]. Exemplary, VP30 contains a RGRPR sequence in its N-terminus, which is methylated in other proteins, but for now arginine methylation of EBOV VP30 is purely speculative[186].

5.2.4 Model of VP30 Phosphorylation

Altogether, our data suggest the following model for VP30 phosphorylation: VP30 interacts with a cellular kinase, whereas NP binds to a VP30-specific cellular phosphatase. Interaction between the two viral proteins increases the local concentration of phosphatases around VP30. VP30 is phosphorylated by the associating kinase and is an indirect target of the phosphatase recruited by NP. Both classes of enzymes localize to perinuclear viral inclusion bodies. The observed rapid turnover of VP30 phosphorylation suggests that viral inclusion bodies represent sites of viral transcription.

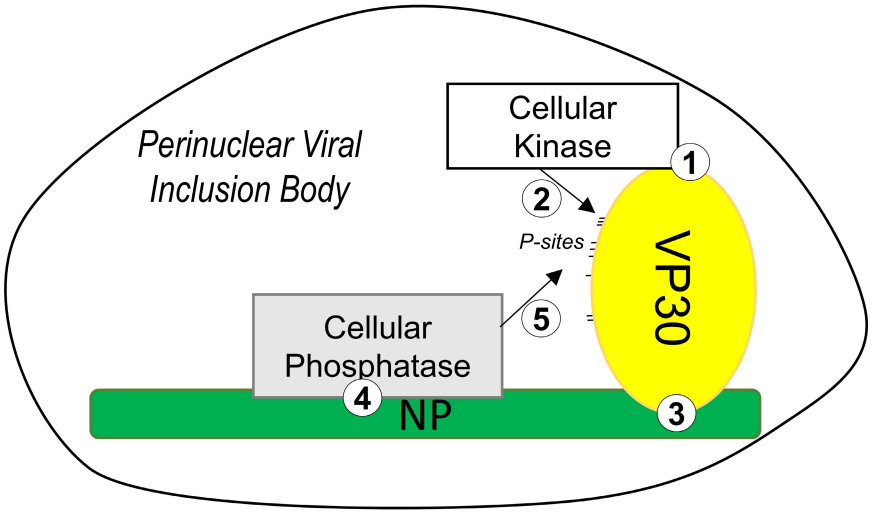

Figure 26: Recruitment of a Complete Phosphorylation / Dephosphorylation System to Viral Inclusion Bodies.

Model of interaction between VP30, NP, cellular kinase(s), and phosphatase(s). (1) VP30 interacts with a cellular kinase, either directly or by adaptor / scaffolding proteins. So far, the region of interaction is not known. (2) The kinase phosphorylates VP30 on the basis of specific phosphorylation motifs. (3) The C-terminus of VP30 interacts with a short peptide in the C-terminal NP. (4) NP interacts with an OA-sensitive phosphatase like PP1 / PP2A. (5) VP30 is an indirect substrate of the phosphatase recruited by NP.

6 Summary

6.1 Summary (English)

Ebola virus is a nonsegmented negative-strand RNA virus of the family *Filoviridae.* Ebola virus is highly pathogenic and classified as a BSL-4 agent. In humans, the virus causes a severe, often fatal disease.

Replication and transcription of the viral genome are achieved by viral proteins of the nucleocapsid complex, which consists of the viral RNA genome and the viral proteins NP, VP24, L, VP35, and VP30. For replication of the viral genome, only NP, VP35, and L are needed, whereas transcription of individual genes also requires a functional VP30. Previous studies indicated that extensive serine phosphorylation of VP30 impairs viral transcription. Here, we demonstrated that phosphorylation of two VP30 serine residues, namely serine 29 and 31, is both necessary and sufficient for downregulation of VP30's transcriptional support activity.

Phosphorylation of VP30 also dynamically modulates the interaction with other viral proteins. For primary transcription immediately after infection of new cells, a phosphorylatable VP30 is a prerequisite. We were able to show that VP30 phosphorylation is essential at early time points of infection to ensure transport of VP30 with the incoming nucleocapsids to the site of primary viral transcription.

With the help of a phosphospecific peptide VP30 antibody directed against serine 29 phosphorylation, we further demonstrated that the majority of VP30 is dephosphorylated at position 29 during infection with recombinant Ebola virus. By recombinantly expressing different combinations of viral proteins, we could show that other viral proteins, especially the nucleoprotein NP, decisively influence VP30 phosphorylation. We gathered first evidence showing that VP30 is a substrate of phosphatases recruited by NP into spatial proximity of VP30. Furthermore, we demonstrated that VP30 directly interacts with a so far unknown cellular kinase, which recognizes a common R-X-X-S phosphorylation motif for VP30 serine residue 29. On the basis of these interactions, both VP30-specific phosphatases and kinases are recruited to perinuclear viral inclusion bodies, where they modulate viral transcription and replication.

6.2 Zusammenfassung (Deutsch)

Das Ebolavirus gehört zur Familie der *Filoviridae*, die ein nicht-segementiertes RNA-Genom in negativer Orientierung besitzen. Da das Virus hochpathogen ist und bei Infektion von Menschen eine schwere, oft tödlich verlaufende Krankheit verursacht, wird der Erreger der biologischen Risikogruppe 4 zugeordnet.

Replikation und Transkription des viralen Genoms werden durch Proteine des viralen Nukleokapsidkomplexes unterstützt, welcher aus dem RNA-Genom sowie den viralen Proteinen NP, VP24, L, VP35 und VP30 besteht. Während für die Replikation des viralen Genoms NP, VP35 und L ausreichend sind, wird für die Transkription individueller Gene zusätzlich ein funktionstüchtiges VP30 benötigt. Vorangegangene Studien zeigten, dass eine extensive Serin-Phosphorylierung des VP30 zu einer Inhibierung der Transkription führt. In unseren Studien konnten wir nun zeigen, dass die Phosphorylierung von zwei Serin-Resten, genauer gesagt an Serin 29 und Serin 31, sowohl notwendig als auch hinreichend ist, um die Funktion von VP30 als Transkriptionsaktivator herunter zu regulieren.

Die Phosphorylierung von VP30 erlaubt auch eine dynamische Interaktion mit anderen viralen Proteinen. Für die primäre Transkription unmittelbar nach der Infektion neuer Zellen muss VP30 phosphorylierbar sein. Wir konnten zeigen, dass die VP30 Phosphorylierung essentiell ist, um den Transport von VP30 mit den Nukleokapsiden zum Ort der primären Transkription sicherzustellen.

Mit Hilfe eines phosphospezifischen VP30 Peptidantikörpers, der gegen die Phosphorylierung an Position S29 gerichtet ist, konnten wir darlegen, dass VP30 während der Infektion mit rekombinanten Ebolaviren an Position 29 hauptsächlich dephosphoryliert ist. Während der rekombinanten Expression verschiedener Kombinationen der viralen Proteine zeigte sich, dass andere virale Proteine, besonders das Nukleoprotein NP, die Phosphorylierung des VP30 entscheidend beeinflussen. Wir haben erste Hinweise dafür gesammelt, dass VP30 ein Substrat einer Phosphatase ist, die durch NP in die räumliche Nähe von VP30 rekruitert wird. Darüberhinaus konnten wir zeigen, dass VP30 direkt mit einer bisher unbekannten Kinase interagiert, die ein weit verbreitetes R-X-X-S Phosphorylierungsmotiv für VP30 Serin 29 erkennt. Auf Basis dieser Interaktionen werden die VP30-spezifischen Phosphatasen und Kinasen in virale Einschlusskörper rekrutiert, wo beide Enzyme die virale Transkription und Replikation modulieren.

7 References

1. Abbate JL, Murall CL, Richner H, Althaus CL. Potential Impact of Sexual Transmission on Ebola Virus Epidemiology: Sierra Leone as a Case Study. PLoS Negl Trop Dis 2016;10:e0004676.
2. Adams JA. Kinetic and catalytic mechanisms of protein kinases. Chem Rev 2001;101:2271–90.
3. Agnandji ST, Huttner A, Zinser ME, et al. Phase 1 Trials of rVSV Ebola Vaccine in Africa and Europe. N Engl J Med 2016;374:1647–60.
4. Akinfeyeva LA, Aksyonova OI, Vasilyevich IV, et al. A case of Ebola hemorrhagic fever. Infektsionnye Bolezni (Moscow);2005:85–8.
5. Aledo JC. Multisite phosphorylation provides a reliable mechanism for making decisions in noisy environments. The FEBS Journal 2018.
6. Aleksandrowicz P, Wolf K, Falzarano D, Feldmann H, Seebach J, Schnittler H. Viral haemorrhagic fever and vascular alterations. Hamostaseologie 2008;28:77–84.
7. Alonso A, Sasin J, Bottini N, et al. Protein tyrosine phosphatases in the human genome. Cell 2004;117:699–711.
8. Alvarez CP, Lasala F, Carrillo J, Muñiz O, Corbí AL, Delgado R. C-type lectins DC-SIGN and L-SIGN mediate cellular entry by Ebola virus in cis and in trans. J Virol 2002;76:6841–4.
9. Amanchy R, Periaswamy B, Mathivanan S, Reddy R, Tattikota SG, Pandey A. A curated compendium of phosphorylation motifs. Nat Biotechnol 2007;25:285–6.
10. Banadyga L, Hoenen T, Ambroggio X, Dunham E, Groseth A, Ebihara H. Ebola virus VP24 interacts with NP to facilitate nucleocapsid assembly and genome packaging. Sci Rep 2017;7:7698.
11. Barik S, Banerjee AK. Phosphorylation by cellular casein kinase II is essential for transcriptional activity of vesicular stomatitis virus phosphoprotein P. Proc Natl Acad Sci U S A 1992;89:6570–4.
12. Barik S, Banerjee AK. Sequential phosphorylation of the phosphoprotein of vesicular stomatitis virus by cellular and viral protein kinases is essential for transcription activation. J Virol 1992;66:1109–18.
13. Barrette RW, Metwally SA, Rowland JM, et al. Discovery of swine as a host for the Reston ebolavirus. Science 2009;325:204–6.
14. Baskerville A, Fisher-Hoch SP, Neild GH, Dowsett AB. Ultrastructural pathology of experimental Ebola haemorrhagic fever virus infection. J Pathol 1985;147:199–209.
15. Bausch DG, Nichol ST, Muyembe-Tamfum JJ, et al. Marburg hemorrhagic fever associated with multiple genetic lineages of virus. N Engl J Med 2006;355:909–19.
16. Bausch DG, Towner JS, Dowell SF, et al. Assessment of the risk of Ebola virus transmission from bodily fluids and fomites. J Infect Dis 2007;196 Suppl 2:S142-7.
17. Bavari S, Bosio CM, Wiegand E, et al. Lipid raft microdomains: a gateway for compartmentalized trafficking of Ebola and Marburg viruses. J Exp Med 2002;195:593–602.

18. Becker S, Huppertz S, Klenk HD, Feldmann H. The nucleoprotein of Marburg virus is phosphorylated. J Gen Virol 1994;75 (Pt 4):809–18.
19. Becker S, Rinne C, Hofsäss U, Klenk HD, Mühlberger E. Interactions of Marburg virus nucleocapsid proteins. Virology 1998;249:406–17.
20. Becker S, Spiess M, Klenk HD. The asialoglycoprotein receptor is a potential liver-specific receptor for Marburg virus. J Gen Virol 1995;76 (Pt 2):393–9.
21. Bermejo M, Rodríguez-Teijeiro JD, Illera G, Barroso A, Vilà C, Walsh PD. Ebola outbreak killed 5000 gorillas. Science 2006;314:1564.
22. Bharat TAM, Noda T, Riches JD, et al. Structural dissection of Ebola virus and its assembly determinants using cryo-electron tomography. PNAS 2012;109:4275–80.
23. Biedenkopf N. Die Phosphorylierung des Ebolavirus VP30 reguliert die virale Transkription und Replikation, 2012.
24. Biedenkopf N, Hartlieb B, Hoenen T, Becker S. Phosphorylation of Ebola virus VP30 influences the composition of the viral nucleocapsid complex: impact on viral transcription and replication. J Biol Chem 2013;288:11165–74.
25. Biedenkopf N, Hoenen T. Modeling the Ebolavirus Life Cycle with Transcription and Replication-Competent Viruslike Particle Assays. Methods Mol Biol 2017;1628:119–31.
26. Biedenkopf N, Lier C, Becker S. Dynamic Phosphorylation of VP30 Is Essential for Ebola Virus Life Cycle. J Virol 2016;90:4914–25.
27. Biedenkopf N, Schlereth J, Grünweller A, Becker S, Hartmann RK. RNA Binding of Ebola Virus VP30 Is Essential for Activating Viral Transcription. J Virol 2016;90:7481–96.
28. Bociaga-Jasik M, Piatek A, Garlicki A. Ebola virus disease - pathogenesis, clinical presentation and management. Folia Med Cracov 2014;54:49–55.
29. Boehmann Y, Enterlein S, Randolf A, Mühlberger E. A reconstituted replication and transcription system for Ebola virus Reston and comparison with Ebola virus Zaire. Virology 2005;332:406–17.
30. Borisevich IV, Markin VA, Firsova IV, et al. Hemorrhagic (Marburg, Ebola, Lassa, and Bolivian) fevers: epidemiology, clinical pictures, and treatment. Voprosy Virusologii – Problems of Virology (Moscow) 2006;(51):8–16.
31. Bosio CM, Aman MJ, Grogan C, et al. Ebola and Marburg viruses replicate in monocyte-derived dendritic cells without inducing the production of cytokines and full maturation. J Infect Dis 2003;188:1630–8.
32. Bowen ET, Platt GS, Simpson DI, McArdell LB, Raymond RT. Ebola haemorrhagic fever: experimental infection of monkeys. Trans R Soc Trop Med Hyg 1978;72:188–91.
33. Bray M, Geisbert TW. Ebola virus: the role of macrophages and dendritic cells in the pathogenesis of Ebola hemorrhagic fever. Int J Biochem Cell Biol 2005;37:1560–6.
34. Breman JG, Johnson KM, van der Groen G, et al. A search for Ebola virus in animals in the Democratic Republic of the Congo and Cameroon: ecologic, virologic, and serologic surveys, 1979-1980. Ebola Virus Study Teams. J Infect Dis 1999;179 Suppl 1:S139-47.
35. Broadhurst MJ, Brooks TJG, Pollock NR. Diagnosis of Ebola Virus Disease, Past, Present, and Future. Clin. Microbiol. Rev. 2016;29:773–93.

36. Busico KM, Marshall KL, Ksiazek TG, et al. Prevalence of IgG antibodies to Ebola virus in individuals during an Ebola outbreak, Democratic Republic of the Congo, 1995. J Infect Dis 1999;179 Suppl 1:S102-7.
37. Caillaud D, Levréro F, Cristescu R, et al. Gorilla susceptibility to Ebola virus: the cost of sociality. Curr Biol 2006;16:R489-91.
38. Cantin R, Méthot S, Tremblay MJ. Plunder and stowaways: incorporation of cellular proteins by enveloped viruses. J Virol 2005;79:6577–87.
39. Carette JE, Raaben M, Wong AC, et al. Ebola virus entry requires the cholesterol transporter Niemann-Pick C1. Nature 2011;477:340–3.
40. Cartee TL, Wertz GW. Respiratory syncytial virus M2-1 protein requires phosphorylation for efficient function and binds viral RNA during infection. J Virol 2001;75:12188–97.
41. Cartier C, Deckert M, Grangeasse C, et al. Association of ERK2 mitogen-activated protein kinase with human immunodeficiency virus particles. J Virol 1997;71:4832–7.
42. Chan SY, Empig CJ, Welte FJ, et al. Folate receptor-alpha is a cofactor for cellular entry by Marburg and Ebola viruses. Cell 2001;106:117–26.
43. Chandran K, Sullivan NJ, Felbor U, Whelan SP, Cunningham JM. Endosomal proteolysis of the Ebola virus glycoprotein is necessary for infection. Science 2005;308:1643–5.
44. Chua AC, Cunningham J, Moussy F, Perkins MD, Formenty P. The Case for Improved Diagnostic Tools to Control Ebola Virus Disease in West Africa and How to Get There. PLoS Negl Trop Dis 2015;9:e0003734.
45. Chughtai AA, Barnes M, Macintyre CR. Persistence of Ebola virus in various body fluids during convalescence: evidence and implications for disease transmission and control. Epidemiol Infect 2016;144:1652–60.
46. Clark DV, Kibuuka H, Millard M, et al. Long-term sequelae after Ebola virus disease in Bundibugyo, Uganda, A retrospective cohort study. The Lancet Infectious Diseases 2015;15:905–12.
47. Cohen P. The regulation of protein function by multisite phosphorylation--a 25 year update. Trends Biochem Sci 2000;25:596–601.
48. Collins PL, Hill MG, Cristina J, Grosfeld H. Transcription elongation factor of respiratory syncytial virus, a nonsegmented negative-strand RNA virus. Proc Natl Acad Sci U S A 1996;93:81–5.
49. Coltart CEM, Lindsey B, Ghinai I, Johnson AM, Heymann DL. The Ebola outbreak, 2013-2016: old lessons for new epidemics. Philos Trans R Soc Lond , B, Biol Sci 2017;372.
50. Cox NJ, McCormick JB, Johnson KM, Kiley MP. Evidence for two subtypes of Ebola virus based on oligonucleotide mapping of RNA. J Infect Dis 1983;147:272–5.
51. Dai J, Zhang J, Sun Y, et al. Characterization of a novel human protein phosphatase 2C family member, PP2Ckappa. Int J Mol Med 2006;17:1117–23.
52. Davey NE, Cyert MS, Moses AM. Short linear motifs - ex nihilo evolution of protein regulation. Cell Commun Signal 2015;13:43.
53. Davey NE, Travé G, Gibson TJ. How viruses hijack cell regulation. Trends Biochem Sci 2011;36:159–69.

54. Davey RT, Dodd L, Proschan MA, et al. A Randomized, Controlled Trial of ZMapp for Ebola Virus Infection. N Engl J Med 2016;375:1448–56.
55. De BP, Gupta S, Banerjee AK. Cellular protein kinase C isoform zeta regulates human parainfluenza virus type 3 replication. Proc Natl Acad Sci U S A 1995;92:5204–8.
56. Deen GF, Knust B, Broutet N, et al. Ebola RNA Persistence in Semen of Ebola Virus Disease Survivors - Preliminary Report. N Engl J Med 2015.
57. Deminoff SJ, Ramachandran V, Herman PK. Distal recognition sites in substrates are required for efficient phosphorylation by the cAMP-dependent protein kinase. Genetics 2009;182:529–39.
58. Diallo B, Sissoko D, Loman NJ, et al. Resurgence of Ebola Virus Disease in Guinea Linked to a Survivor With Virus Persistence in Seminal Fluid for More Than 500 Days. Clin Infect Dis 2016;63:1353–6.
59. DiCarlo A, Biedenkopf N, Hartlieb B, Klussmeier A, Becker S. Phosphorylation of Marburg virus NP region II modulates viral RNA synthesis. J Infect Dis 2011;204 Suppl 3:S927-33.
60. Donella-Deana A, Krinks MH, Ruzzene M, Klee C, Pinna LA. Dephosphorylation of phosphopeptides by calcineurin (protein phosphatase 2B). Eur J Biochem 1994;219:109–17.
61. Dowell SF, Mukunu R, Ksiazek TG, Khan AS, Rollin PE, Peters CJ. Transmission of Ebola hemorrhagic fever: a study of risk factors in family members, Kikwit, Democratic Republic of the Congo, 1995. Commission de Lutte contre les Epidémies à Kikwit. J Infect Dis 1999;179 Suppl 1:S87-91.
62. Dunning J, Kennedy SB, Antierens A, et al. Experimental Treatment of Ebola Virus Disease with Brincidofovir. PLoS ONE 2016;11:e0162199.
63. Dunning J, Sahr F, Rojek A, et al. Experimental Treatment of Ebola Virus Disease with TKM-130803: A Single-Arm Phase 2 Clinical Trial. PLoS Med 2016;13:e1001997.
64. Dziubańska PJ, Derewenda U, Ellena JF, Engel DA, Derewenda ZS. The structure of the C-terminal domain of the Zaire ebolavirus nucleoprotein. Acta Crystallogr D Biol Crystallogr 2014;70:2420–9.
65. Ebola haemorrhagic fever in Sudan, 1976. Bull World Health Organ 1978;56:247–70.
66. Ebola haemorrhagic fever in Zaire, 1976. Bull World Health Organ 1978;56:271–93.
67. Ebola virus disease. (Accessed December 5, 2018, at http://www.who.int/en/news-room/fact-sheets/detail/ebola-virus-disease).
68. Elliott LH, Kiley MP, McCormick JB. Descriptive analysis of Ebola virus proteins. Virology 1985;147:169–76.
69. Emond RT, Evans B, Bowen ET, Lloyd G. A case of Ebola virus infection. Br Med J 1977;2:541–4.
70. Empig CJ, Goldsmith MA. Association of the caveola vesicular system with cellular entry by filoviruses. J Virol 2002;76:5266–70.
71. Enterlein S, Volchkov V, Weik M, et al. Rescue of recombinant Marburg virus from cDNA is dependent on nucleocapsid protein VP30. J Virol 2006;80:1038–43.
72. Ewer K, Rampling T, Venkatraman N, et al. A Monovalent Chimpanzee Adenovirus Ebola Vaccine Boosted with MVA. N Engl J Med 2016;374:1635–46.

73. Feldmann H, Geisbert TW. Ebola haemorrhagic fever. The Lancet 2011;377:849–62.
74. Feldmann H, Nichol ST, Klenk HD, Peters CJ, Sanchez A. Characterization of filoviruses based on differences in structure and antigenicity of the virion glycoprotein. Virology 1994;199:469–73.
75. Ficarro SB, McCleland ML, Stukenberg PT, et al. Phosphoproteome analysis by mass spectrometry and its application to Saccharomyces cerevisiae. Nat Biotechnol 2002;20:301–5.
76. Fiol CJ, Wang A, Roeske RW, Roach PJ. Ordered multisite protein phosphorylation. Analysis of glycogen synthase kinase 3 action using model peptide substrates. J. Biol. Chem. 1990;265:6061–5.
77. Formenty P, Boesch C, Wyers M, et al. Ebola virus outbreak among wild chimpanzees living in a rain forest of Côte d'Ivoire. J Infect Dis 1999;179 Suppl 1:S120-6.
78. Fowler RA, Fletcher T, Fischer WA, et al. Caring for critically ill patients with ebola virus disease. Perspectives from West Africa. Am J Respir Crit Care Med 2014;190:733–7.
79. Garton AJ, Yeaman SJ. Identification and role of the basal phosphorylation site on hormone-sensitive lipase. Eur J Biochem 1990;191:245–50.
80. Geisbert TW, Hensley LE, Gibb TR, Steele KE, Jaax NK, Jahrling PB. Apoptosis induced in vitro and in vivo during infection by Ebola and Marburg viruses. Lab Invest 2000;80:171–86.
81. Geisbert TW, Hensley LE, Larsen T, et al. Pathogenesis of Ebola Hemorrhagic Fever in Cynomolgus Macaques. The American Journal of Pathology 2003;163:2347–70.
82. Geisbert TW, Jahrling PB. Differentiation of filoviruses by electron microscopy. Virus Res 1995;39:129–50.
83. Geisbert TW, Young HA, Jahrling PB, Davis KJ, Kagan E, Hensley LE. Mechanisms underlying coagulation abnormalities in ebola hemorrhagic fever: overexpression of tissue factor in primate monocytes/macrophages is a key event. J Infect Dis 2003;188:1618–29.
84. Giroud C, Chazal N, Briant L. Cellular kinases incorporated into HIV-1 particles: passive or active passengers? Retrovirology 2011;8:71.
85. Gógl G, Schneider KD, Yeh BJ, et al. The Structure of an NDR/LATS Kinase-Mob Complex Reveals a Novel Kinase-Coactivator System and Substrate Docking Mechanism. PLoS Biol 2015;13:e1002146.
86. Gramberg T, Hofmann H, Möller P, et al. LSECtin interacts with filovirus glycoproteins and the spike protein of SARS coronavirus. Virology 2005;340:224–36.
87. Groseth A, Charton JE, Sauerborn M, et al. The Ebola virus ribonucleoprotein complex, A novel VP30–L interaction identified. Virus Res 2009;140:8–14.
88. Guergnon J, Godet AN, Galioot A, et al. PP2A targeting by viral proteins: a widespread biological strategy from DNA/RNA tumor viruses to HIV-1. Biochim Biophys Acta 2011;1812:1498–507.

89. Hartlieb B, Modrof J, Mühlberger E, Klenk H-D, Becker S. Oligomerization of Ebola Virus VP30 Is Essential for Viral Transcription and Can Be Inhibited by a Synthetic Peptide. J. Biol. Chem. 2003;278:41830–6.
90. Hartlieb B, Muziol T, Weissenhorn W, Becker S. Crystal structure of the C-terminal domain of Ebola virus VP30 reveals a role in transcription and nucleocapsid association. Proc Natl Acad Sci U S A 2007;104:624–9.
91. Harty RN, Brown ME, Wang G, Huibregtse J, Hayes FP. A PPxY motif within the VP40 protein of Ebola virus interacts physically and functionally with a ubiquitin ligase: implications for filovirus budding. Proc Natl Acad Sci U S A 2000;97:13871–6.
92. Hayden FG, Friede M, Bausch DG. Experimental Therapies for Ebola Virus Disease: What Have We Learned? J Infect Dis 2017;215:167–70.
93. Hayes CG, Burans JP, Ksiazek TG, et al. Outbreak of fatal illness among captive macaques in the Philippines caused by an Ebola-related filovirus. Am J Trop Med Hyg 1992;46:664–71.
94. Henao-Restrepo AM, Camacho A, Longini IM, et al. Efficacy and effectiveness of an rVSV-vectored vaccine in preventing Ebola virus disease, Final results from the Guinea ring vaccination, open-label, cluster-randomised trial (Ebola Ça Suffit!). The Lancet 2017;389:505–18.
95. Henao-Restrepo AM, Longini IM, Egger M, et al. Efficacy and effectiveness of an rVSV-vectored vaccine expressing Ebola surface glycoprotein, Interim results from the Guinea ring vaccination cluster-randomised trial. The Lancet 2015;386:857–66.
96. Hertz EPT, Kruse T, Davey NE, et al. A Conserved Motif Provides Binding Specificity to the PP2A-B56 Phosphatase. Mol Cell 2016;63:686–95.
97. Heymann DL, Weisfeld JS, Webb PA, Johnson KM, Cairns T, Berquist H. Ebola hemorrhagic fever: Tandala, Zaire, 1977-1978. J Infect Dis 1980;142:372–6.
98. Hoenen T, Shabman RS, Groseth A, et al. Inclusion bodies are a site of ebolavirus replication. J Virol 2012;86:11779–88.
99. Hoenen T, Watt A, Mora A, Feldmann H. Modeling the lifecycle of Ebola virus under biosafety level 2 conditions with virus-like particles containing tetracistronic minigenomes. J Vis Exp 2014;(91):52381.
100. Hood CL, Abraham J, Boyington JC, Leung K, Kwong PD, Nabel GJ. Biochemical and structural characterization of cathepsin L-processed Ebola virus glycoprotein: implications for viral entry and immunogenicity. J Virol 2010;84:2972–82.
101. Hopfield JJ. Kinetic Proofreading, A New Mechanism for Reducing Errors in Biosynthetic Processes Requiring High Specificity. Proc Natl Acad Sci U S A 1974;71:4135–9.
102. Hsu CH, Kingsbury DW. Topography of phosphate residues in Sendai virus proteins. Virology 1982;120:225–34.
103. Huang M, Sato H, Hagiwara K, et al. Determination of a phosphorylation site in Nipah virus nucleoprotein and its involvement in virus transcription. J Gen Virol 2011;92:2133–41.
104. Huang Q, Fu W-L, You J-P, Mao Q. Laboratory diagnosis of Ebola virus disease and corresponding biosafety considerations in the China Ebola Treatment Center. Crit Rev Clin Lab Sci 2016;53:326–40.

105. Huang Y, Xu L, Sun Y, Nabel GJ. The assembly of Ebola virus nucleocapsid requires virion-associated proteins 35 and 24 and posttranslational modification of nucleoprotein. Mol Cell 2002;10:307–16.
106. Huijbregts B, Wachter P de, Obiang LSN, Akou ME. Ebola and the decline of gorilla Gorilla gorilla and chimpanzee Pan troglodytes populations in Minkebe Forest, north-eastern Gabon. ORX 2003;37.
107. Hunt CL, Kolokoltsov AA, Davey RA, Maury W. The Tyro3 receptor kinase Axl enhances macropinocytosis of Zaire ebolavirus. J. Virol. 2011;85:334–47.
108. Hunt L, Gupta-Wright A, Simms V, et al. Clinical presentation, biochemical, and haematological parameters and their association with outcome in patients with Ebola virus disease, An observational cohort study. The Lancet Infectious Diseases 2015;15:1292–9.
109. Iacovides DC, O'Shea CC, Oses-Prieto J, Burlingame A, McCormick F. Critical role for arginine methylation in adenovirus-infected cells. J. Virol. 2007;81:13209–17.
110. Iakoucheva LM, Radivojac P, Brown CJ, et al. The importance of intrinsic disorder for protein phosphorylation. Nucleic Acids Res 2004;32:1037–49.
111. Iampietro M, Younan P, Nishida A, et al. Ebola virus glycoprotein directly triggers T lymphocyte death despite of the lack of infection. PLoS Pathog 2017;13:e1006397.
112. Ilinykh PA, Tigabu B, Ivanov A, et al. Role of protein phosphatase 1 in dephosphorylation of Ebola virus VP30 protein and its targeting for the inhibition of viral transcription. J Biol Chem 2014;289:22723–38.
113. International Committee on Taxonomy of Viruses (ICTV). (Accessed December 5, 2018, at https://talk.ictvonline.org/information/w/faq/386/how-to-write-a-virus-name).
114. Jaax NK, Davis KJ, Geisbert TJ, et al. Lethal experimental infection of rhesus monkeys with Ebola-Zaire (Mayinga) virus by the oral and conjunctival route of exposure. Arch Pathol Lab Med 1996;120:140–55.
115. Jacob T, van den Broeke C, Favoreel HW. Viral serine/threonine protein kinases. J. Virol. 2011;85:1158–73.
116. Jacobs M, Rodger A, Bell DJ, et al. Late Ebola virus relapse causing meningoencephalitis, A case report. The Lancet 2016;388:498–503.
117. Jahrling PB, Geisbert TW, Dalgard DW, et al. Preliminary report: isolation of Ebola virus from monkeys imported to USA. Lancet 1990;335:502–5.
118. Jasenosky LD, Neumann G, Lukashevich I, Kawaoka Y. Ebola virus VP40-induced particle formation and association with the lipid bilayer. J Virol 2001;75:5205–14.
119. John SP, Wang T, Steffen S, Longhi S, Schmaljohn CS, Jonsson CB. Ebola virus VP30 is an RNA binding protein. J Virol 2007;81:8967–76.
120. Johnson E, Jaax N, White J, Jahrling P. Lethal experimental infections of rhesus monkeys by aerosolized Ebola virus. Int J Exp Pathol 1995;76:227–36.
121. Johnson ED, Johnson BK, Silverstein D, et al. Characterization of a new Marburg virus isolated from a 1987 fatal case in Kenya. Arch Virol Suppl 1996;11:101–14.
122. Johnson LN, Barford D. The effects of phosphorylation on the structure and function of proteins. Annu Rev Biophys Biomol Struct 1993;22:199–232.

123. Keck F, Ataey P, Amaya M, Bailey C, Narayanan A. Phosphorylation of Single Stranded RNA Virus Proteins and Potential for Novel Therapeutic Strategies. Viruses 2015;7:5257–73.
124. Khan AS, Tshioko FK, Heymann DL, et al. The reemergence of Ebola hemorrhagic fever, Democratic Republic of the Congo, 1995. Commission de Lutte contre les Epidémies à Kikwit. J Infect Dis 1999;179 Suppl 1:S76-86.
125. Kirchdoerfer RN, Moyer CL, Abelson DM, Saphire EO. The Ebola Virus VP30-NP Interaction Is a Regulator of Viral RNA Synthesis. PLoS Pathog 2016;12:e1005937.
126. Kõivomägi M, Valk E, Venta R, et al. Dynamics of Cdk1 substrate specificity during the cell cycle. Mol Cell 2011;42:610–23.
127. Kolesnikova L, Berghöfer B, Bamberg S, Becker S. Multivesicular bodies as a platform for formation of the Marburg virus envelope. J Virol 2004;78:12277–87.
128. Kolesnikova L, Bohil AB, Cheney RE, Becker S. Budding of Marburgvirus is associated with filopodia. Cell Microbiol 2007;9:939–51.
129. Komaki K-i, Katsura K, Ohnishi M, et al. Molecular cloning of PP2Ceta, a novel member of the protein phosphatase 2C family. Biochim Biophys Acta 2003;1630:130–7.
130. Kondratowicz AS, Lennemann NJ, Sinn PL, et al. T-cell immunoglobulin and mucin domain 1 (TIM-1) is a receptor for Zaire Ebolavirus and Lake Victoria Marburgvirus. PNAS 2011;108:8426–31.
131. Kreuels B, Wichmann D, Emmerich P, et al. A case of severe Ebola virus infection complicated by gram-negative septicemia. N Engl J Med 2014;371:2394–401.
132. Kruse T, Biedenkopf N, Hertz EPT, et al. The Ebola Virus Nucleoprotein Recruits the Host PP2A-B56 Phosphatase to Activate Transcriptional Support Activity of VP30. Mol Cell 2018;69:136-145.e6.
133. Ksiazek TG, West CP, Rollin PE, Jahrling PB, Peters CJ. ELISA for the detection of antibodies to Ebola viruses. J Infect Dis 1999;179 Suppl 1:S192-8.
134. Lammers T, Lavi S. Role of type 2C protein phosphatases in growth regulation and in cellular stress signaling. Crit Rev Biochem Mol Biol 2007;42:437–61.
135. Le Guenno B, Formenty P, Wyers M, Gounon P, Walker F, Boesch C. Isolation and partial characterisation of a new strain of Ebola virus. Lancet 1995;345:1271–4.
136. Leader DP, Katan M. Viral aspects of protein phosphorylation. J Gen Virol 1988;69 (Pt 7):1441–64.
137. Lee JE, Fusco ML, Hessell AJ, Oswald WB, Burton DR, Saphire EO. Structure of the Ebola virus glycoprotein bound to an antibody from a human survivor. Nature 2008;454:177–82.
138. Leirs H, Mills JN, Krebs JW, et al. Search for the Ebola virus reservoir in Kikwit, Democratic Republic of the Congo: reflections on a vertebrate collection. J Infect Dis 1999;179 Suppl 1:S155-63.
139. Lenard J. Host cell protein kinases in nonsegmented negative-strand virus (mononegavirales) infection. Pharmacology & Therapeutics 1999;83:39–48.
140. Leroy EM, Epelboin A, Mondonge V, et al. Human Ebola outbreak resulting from direct exposure to fruit bats in Luebo, Democratic Republic of Congo, 2007. Vector Borne Zoonotic Dis 2009;9:723–8.

141. Leroy EM, Kumulungui B, Pourrut X, et al. Fruit bats as reservoirs of Ebola virus. Nature 2005;438:575–6.
142. Leroy EM, Rouquet P, Formenty P, et al. Multiple Ebola virus transmission events and rapid decline of central African wildlife. Science 2004;303:387–90.
143. Licata JM, Johnson RF, Han Z, Harty RN. Contribution of ebola virus glycoprotein, nucleoprotein, and VP24 to budding of VP40 virus-like particles. J Virol 2004;78:7344–51.
144. Licata JM, Simpson-Holley M, Wright NT, Han Z, Paragas J, Harty RN. Overlapping motifs (PTAP and PPEY) within the Ebola virus VP40 protein function independently as late budding domains: involvement of host proteins TSG101 and VPS-4. J Virol 2003;77:1812–9.
145. Lier C, Becker S, Biedenkopf N. Dynamic phosphorylation of Ebola virus VP30 in NP-induced inclusion bodies. Virology 2017;512:39–47.
146. Lötfering B, Mühlberger E, Tamura T, Klenk HD, Becker S. The nucleoprotein of Marburg virus is target for multiple cellular kinases. Virology 1999;255:50–62.
147. Lötsch F, Schnyder J, Goorhuis A, Grobusch MP. Neuropsychological long-term sequelae of Ebola virus disease survivors - A systematic review. Travel Med Infect Dis 2017;18:18–23.
148. Ma C-T, Velazquez-Dones A, Hagopian JC, Ghosh G, Fu X-D, Adams JA. Ordered multi-site phosphorylation of the splicing factor ASF/SF2 by SRPK1. J Mol Biol 2008;376:55–68.
149. Mahanty S, Hutchinson K, Agarwal S, McRae M, Rollin PE, Pulendran B. Cutting edge: impairment of dendritic cells and adaptive immunity by Ebola and Lassa viruses. J Immunol 2003;170:2797–801.
150. Manguvo A, Mafuvadze B. The impact of traditional and religious practices on the spread of Ebola in West Africa: time for a strategic shift. Pan Afr Med J 2015;22 Suppl 1:9.
151. Manning G, Whyte DB, Martinez R, Hunter T, Sudarsanam S. The protein kinase complement of the human genome. Science 2002;298:1912–34.
152. Martinez MJ, Volchkova VA, Raoul H, Alazard-Dany N, Reynard O, Volchkov VE. Role of VP30 phosphorylation in the Ebola virus replication cycle. J Infect Dis 2011;204 Suppl 3:S934-40.
153. Martínez MJ, Biedenkopf N, Volchkova V, et al. Role of Ebola virus VP30 in transcription reinitiation. J Virol 2008;82:12569–73.
154. Martini GA. Marburg agent disease: in man. Trans R Soc Trop Med Hyg 1969;63:295–302.
155. Mate SE, Kugelman JR, Nyenswah TG, et al. Molecular Evidence of Sexual Transmission of Ebola Virus. N Engl J Med 2015;373:2448–54.
156. McElroy AK, Akondy RS, Davis CW, et al. Human Ebola virus infection results in substantial immune activation. PNAS 2015;112:4719–24.
157. McGivern DR, Collins PL, Fearns R. Identification of internal sequences in the 3' leader region of human respiratory syncytial virus that enhance transcription and confer replication processivity. J Virol 2005;79:2449–60.
158. Mehedi M, Falzarano D, Seebach J, et al. A new Ebola virus nonstructural glycoprotein expressed through RNA editing. J Virol 2011;85:5406–14.

159. Meiselbach H, Sticht H, Enz R. Structural analysis of the protein phosphatase 1 docking motif: molecular description of binding specificities identifies interacting proteins. Chem Biol 2006;13:49–59.
160. Michael Klüwer, working group Stephan Becker. Unpublished data.
161. Miranda ME, Ksiazek TG, Retuya TJ, et al. Epidemiology of Ebola (subtype Reston) virus in the Philippines, 1996. J Infect Dis 1999;179 Suppl 1:S115-9.
162. Miranda ME, White ME, Dayrit MM, Hayes CG, Ksiazek TG, Burans JP. Seroepidemiological study of filovirus related to Ebola in the Philippines. Lancet 1991;337:425–6.
163. Modrof J, Becker S, Muhlberger E. Ebola Virus Transcription Activator VP30 Is a Zinc-Binding Protein. J Virol 2003;77:3334–8.
164. Modrof J, Möritz C, Kolesnikova L, et al. Phosphorylation of Marburg virus VP30 at serines 40 and 42 is critical for its interaction with NP inclusions. Virology 2001;287:171–82.
165. Modrof J, Mühlberger E, Klenk H-D, Becker S. Phosphorylation of VP30 impairs ebola virus transcription. J Biol Chem 2002;277:33099–104.
166. Mohl B-P, Roy P. Cellular Casein Kinase 2 and Protein Phosphatase 2A Modulate Replication Site Assembly of Bluetongue Virus. J Biol Chem 2016;291:14566–74.
167. Moorhead GBG, Trinkle-Mulcahy L, Ulke-Lemée A. Emerging roles of nuclear protein phosphatases. Nat Rev Mol Cell Biol 2007;8:234–44.
168. Morvan JM, Deubel V, Gounon P, et al. Identification of Ebola virus sequences present as RNA or DNA in organs of terrestrial small mammals of the Central African Republic. Microbes Infect 1999;1:1193–201.
169. Mühlberger E. Filovirus replication and transcription. Future Virol 2007;2:205–15.
170. Mühlberger E, Weik M, Volchkov VE, Klenk H-D, Becker S. Comparison of the Transcription and Replication Strategies of Marburg Virus and Ebola Virus by Using Artificial Replication Systems. J Virol 1999;73:2333–42.
171. Mulangu S, Borchert M, Paweska J, et al. High prevalence of IgG antibodies to Ebola virus in the Efé pygmy population in the Watsa region, Democratic Republic of the Congo. BMC Infect Dis 2016;16:263.
172. Nanbo A, Imai M, Watanabe S, et al. Ebolavirus is internalized into host cells via macropinocytosis in a viral glycoprotein-dependent manner. PLoS Pathog 2010;6:e1001121.
173. Nanbo A, Watanabe S, Halfmann P, Kawaoka Y. The spatio-temporal distribution dynamics of Ebola virus proteins and RNA in infected cells. Sci Rep 2013;3:1206.
174. Nanyonga M, Saidu J, Ramsay A, Shindo N, Bausch DG. Sequelae of Ebola Virus Disease, Kenema District, Sierra Leone. Clin Infect Dis 2016;62:125–6.
175. Naruse H, Nagai Y, Yoshida T, et al. The polypeptides of mumps virus and their synthesis in infected chick embryo cells. Virology 1981;112:119–30.
176. Negredo A, Palacios G, Vázquez-Morón S, et al. Discovery of an ebolavirus-like filovirus in europe. PLoS Pathog 2011;7:e1002304.

177. Ngo JCK, Chakrabarti S, Ding J-H, et al. Interplay between SRPK and Clk/Sty kinases in phosphorylation of the splicing factor ASF/SF2 is regulated by a docking motif in ASF/SF2. Mol Cell 2005;20:77–89.
178. Noda T, Aoyama K, Sagara H, Kida H, Kawaoka Y. Nucleocapsid-like structures of Ebola virus reconstructed using electron tomography. J Vet Med Sci 2005;67:325–8.
179. Noda T, Ebihara H, Muramoto Y, et al. Assembly and budding of Ebolavirus. PLoS Pathog 2006;2:e99.
180. Noda T, Hagiwara K, Sagara H, Kawaoka Y. Characterization of the Ebola virus nucleoprotein-RNA complex. J Gen Virol 2010;91:1478–83.
181. Noda T, Halfmann P, Sagara H, Kawaoka Y. Regions in Ebola virus VP24 that are important for nucleocapsid formation. J Infect Dis 2007;196 Suppl 2:S247-50.
182. Noda T, Sagara H, Suzuki E, Takada A, Kida H, Kawaoka Y. Ebola virus VP40 drives the formation of virus-like filamentous particles along with GP. J Virol 2002;76:4855–65.
183. Noda T, Watanabe S, Sagara H, Kawaoka Y. Mapping of the VP40-binding regions of the nucleoprotein of Ebola virus. J Virol 2007;81:3554–62.
184. Okware SI, Omaswa FG, Zaramba S, et al. An outbreak of Ebola in Uganda. Trop Med Int Health 2002;7:1068–75.
185. Olsen JV, Blagoev B, Gnad F, et al. Global, in vivo, and site-specific phosphorylation dynamics in signaling networks. Cell 2006;127:635–48.
186. Ong S-E, Mittler G, Mann M. Identifying and quantifying in vivo methylation sites by heavy methyl SILAC. Nat Methods 2004;1:119–26.
187. Outbreak of Marburg virus hemorrhagic fever--Angola, October 1, 2004-March 29, 2005. MMWR Morb Mortal Wkly Rep 2005;54:308–9.
188. Outbreak Table | Marburg Hemorrhagic Fever | CDC. (Accessed December 5, 2018, at https://www.cdc.gov/vhf/marburg/resources/outbreak-table.html).
189. Pattyn SR. Ebola virus haemorrhagic fever, Proceedings of an International Colloquium on Ebola Virus Infection and other Haemorrhagic Feversheld in Antwerp, Belgium 6-8 December, 1977. International Colloquium on Ebola Virus Infection and other Haemorrhagic Fevers. Amsterdam, New York: Elsevier North-Holland Biomedical Press, 1978. XII, 436 S. ISBN: 9780444800602.
190. Peters CJ. Marburg and Ebola--arming ourselves against the deadly filoviruses. N Engl J Med 2005;352:2571–3.
191. Pinna LA, Ruzzene M. How do protein kinases recognize their substrates? Biochim Biophys Acta 1996;1314:191–225.
192. Piot P. No time to lose, A life in pursuit of deadly viruses. New York, London: W.W. Norton, 2013. 1 online resource (1 volume). ISBN: 0393084116.
193. Pourrut X, Délicat A, Rollin PE, Ksiazek TG, Gonzalez J-P, Leroy EM. Spatial and temporal patterns of Zaire ebolavirus antibody prevalence in the possible reservoir bat species. J Infect Dis 2007;196 Suppl 2:S176-83.
194. Prevention | Ebola (Ebola Virus Disease) | CDC, 2018. (Accessed December 5, 2018, at https://www.cdc.gov/vhf/ebola/prevention/index.html).
195. Regnery RL, Johnson KM, Kiley MP. Virion nucleic acid of Ebola virus. J Virol 1980;36:465–9.

196. Reiter P, Turell M, Coleman R, et al. Field investigations of an outbreak of Ebola hemorrhagic fever, Kikwit, Democratic Republic of the Congo, 1995: arthropod studies. J Infect Dis 1999;179 Suppl 1:S148-54.
197. Reynard O, Nemirov K, Page A, et al. Conserved proline-rich region of Ebola virus matrix protein VP40 is essential for plasma membrane targeting and virus-like particle release. J Infect Dis 2011;204 Suppl 3:S884-91.
198. Rimoin AW, Lu K, Bramble MS, et al. Ebola Virus Neutralizing Antibodies Detectable in Survivors of theYambuku, Zaire Outbreak 40 Years after Infection. J Infect Dis 2018;217:223–31.
199. Roach PJ. Multisite and hierarchal protein phosphorylation. J. Biol. Chem. 1991;266:14139–42.
200. Rollin P. Ebola and Marburg Viruses, A View of Infection Using Electron Microscopy. Emerg. Infect. Dis. 2004;10:1517.
201. Rollin PE, Williams RJ, Bressler DS, et al. Ebola (subtype Reston) virus among quarantined nonhuman primates recently imported from the Philippines to the United States. J Infect Dis 1999;179 Suppl 1:S108-14.
202. Rouquet P, Froment J-M, Bermejo M, et al. Wild animal mortality monitoring and human Ebola outbreaks, Gabon and Republic of Congo, 2001-2003. Emerging Infect Dis 2005;11:283–90.
203. Rubin CS, Rosen OM. Protein phosphorylation. Annu Rev Biochem 1975;44:831–87.
204. Rust HL, Thompson PR. Kinase consensus sequences: a breeding ground for crosstalk. ACS Chem Biol 2011;6:881–92.
205. Ryabchikova EI, Kolesnikova LV, Luchko SV. An analysis of features of pathogenesis in two animal models of Ebola virus infection. J Infect Dis 1999;179 Suppl 1:S199-202.
206. Saeed MF, Kolokoltsov AA, Albrecht T, Davey RA. Cellular entry of ebola virus involves uptake by a macropinocytosis-like mechanism and subsequent trafficking through early and late endosomes. PLoS Pathog 2010;6:e1001110.
207. Sanchez A. Analysis of filovirus entry into vero e6 cells, using inhibitors of endocytosis, endosomal acidification, structural integrity, and cathepsin (B and L) activity. J Infect Dis 2007;196 Suppl 2:S251-8.
208. Sanchez A, Kiley MP. Identification and analysis of Ebola virus messenger RNA. Virology 1987;157:414–20.
209. Sanchez A, Kiley MP, Holloway BP, Auperin DD. Sequence analysis of the Ebola virus genome: organization, genetic elements, and comparison with the genome of Marburg virus. Virus Res 1993;29:215–40.
210. Sanchez A, Kiley MP, Holloway BP, McCormick JB, Auperin DD. The nucleoprotein gene of Ebola virus: cloning, sequencing, and in vitro expression. Virology 1989;170:81–91.
211. Sanchez A, Yang ZY, Xu L, Nabel GJ, Crews T, Peters CJ. Biochemical analysis of the secreted and virion glycoproteins of Ebola virus. J Virol 1998;72:6442–7.
212. Schieffelin JS, Jacob ST. Raising the standard for clinical care of patients with Ebola virus disease. The Lancet Infectious Diseases 2015;15:1247–8.

213. Schieffelin JS, Shaffer JG, Goba A, et al. Clinical illness and outcomes in patients with Ebola in Sierra Leone. N Engl J Med 2014;371:2092–100.
214. Schlereth J, Grünweller A, Biedenkopf N, Becker S, Hartmann RK. RNA binding specificity of Ebola virus transcription factor VP30. RNA Biol 2016;13:783–98.
215. Schornberg K, Matsuyama S, Kabsch K, Delos S, Bouton A, White J. Role of endosomal cathepsins in entry mediated by the Ebola virus glycoprotein. J Virol 2006;80:4174–8.
216. Schornberg KL, Shoemaker CJ, Dube D, et al. Alpha5beta1-integrin controls ebolavirus entry by regulating endosomal cathepsins. PNAS 2009;106:8003–8.
217. Schudt G, Dolnik O, Kolesnikova L, Biedenkopf N, Herwig A, Becker S. Transport of Ebolavirus Nucleocapsids Is Dependent on Actin Polymerization: Live-Cell Imaging Analysis of Ebolavirus-Infected Cells. J Infect Dis 2015;212 Suppl 2:S160-6.
218. Schudt G, Kolesnikova L, Dolnik O, Sodeik B, Becker S. Live-cell imaging of Marburg virus-infected cells uncovers actin-dependent transport of nucleocapsids over long distances. Proc Natl Acad Sci U S A 2013;110:14402–7.
219. Shi W, Huang Y, Sutton-Smith M, et al. A filovirus-unique region of Ebola virus nucleoprotein confers aberrant migration and mediates its incorporation into virions. J Virol 2008;82:6190–9.
220. Shi Y. Serine/Threonine Phosphatases, Mechanism through Structure. Cell 2009;139:468–84.
221. Shimojima M, Takada A, Ebihara H, et al. Tyro3 family-mediated cell entry of Ebola and Marburg viruses. J Virol 2006;80:10109–16.
222. Simmons G, Reeves JD, Grogan CC, et al. DC-SIGN and DC-SIGNR bind ebola glycoproteins and enhance infection of macrophages and endothelial cells. Virology 2003;305:115–23.
223. Sissoko D, Duraffour S, Kerber R, et al. Persistence and clearance of Ebola virus RNA from seminal fluid of Ebola virus disease survivors, A longitudinal analysis and modelling study. The Lancet Global Health 2017;5:e80-e88.
224. Sissoko D, Laouenan C, Folkesson E, et al. Experimental Treatment with Favipiravir for Ebola Virus Disease (the JIKI Trial): A Historically Controlled, Single-Arm Proof-of-Concept Trial in Guinea. PLoS Med 2016;13:e1001967.
225. Smith CE, Simpson DI, Bowen ET, Zlotnik I. Fatal human disease from vervet monkeys. Lancet 1967;2:1119–21.
226. Sobarzo A, Ochayon DE, Lutwama JJ, et al. Persistent immune responses after Ebola virus infection. N Engl J Med 2013;369:492–3.
227. Ströher U, West E, Bugany H, Klenk HD, Schnittler HJ, Feldmann H. Infection and activation of monocytes by Marburg and Ebola viruses. J Virol 2001;75:11025–33.
228. Sugai A, Sato H, Yoneda M, Kai C. Phosphorylation of measles virus phosphoprotein at S86 and/or S151 downregulates viral transcriptional activity. FEBS Lett 2012;586:3900–7.
229. Sun D, Luthra P, Li Z, He B. PLK1 down-regulates parainfluenza virus 5 gene expression. PLoS Pathog 2009;5:e1000525.
230. Sun M, Fuentes SM, Timani K, et al. Akt plays a critical role in replication of nonsegmented negative-stranded RNA viruses. J. Virol. 2008;82:105–14.

231. Swain PS, Siggia ED. The role of proofreading in signal transduction specificity. Biophys J 2002;82:2928–33.
232. Swanepoel R, Leman PA, Burt FJ, et al. Experimental inoculation of plants and animals with Ebola virus. Emerging Infect Dis 1996;2:321–5.
233. Swingle M, Ni L, Honkanen RE. Small-molecule inhibitors of ser/thr protein phosphatases: specificity, use and common forms of abuse. Methods Mol Biol 2007;365:23–38.
234. Takada A, Robison C, Goto H, et al. A system for functional analysis of Ebola virus glycoprotein. Proc Natl Acad Sci U S A 1997;94:14764–9.
235. Takada A, Watanabe S, Ito H, Okazaki K, Kida H, Kawaoka Y. Downregulation of beta1 integrins by Ebola virus glycoprotein: implication for virus entry. Virology 2000;278:20–6.
236. Tanner SJ, Ariza A, Richard C-A, et al. Crystal structure of the essential transcription antiterminator M2-1 protein of human respiratory syncytial virus and implications of its phosphorylation. Proc Natl Acad Sci U S A 2014;111:1580–5.
237. Tarrant MK, Cole PA. The chemical biology of protein phosphorylation. Annu Rev Biochem 2009;78:797–825.
238. Timmins J, Scianimanico S, Schoehn G, Weissenhorn W. Vesicular release of ebola virus matrix protein VP40. Virology 2001;283:1–6.
239. Tompa P, Davey NE, Gibson TJ, Babu MM. A million peptide motifs for the molecular biologist. Mol Cell 2014;55:161–9.
240. Towner JS, Amman BR, Sealy TK, et al. Isolation of genetically diverse Marburg viruses from Egyptian fruit bats. PLoS Pathog 2009;5:e1000536.
241. Towner JS, Khristova ML, Sealy TK, et al. Marburgvirus genomics and association with a large hemorrhagic fever outbreak in Angola. J Virol 2006;80:6497–516.
242. Towner JS, Sealy TK, Khristova ML, et al. Newly discovered ebola virus associated with hemorrhagic fever outbreak in Uganda. PLoS Pathog 2008;4:e1000212.
243. Turell MJ, Bressler DS, Rossi CA. Short report: lack of virus replication in arthropods after intrathoracic inoculation of Ebola Reston virus. Am J Trop Med Hyg 1996;55:89–90.
244. Ubersax JA, Ferrell JE. Mechanisms of specificity in protein phosphorylation. Nat Rev Mol Cell Biol 2007;8:530–41.
245. Uehara Y, Fukazawa H, Murakami Y, Mizuno S. Irreversible inhibition of v-src tyrosine kinase activity by herbimycin A and its abrogation by sulfhydryl compounds. Biochem Biophys Res Commun 1989;163:803–9.
246. Uyeki TM, Mehta AK, Davey RT, et al. Clinical Management of Ebola Virus Disease in the United States and Europe. N Engl J Med 2016;374:636–46.
247. van de Weerdt BCM, Littler DR, Klompmaker R, et al. Polo-box domains confer target specificity to the Polo-like kinase family. Biochim Biophys Acta 2008;1783:1015–22.
248. van Griensven J, Bah EI, Haba N, et al. Electrolyte and Metabolic Disturbances in Ebola Patients during a Clinical Trial, Guinea, 2015. Emerging Infect Dis 2016;22.

249. van Griensven J, Weiggheleire A de, Delamou A, et al. The Use of Ebola Convalescent Plasma to Treat Ebola Virus Disease in Resource-Constrained Settings: A Perspective From the Field. Clin Infect Dis 2016;62:69–74.
250. Varkey JB, Shantha JG, Crozier I, et al. Persistence of Ebola Virus in Ocular Fluid during Convalescence. N Engl J Med 2015;372:2423–7.
251. Vidal S, Kolakofsky D. Modified model for the switch from Sendai virus transcription to replication. J Virol 1989;63:1951–8.
252. Villanueva N, Hardy R, Asenjo A, Yu Q, Wertz G. The bulk of the phosphorylation of human respiratory syncytial virus phosphoprotein is not essential but modulates viral RNA transcription and replication. J Gen Virol 2000;81:129–33.
253. Villanueva N, Navarro J, Méndez E, García-Albert I. Identification of a protein kinase involved in the phosphorylation of the C-terminal region of human respiratory syncytial virus P protein. J Gen Virol 1994;75 (Pt 3):555–65.
254. Volchkov VE, Becker S, Volchkova VA, et al. GP mRNA of Ebola virus is edited by the Ebola virus polymerase and by T7 and vaccinia virus polymerases. Virology 1995;214:421–30.
255. Volchkov VE, Feldmann H, Volchkova VA, Klenk HD. Processing of the Ebola virus glycoprotein by the proprotein convertase furin. Proc Natl Acad Sci U S A 1998;95:5762–7.
256. Volchkov VE, Volchkova VA, Chepurnov AA, et al. Characterization of the L gene and 5' trailer region of Ebola virus. J Gen Virol 1999;80 (Pt 2):355–62.
257. Votteler J, Sundquist WI. Virus budding and the ESCRT pathway. Cell Host Microbe 2013;14:232–41.
258. Walsh PD, Abernethy KA, Bermejo M, et al. Catastrophic ape decline in western equatorial Africa. Nature 2003;422:611–4.
259. Wang Z, Cole PA. Catalytic mechanisms and regulation of protein kinases. Meth Enzymol 2014;548:1–21.
260. Watanabe S, Noda T, Kawaoka Y. Functional mapping of the nucleoprotein of Ebola virus. J Virol 2006;80:3743–51.
261. Weik M, Modrof J, Klenk H-D, Becker S, Mühlberger E. Ebola virus VP30-mediated transcription is regulated by RNA secondary structure formation. J Virol 2002;76:8532–9.
262. Weingartl HM, Embury-Hyatt C, Nfon C, Leung A, Smith G, Kobinger G. Transmission of Ebola virus from pigs to non-human primates. Sci Rep 2012;2:811.
263. Wenk J, Mieskes G. Cytosolic and nuclear localization of protein phosphatase 2C beta 1 in COS and BHK cells. Eur J Cell Biol 1995;68:377–86.
264. West TE, Saint André-von Arnim A v. Clinical presentation and management of severe Ebola virus disease. Ann Am Thorac Soc 2014;11:1341–50.
265. Willemsen NM, Hitchen EM, Bodetti TJ, et al. Protein methylation is required to maintain optimal HIV-1 infectivity. Retrovirology 2006;3:92.
266. Wittmann TJ, Biek R, Hassanin A, et al. Isolates of Zaire ebolavirus from wild apes reveal genetic lineage and recombinants. PNAS 2007;104:17123–7.
267. Wooten MW. In-gel kinase assay as a method to identify kinase substrates. Sci STKE 2002;2002:pl15.

268. World Health Organization. Ebola virus disease outbreak: World Health Organization. (Accessed December 5, 2018, at http://www.who.int/csr/disease/ebola/en/).
269. Wu X, Gong X, Foley HD, Schnell MJ, Fu ZF. Both viral transcription and replication are reduced when the rabies virus nucleoprotein is not phosphorylated. J Virol 2002;76:4153–61.
270. Xu W, Luthra P, Wu C, et al. Ebola virus VP30 and nucleoprotein interactions modulate viral RNA synthesis. Nat Commun 2017;8.
271. Yamagata K, Daitoku H, Takahashi Y, et al. Arginine methylation of FOXO transcription factors inhibits their phosphorylation by Akt. Mol Cell 2008;32:221–31.
272. Yamayoshi S, Noda T, Ebihara H, et al. Ebola virus matrix protein VP40 uses the COPII transport system for its intracellular transport. Cell Host Microbe 2008;3:168–77.
273. Years of Ebola Virus Disease Outbreaks | 2014-2016 Outbreak West Africa | History | Ebola (Ebola Virus Disease) | CDC, 2018. (Accessed December 5, 2018, at https://www.cdc.gov/vhf/ebola/history/chronology.html).
274. Yuan G, Kaneko M, Masuda H, Hon RB, Kobayashi A, Yamazaki N. Decrease in heart mitochondrial creatine kinase activity due to oxygen free radicals. Biochim Biophys Acta 1992;1140:78–84.
275. Zaki SR, Goldsmith CS. Pathologic features of filovirus infections in humans. Curr Top Microbiol Immunol 1999;235:97–116.
276. Zaki SR, Shieh WJ, Greer PW, et al. A novel immunohistochemical assay for the detection of Ebola virus in skin: implications for diagnosis, spread, and surveillance of Ebola hemorrhagic fever. Commission de Lutte contre les Epidémies à Kikwit. J Infect Dis 1999;179 Suppl 1:S36-47.
277. Zeke A, Bastys T, Alexa A, et al. Systematic discovery of linear binding motifs targeting an ancient protein interaction surface on MAP kinases. Mol Syst Biol 2015;11:837.
278. Zou L, Wang M, Shen Y, Liao J, Li A, Wang M. PKIS: computational identification of protein kinases for experimentally discovered protein phosphorylation sites. BMC Bioinformatics 2013;14:247.

Appendix

Overview of VP30 Mutants

On the following pages, sequences of the VP30 mutants are shown, from amino acid 23 to 50. This region comprises the two N-terminal phosphorylation clusters that are studied in this thesis. Serine is mutated to alanine to mimic a permanently nonphosphorylated serine residue and to aspartate to mimic permanently phosphorylated serine residue. Amino acids of putative VP30 phosphorylation motifs are mutated to uncharged alanine. The amino acids which differ from VP30 wt are framed.

For reasons of simplification, the nomenclature of the VP30 mutants is not in accordance with the suggestions of the Human genome variation society (HGVS). EBOV VP30 serines 29-31 is summarized as a first cluster of serine residues and serines 42 / 44 / 46 as a second cluster of serine residues. When all six serine residues are mutated to alanine, the mutant is abbreviated as VP30_AA. The first A stands for mutation of the first serine cluster to alanine residues, the second A for mutation of the second cluster to alanine residues. Likewise, mutation of the first serine cluster to aspartate and of the second serine cluster to alanine is abbreviated as VP30_DA. Based on this nomenclature, a VP30 mutant with serine only on position 29 and alanine on the other positions can be named VP30_AA_A29S. According to the HGVS, the correct nomenclature for this mutant would be:

p.VP30 [Ser30Ala; Ser31Ala; Ser42Ala; Ser44Ala; Ser46Ala]

Alternative names for the VP30 mutants have previously been used in manuscripts and publications and are presented on the following pages.

Name	Alternative Name	Amino acid sequence																										
		23			26		28	29	30	31	32	33						40		42	43	44		46	47			50
VP30 wt		**H**	**H**	**V**	**R**	**A**	**R**	**S**	**S**	**S**	**R**	**E**	**N**	**Y**	**R**	**G**	**E**	**Y**	**R**	**Q**	**S**	**R**	**S**	**A**	**S**	**Q**	**V**	**R**	**V**
VP30 AA		H	H	V	R	A	R	A	A	A	R	E	N	Y	R	G	E	Y	R	Q	A	R	A	A	A	Q	V	R	V
VP30 DD		H	H	V	R	A	R	D	D	D	R	E	N	Y	R	G	E	Y	R	Q	D	R	D	A	D	Q	V	R	V
VP30 SA		H	H	V	R	A	R	S	S	S	R	E	N	Y	R	G	E	Y	R	Q	A	R	A	A	A	Q	V	R	V
VP30 AS		H	H	V	R	A	R	A	A	A	R	E	N	Y	R	G	E	Y	R	Q	S	R	S	A	S	Q	V	R	V
VP30 DA		H	H	V	R	A	R	D	D	D	R	E	N	Y	R	G	E	Y	R	Q	A	R	A	A	A	Q	V	R	V
VP30 AD		H	H	V	R	A	R	A	A	A	R	E	N	Y	R	G	E	Y	R	Q	D	R	D	A	D	Q	V	R	V
VP30 AA_A29D	VP30 D29	H	H	V	R	A	R	D	A	A	R	E	N	Y	R	G	E	Y	R	Q	A	R	A	A	A	Q	V	R	V
VP30 AA_A29S	VP30 S29	H	H	V	R	A	R	S	A	A	R	E	N	Y	R	G	E	Y	R	Q	A	R	A	A	A	Q	V	R	V
VP30 AA_A30S	VP30 S30	H	H	V	R	A	R	A	S	A	R	E	N	Y	R	G	E	Y	R	Q	A	R	A	A	A	Q	V	R	V
VP30 AA_A31S	VP30 S31	H	H	V	R	A	R	A	A	S	R	E	N	Y	R	G	E	Y	R	Q	A	R	A	A	A	Q	V	R	V
VP30 AA_A42S	VP30 S42	H	H	V	R	A	R	A	A	A	R	E	N	Y	R	G	E	Y	R	Q	S	R	A	A	A	Q	V	R	V
VP30 AA_A44S	VP30 S44	H	H	V	R	A	R	A	A	A	R	E	N	Y	R	G	E	Y	R	Q	A	R	S	A	A	Q	V	R	V
VP30 AA_A46S	VP30 S46	H	H	V	R	A	R	A	A	A	R	E	N	Y	R	G	E	Y	R	Q	A	R	A	A	S	Q	V	R	V

Name	Alternative Name	Amino acid sequence																										
		23			26		28	29	30	31	32	33							40		42	43	44		46	47			50
VP30 wt		**H**	**H**	**V**	**R**	**A**	**R**	**S**	**S**	**S**	**R**	**E**	**N**	**Y**	**R**	**G**	**E**	**Y**	**R**	**Q**	**S**	**R**	**S**	**A**	**S**	**Q**	**V**	**R**	**V**
VP30 S29A	VP30 A29	H	H	V	R	A	R	A	S	S	R	E	N	Y	R	G	E	Y	R	Q	S	R	S	A	S	Q	V	R	V
VP30 S30A	VP30 A30	H	H	V	R	A	R	S	A	S	R	E	N	Y	R	G	E	Y	R	Q	S	R	S	A	S	Q	V	R	V
VP30 S31A	VP30 A31	H	H	V	R	A	R	S	S	A	R	E	N	Y	R	G	E	Y	R	Q	S	R	S	A	S	Q	V	R	V
VP30 S42A	VP30 A42	H	H	V	R	A	R	S	S	S	R	E	N	Y	R	G	E	Y	R	Q	A	R	S	A	S	Q	V	R	V
VP30 S44A	VP30 A44	H	H	V	R	A	R	S	S	S	R	E	N	Y	R	G	E	Y	R	Q	S	R	A	A	S	Q	V	R	V
VP30 S46A	VP30 A46	H	H	V	R	A	R	S	S	S	R	E	N	Y	R	G	E	Y	R	Q	S	R	S	A	A	Q	V	R	V
VP30 R26A		H	H	V	A	A	R	S	S	S	R	E	N	Y	R	G	E	Y	R	Q	S	R	S	A	S	Q	V	R	V
VP30 R28A		H	H	V	R	A	A	S	S	S	R	E	N	Y	R	G	E	Y	R	Q	S	R	S	A	S	Q	V	R	V
VP30 R32A		H	H	V	R	A	R	S	S	S	A	E	N	Y	R	G	E	Y	R	Q	S	R	S	A	S	Q	V	R	V
VP30 R40A		H	H	V	R	A	R	S	S	S	R	E	N	Y	R	G	E	Y	A	Q	S	R	S	A	S	Q	V	R	V
VP30 R40A_R43A		H	H	V	R	A	R	S	S	S	R	E	N	Y	R	G	E	Y	A	Q	S	A	S	A	S	Q	V	R	V
VP30 R26A_R28A_R40A	VP30 3RA	H	H	V	A	A	A	S	S	S	R	E	N	Y	R	G	E	Y	A	Q	S	R	S	A	S	Q	V	R	V
VP30 E33A		H	H	V	R	A	R	S	S	S	R	A	N	Y	R	G	E	Y	R	Q	S	R	S	A	S	Q	V	R	V
VP30 Q47A		H	H	V	R	A	R	S	S	S	R	E	N	Y	R	G	E	Y	R	Q	S	R	S	A	S	A	V	R	V

Name	Alternative Name	Amino acid sequence																										
		23			26		28	29	30	31	32	33						40		42	43	44		46	47			50
VP30 wt		**H**	**H**	**V**	**R**	**A**	**R**	**S**	**S**	**S**	**R**	**E**	**N**	**Y**	**R**	**G**	**E**	**Y**	**R**	**Q**	**S**	**R**	**S**	**A**	**S**	**Q**	**V**	**R**	**V**
VP30 AA_A29S_R26A		H	H	V	A	A	R	S	A	A	R	E	N	Y	R	G	E	Y	R	Q	A	R	A	A	A	Q	V	R	V
VP30 AA_A29S_R28A		H	H	V	R	A	A	S	A	A	R	E	N	Y	R	G	E	Y	R	Q	A	R	A	A	A	Q	V	R	V
VP30 AA_A29S_R26A_R28A		H	H	V	A	A	A	S	A	A	R	E	N	Y	R	G	E	Y	R	Q	A	R	A	A	A	Q	V	R	V
VP30 AA_A29S_A31S		H	H	V	R	A	R	S	A	S	R	E	N	Y	R	G	E	Y	R	Q	A	R	A	A	A	Q	V	R	V
VP30 AA_A29S_A31S_R26A		H	H	V	A	A	R	S	A	S	R	E	N	Y	R	G	E	Y	R	Q	A	R	A	A	A	Q	V	R	V
VP30 AA_A29S_A31S_R28A		H	H	V	R	A	A	S	A	S	R	E	N	Y	R	G	E	Y	R	Q	A	R	A	A	A	Q	V	R	V
VP30 AA_A29S_A31S_R26A_R28A		H	H	V	A	A	A	S	A	S	R	E	N	Y	R	G	E	Y	R	Q	A	R	A	A	A	Q	V	R	V

RPM to RCF Conversion for Centrifuges

For conversion of revolutions per minute (RPM) to the relative centrifugal force (RCF), the following equation can be used. RCF is expressed in multiples of the standard gravity (× g or times g).

R is the radius of the rotor in mm. R_{mid} is used for the average RCF, R_{max} for maximum RCF, and R_{min} for mininum RCF. A table of rotors used in this thesis is shown below.

$$RCF = 1.118 \times R \times RPM^2 \times 10^{-6}$$

or

$$RPM = 10^3 \times \sqrt{\frac{RCF}{R \times 1.118}}$$

Rotor		**R_{min} (in mm)**	**R_{mid} (in mm)**	**R_{max} (in mm)**
Beckmann Coulter	SW32	66.8	109.65	152.5
	SW41	67.4	110.25	153.1
	SW60	63.1	91.7	120.3
Eppendorf centrifuge 5415R – 24 place fixed angle rotor				84
Heraeus Multifuge 3S-R – swinging bucket rotor				~190

Figures

Tables

Abbrevations

aa	amino acid
AKT	protein kinase B
APS	ammonium persulfate
ATM	ataxia telangiectasia mutated
ATP	adenosine triphosphat
ATR	ataxia telangiectasia and rad3-related protein
BDBV	Bundibugyo virus
bp	base pairs
BSA	bovine serum albumin
BSL	biosafety level
CAMK	Ca^{2+} / calmodulin-dependent protein kinase
CDC	Center for Disease Control and Prevention
cDNA	complementary DNA or copy DNA
CEB	cell extraction buffer
CHK	checkpoint kinase
CIP	calf intestinal phosphatase
CK	casein kinase
CLK	cdc2-like kinase
Co-IP	co-immunoprecipitation
COP	coat protein complex
C-terminus	carboxy-terminus
d	day
DA	Dalton
DABCO	1,4-diazabicyclo[2.2.2]octane
DAPI	4',6-diamidino-2-phenylindole
DC-SIGN	dendritic cell-specific ICAM-3 grabbing nonintegrin
dH_2O	distilled H_2O
DMEM	Dulbecco's modified Eagle's medium
DMSO	dimethyl sulfoxide
DNA	deoxyribonucleic acid
dNTP	deoxynucleotide triphosphates
DRC	Democratic Republic of Congo
ds	double-stranded

DTT	dithiothreitol
E. coli	Escherichia coli
e.g.	exempli gratia
EBOV	Ebola virus
EDTA	ethylenediaminetetraacetic acid
EGTA	ethylene glycol tetraacetic acid
EM	electron microscopy
ESCRT	endosomal sorting complexes required for transport
EtOH	ethanol
EVD	Ebola virus disease
f	flag
f.i.	for instance
FCS	fetal calf serum
FF	Firefly
for	forward
g	standard gravity
GER	Germany
gp	guinea pig
GP	glycoprotein
h	hour / hours
HA	hemagglutinin
HEK-293	human embryonic kidney-293 cells
HGVS	Human Genome Variation Society
HUH-7	human hepatoma-7 cells
IC	inhibitory concentration
IC50	half maximal inhibitory concentration
ICTV	International Committee on Taxonomy of Viruses (ICTV)
IFA	immunofluorescence analysis
INR	international normalised ratio
k	kilo
kb	kilobases
L	large (protein)
LB	lysogeny broth
LLOV	Lloviu virus

L-SIGN	liver / lymph node-specific ICAM-3 grabbing nonintegrin
M	mol / l
MARV	Marburg virus
MCS	multiple cloning site
min	minute / minutes
MM	mastermix
MOI	multiplicity of infection
mRNA	messenger RNA
MVB	multivesicular bodies
NaF	sodium fluoride
NC	nitrocellulose
NEM	N-ethylmaleimide
NP	nucleoprotein
NP-40	nonyl phenoxypolyethoxylethanol
N-terminus	amino-terminus
OA	okadaic acid
p.i.	post infectionem
P.K	proteinase K
p.t.	post transfectionem
P/S	penicillin / streptomycin
PAGE	polyacrylamide gel electrophoresis
PBS	phosphate-buffered saline
PBS_{def}	phosphate-buffered saline deficient in calcium and magnesium
PCR	polymerase chain reaction
PEG	polyethylene glycol
PFA	paraformaldehyd
Pfu	Pyrococcus furiosus
pfu	plaque-forming unit
pH	potentia hydrogenii
PKA	protein kinase a
PKB	protein kinase b
PKC	protein kinase c
PKG	protein kinase g
PLK1	Polo-like-kinase 1

PMSF	phenylmethane sulfonyl fluoride
PP	protein phosphatase
PRMT	protein arginine methyl transferase
pS29	phosphoserine at position 29 of VP30
P-site	phosphorylation site
PTT	prothrombin time
R	radius
RCF	relative centrifugal force
rec	recombinant
REN	Renilla
RESTV	Reston ebolavirus
rev	reverse
rel.	relative
RLU	relative light units
RNA	ribonucleic acid
ROCK	Rho-associated protein kinase
RPM	revolutions per minute
RSK	ribosomal s6 kinase
RSV	respiratory syncytial virus
rt	room temperature
RT-PCR	reverse transcriptase-PCR
SDM	site-directed mutagenesis
SDS	sodium dodecyl sulfate
sec	seconds
sGP	soluble glycoprotein
siRNA	small interfering RNA
SLIM	short linear motif
SOB	super optimal broth
ssGP	small soluble glycoprotein
SUDV	Sudan virus
T7-pol	T7 DNA-dependent RNA polymerase
TAFV	Taï Forest virus
TBCA	tetrabromocinnamic acid
TBS	Tris-buffered saline

TE	Tris-EDTA
TEMED	tetramethylethylenediamine
TM	Tris-Magnesium
TNE	Tris-NaCl-EDTA buffer
trVLP	transcription and replication competent VLP
U	units
UV	ultraviolett
VLP	virus-like particle
VP	viral protein
WB	western blot
WHO	World Health Organization
wt	wild type
α	anti

Amino Acid Abbrevations

Alanine	Ala	A
Arginine	Arg	R
Asparagine	Asn	N
Aspartic acid	Asp	D
Cysteine	Cys	C
Glutamine	Gln	Q
Glutamic acid	Glu	E
Glycine	Gly	G
Histidine	His	H
Isoleucine	Ile	I
Leucine	Leu	L
Lysine	Lys	K
Methionine	Met	M
Phenylalanine	Phe	F
Proline	Pro	P
Serine	Ser	S
Threonine	Thr	T
Tryptophan	Trp	W
Tyrosine	Tyr	Y
Valine	Val	V
Any amino acid		X

Nucleic Acid Notation

Adenine	A
Thymine	T
Guanine	G
Cytosine	C
Uracil	U

Publications and Posters

Publications

- Biedenkopf N, Lier C, Becker S. Dynamic Phosphorylation of VP30 Is - Essential for Ebola Virus Life Cycle. J Virol 2016;90:4914–25.

- Lier C, Becker S, Biedenkopf N. Dynamic phosphorylation of Ebola virus VP30 in NP-induced inclusion bodies. Virology 2017;512:39–47.

Posters

- Characterization of Ebola virus VP30 Phosphorylation (Clemens Lier, Nadine Biedenkopf, and Stephan Becker; DZIF-Standorttreffen Langen 2014)

- Studying Ebola virus VP30 phosphorylation with a phosphospecific VP30 antibody (Clemens Lier, Stephan Becker, and Nadine Biedenkopf; GfV-Tagung Bochum 2015)

- Role of Protein Phosphatase 1 for Ebola virus VP30 Phosphorylation (Gertrud Stalmann, Clemens Lier, Stephan Becker, and Nadine Biedenkopf; DZIF-Standorttreffen Langen 2015)

- Dynamic Phosphorylation of VP30 Is Essential for Ebola Virus Life Cycle (Nadine Biedenkopf, Clemens Lier, and Stephan Becker; GfV-Tagung Marburg 2017)

Verzeichnis der Akademischen Lehrer

Meine akademischen Lehrer an der Philipps-Universität Marburg waren die Damen und Herren:

Vorklinik

Adamkiewicz, Bette, Braun, Brehm, Cetin, Daut, Decher, del Rey, Feuser, Kinscherf, Koolman, Lill, Oliver, Preisig-Müller, Rausch, Rost, Schütz, Seitz, Stiewe, Suske, Weihe, Westermann, Wilhelm, Wrocklage

Klinik

Baarlink, Bartsch, Bauer, Baum, Baumann, Becker K, Becker S, Bender, Bliemel, Bohlander, Burchert, Czubayko, Dettmeyer, Dodel, Donner-Banzhoff, Eming, Fendrich, Fritz, Fuchs-Winkelmann, Gallmeier, Geks, Görg, Gress, Grimm, Grosse, Hertl, Hofmann, Hoyer, Hundt, Jaques, Jerrentrup, Kann, Kill, Kircher, Klose, Kolb-Niemann, König, Lohoff, Löw, Mahnken, Maier, Maisner, Mandic, Mittag, Moll, Moosdorf, Müller, Mutters, Nenadic, Neubauer, Nimsky, Oertel, Opitz, Pagenstecher, Pfützner, Plant, Reese, Renz, Richter, Rierra-Knorrenschild, Riße, Ruchholtz, Schäfer, Schieffer, Schneider, Schröder, Schu, Schulze, Sekundo, Sevinc, Shams-Eldin, Sommer, Tackenberg, Vogelmeier, Wagner, Werner, Wulf, Zemlin

Acknowledgements

Ich möchte mich herzlich bei Prof. Dr. Stephan Becker bedanken, der es mir ermöglicht hat, eine medizinische Doktorarbeit am Institut für Virologie anzufertigen. Vielen Dank für das Vertrauen, für viele hilfreiche Anregungen und die Bereitschaft zu zahlreichen Diskussionen.

Besonders möchte ich mich bei Dr. Nadine Biedenkopf bedanken, die mich während der gesamten Zeit hervorragend betreut hat, mir jederzeit mit Rat und Tat zur Seite stand, Versuche im BSL-4 Labor durchgeführt hat und mir beim Schreiben wissenschaftlicher Texte geholfen hat.

Ebenso möchte ich mich bei der gesamten AG Becker für die freundliche Aufnahme und die angenehme Arbeitsatmosphäre herzlich bedanken.

Zu guter Letzt geht mein Dank auch an das Deutsche Zentrum für Infektionsforschung (DZIF) für die Unterstützung mittels eines Promotionsstipendiums.